TEMPLATE INDUCED POLYMORPHIC SELECTIVITY IN PHARMACEUTICAL CRYSTALLISATION

JOSE VARGHESE PARAMBIL

NATIONAL UNIVERSITY OF SINGAPORE

2015

TEMPLATE INDUCED POLYMORPHIC SELECTIVITY IN PHARMACEUTICAL CRYSTALLISATION

JOSE VARGHESE PARAMBIL

(*MSc. IMPERIAL COLLEGE LONDON*)

A THESIS SUBMITTED FOR THE

NATIONAL UNIVERSITY OF SINGAPORE – IMPERIAL COLLEGE LONDON JOINT DEGREE OF DOCTOR OF PHILOSOPHY

DEPARTMENT OF CHEMICAL AND BIOMOLECULAR ENGINEERING

NATIONAL UNIVERSITY OF SINGAPORE

2015

Declaration

I hereby declare that this thesis is my original work and it has been written by me in its entirety. I have duly acknowledged all the sources of information which have been used in the thesis.

This thesis has also not been submitted for any degree in any university previously.

_____

Jose Varghese Parambil

29 December 2014

Acknowledgements

I would like to express my utmost gratitude to Prof. Reginald B. H. Tan and Dr. Jerry Y. Y. Heng for their supervision, support and guidance throughout the duration of this doctoral study. Prof. Tan has expressed his faith in my capabilities and has provided insights into new directions in my work. Dr. Heng has always been patient and helpful during adversities. He has encouraged me to take a step further in all endeavours, helping both professional and personal development.

My research work at Institute of Chemical and Engineering Sciences (ICES) would not have been fruitful without the guidance and help of Dr. Sendhil K. Poornachary. Regular discussions with Dr. Poornachary have played a significant role in shaping up of this research work. I am thankful to Dr. Jin Wang Kwek and Dr. Alvin Yeoh Chong at ICES who were very resourceful and trained me on different techniques during my work. I am also grateful to other members in the Crystallisation and Particle Science group at ICES who has supported me through technical assistances and useful discussions during my time there.

It was a rewarding experience to be the part of Surface and Particle Engineering Lab (SPEL) during my term at Imperial College London (ICL). It provided me the opportunity to engage with variety of research topics and learn different surface specific characterisation techniques. Dr. Umang Shah supported me in coping up with the transfer from ICES lab and setting up my experiments at ICL. I am thankful to Dr. Steve J. Hinder at the Department of Mechanical Engineering Sciences at the University of Surrey for his help with the X-ray photoelectron spectroscopy analysis. I am also very grateful to

Dr. Stephane Kena-Cohen and Mr. Tarik Abdelmoula in the Department of Physics at ICL for their help with spectroscopic ellipsometry analysis. Dr. Andrew J. P. White at the Chemical Crystallography laboratory, ICL aided the single crystal X-ray diffraction analysis for face indexing study.

This project would not have been possible without the financial aid from the National University of Singapore (NUS). I am also honoured to be the recipient of President's Graduate Fellowship bestowed by NUS which encourages me to aim higher in life. I sincerely thank Prof. Tan and Dr. Heng for nominating me for this honour.

I am greatly indebted to my family and friends for their support and understanding which helped me to boldly face every challenge and failure encountered in my research work. Thanks to all my colleagues at ICES, NUS and ICL who have made my work more pleasant and memorable.

Jose V Parambil

Table of Contents

List of Figures

List of Tables

Summary

Polymorphism in pharmaceutical drug crystals causes differences in their bioavailability, stability and processability. Hence, identifying different crystal polymorphs of an active ingredient during the early stages of drug development and controlling crystal polymorphism during the manufacturing process are important aspects of pharmaceutical crystallisation. Nucleation and growth of different polymorphs in a crystallising solution are regulated by a delicate balance between thermodynamic and kinetic factors. Crystal nucleation predominantly occurs via heterogeneous nucleation pathway as it is energetically favourable than homogeneous nucleation. Template-induced nucleation approach aims to utilise the advantage of heterogeneous nucleation to induce nucleation of specific crystal polymorphs through interfacial interactions between a preformed solid surface and solute molecules at the nucleation stage.

In template-induced crystallisation, templates with specific surface properties that can act as heterogeneous nucleation sites are introduced in contact with the crystallising solution. Specific interactions between the template surface and solute molecules are known to influence nucleation and growth of crystal polymorphs. However, the effects of template surface chemistry and other operating conditions such as temperature and supersaturation on template-induced crystallisation is not clearly understood. Hence, the aim of this study is to probe the combined effects of surface chemistry, crystallisation temperature, supersaturation, and solvent on template-induced crystallisation experimentally and consequent development of a molecular modelling approach to study template-induced nucleation. This

could help in establishing template-induced nucleation as a method to achieve preferential nucleation of crystal polymorphs and to support template chemistry as a novel parameter for polymorph screenings.

Carbamazepine (CBZ) was selected as the model drug compound and silanised glass vials were chosen as the template surfaces. CBZ crystallisation from ethanol solutions on templates with cyano functional surface groups led to selective nucleation of metastable form II crystals while the control surfaces resulted in concomitant nucleation of both form II and stable form III crystals. On mercapto and fluoro templates, CBZ crystallised preferentially as form III polymorph. These variations in the polymorphic outcome with template chemistry, temperature and supersaturation were mapped on to template-induced polymorphic domain (TiPoD) plots. The analysis of TiPoD plots showed that the template-induced nucleation mechanism was prominent within a narrow range of supersaturation across the temperature range studied. The influence of solvents on template-induced nucleation of CBZ polymorphs was also investigated by constructing TiPoD plots in five different solvents. These studies revealed that the templates were less effective in altering polymorphic outcome in highly polar solvent in comparison with the less polar solvents.

Interfacial interactions between the template surface and CBZ crystal polymorphs were calculated through molecular modelling. The simulation results suggest that those templates exhibiting favourable interaction energies with the dominant crystal facets of a specific polymorph preferentially induce nucleation of that crystal form.

List of Symbols and Abbreviations

Symbols

A	Helmholtz energy
A_n	Pre-exponential factor in Arrhenius type equation
a_{solute}^{ss}	Activity of solute in supersaturated solution
a_{solute}^{eq}	Activity of solute at equilibrium
C_p	Specific heat capacity
C^{ss}	Solution concentration in supersaturation solution
C^{eq}	Equilibrium solution concentration (solubility)
E	Internal energy
E_B	Electron binding energy
E_K	Kinetic energy of electron
G	Gibbs free energy
H	Enthalpy
J	Nucleation rate
$n(\lambda)$	Refractive index
R	Universal gas constant
r_{crit}	Critical radius of nucleus
S	Entropy
T	Temperature
T_p	Transition point for enantiotropes
V_m	Molecular volume
x	Mol fraction of solute
γ^+	Acidic component of surface energy
γ^-	Basic component of surface energy
γ^{AB}	Acid-base component of surface energy

γ^{LW}	Lifshitz-van der Waals component of surface energy
γ_{LV}	Surface tension of liquid
γ_{LV}^{d}	Dispersive component of liquid surface energy
γ_{LV}^{p}	Polar component of liquid surface energy
γ_{SL}	Interfacial energy at solid-liquid interface
γ_{SV}	Surface energy of solid
γ_{SV}^{d}	Dispersive component of solid surface energy
γ_{SV}^{h}	Hydrogen-bonding component of solid surface energy
γ_{SV}^{i}	Induction bonding component of solid surface energy
γ_{SV}^{m}	Metallic bonding component of solid surface energy
γ_{SV}^{p}	Polar component of solid surface energy
Δ	Phase difference
ΔG^{diss}	Free energy of dissolution
ΔG_{crit}	Gibbs free energy for nucleus of critical radius
ΔH^{diss}	Enthalpy of dissolution
ΔS^{diss}	Entropy of dissolution
θ	Contact angle
λ	Wavelength
μ^{ss}	Chemical potential of solute in supersaturated solution
μ^{eq}	Chemical potential of solute at equilibrium
σ	Solution supersaturation
ϕ	Spectrometer work function
Ψ	Amplitude component of polarised light

Abbreviations

ACN	Acetonitrile
AE	Attachment energy model
API	Active Pharmaceutical Ingredient
BFDH	Bravais–Friedel–Donnay–Harker model
CBZ	Carbamazepine
CCDC	Cambridge Crystallographic Data Centre
CNT	Classical Nucleation Theory
COMPASS	Condensed-phase Optimised Molecular Potentials for Atomistic Simulation
EtOH	Ethanol
IPA	Iso-propanol
MD	Molecular Dynamics
MeOH	Methanol
MS	Materials Studio®
OW	Owens-Wendt method
PoD	Polymorphic Domain
PXRD	Powder X-ray Diffraction
QCM	Quartz Crystal Microbalance
SAM	Self Assembled Monolayer
TiPoD	Template-induced Polymorphic Domain
TOL	Toluene
vOCG	van Oss, Chaudhury and Good method (Acid-base method)
XPS	X-ray Photoelectron Spectroscopy
XRD	X-ray Diffraction

Chapter 1

Introduction

Crystallisation is a unit operation widely used in many chemical plants. Electronics, food, pharmaceutical, agrochemical and speciality chemical industry utilises crystallisation for purification and formulation purposes. The pharmaceutical industry prefers developing molecular crystals as dosage forms largely due to stability and manufacturability reasons (Lee *et al.*, 2011). Crystallisation often serves as the final stage in the manufacture of active pharmaceutical ingredients (API) and excipients (Chen *et al.*, 2011). More than 90% of solid phase pharmaceutical products contain particulate drug, mostly in crystalline form (Shekunov & York, 2000). It is one of the most economical ways to produce high purity solid products and at times help to bypass expensive multistage purification processes such as chromatographic separations.

The most significant aspect of crystals is their well-ordered long range molecular arrangement. The molecular ordering in crystals imparts very specific physicochemical properties such as density, compressibility, melting point and solubility to the solid form. Many times molecules can form ordered molecular structures in more than one way and hence result in crystals of the same molecule with different molecular arrangements, known as polymorphs. McCrone defined polymorphs as "a solid crystalline phase of a given compound that results from the possibility of at least two crystalline arrangements of the molecules of that compound in the solid state" (Haleblian & McCrone, 1969). While many variations to this definition has been

proposed by further researchers over the years (Aitipamula & Nangia, 2012), the general understanding is that polymorphs of a molecule are chemically identical solid forms that differ in their structural arrangement, which in turn leads to difference in physicochemical properties. Although the term polymorphism was coined only in 1822, the phenomenon was recognised in inorganic materials and elements much before that. Klaproth reported that calcium carbonate can crystallise both as calcite and aragonite in 1788 (Haleblian & McCrone, 1969). It is estimated that about 50% of organic compounds could potentially exhibit polymorphism (Stahly, 2007).

In pharmaceuticals, difference in the physicochemical properties between polymorphic crystal forms can result in modification of stability, bioavailability and processability of the solids. For example, solubilities of different polymorphs of a compound can differ by 2–3 times due to the free energy difference between their structures (Singhal & Curatolo, 2004). Faster photolytic degradation kinetics of a photo-sensitive molecule in metastable polymorph than in stable polymorph is another instance where polymorphism can affect product quality (De Villiers *et al.*, 1992). Polymorph transformation of rotigotine in transdermal patches (Neupro®, Schwarz Pharma) used in the treatment of Parkinson's disease has led to large scale recall of the product in 2008. The new crystal form was more stable and less soluble than the initial formulated form, thereby lowering the effectiveness of the drug (Chaudhuri, 2008). Due to these concerns, regulatory approval of new drugs now require extensive data on polymorphic study of the molecules, drug stability, and their implications on final product characteristics (Byrn *et al.*, 1995).

In addition to the impact of product quality, polymorphism is also relevant in the domain of intellectual property. Since each polymorph of a new drug molecule can be patented, drug manufactures endeavour to patent every viable solid form, their methods of use, and process of manufacture in order to secure exclusive intellectual right to the molecule (Lee *et al.*, 2011). Consequently, systematic search for all polymorphs as well as other solid forms of the drugs has become a norm throughout the entire drug development process.

Polymorph screening often starts with crystallisation of drug from different solvents, typically with the solvents that are frequently used in final processing and formulation steps (Shekunov & York, 2000). Solvent effects on polymorph occurrence are well recognised though the effect of solvent on crystal nucleation is not thoroughly understood (Allesø *et al.*, 2008). There are examples reported in literature where a particular solvent resulted in selective crystallisation of specific polymorph(s). For example, sulfathiazole crystallisation from n-propanol results exclusively in form I polymorph while form II and III are crystallised with water as solvent (Khoshkhoo & Anwar, 1993). Other polymorph screening parameters may also include temperature, pH, degree of supersaturation, ionic strength and the presence of additives such as commonly used salts and excipients. These factors are compounded with the use of different crystallisation methods such as cooling, evaporative and anti-solvent crystallisation (Morissette *et al.*, 2004). This enables exploration of wide spectrum of thermodynamic and kinetic factors during the screening process in order to identify conditions that may lead to the formation of new polymorphs. However, it is to be noted that no universal protocol

exists for polymorph screening and the process selection is often guided by the experience and observations of the experimenter than by any rational scientific basis (Cross *et al.*, 2002). Predictive models of crystal polymorphism based on identifying conditions that could result in specific polymorphic crystals are yet to be fully realised (Price, 2008).

Crystallisation generally occurs through nucleation and growth process. It is supposed that the polymorphic identity of a crystal could be determined during early nucleation stage (Davey *et al.*, 2002; Mattei & Li, 2011). Hence, understanding and controlling crystal nucleation could go a long way towards predicting polymorph occurrence. Although nucleation could be either homogeneous or heterogeneous, the latter exhibits significant energy advantage due to lower activation energy requirement. Hence, heterogeneous nucleation is easier to achieve and expected to contribute to most of the experimentally observed nucleation processes (Price *et al.*, 2005). Heterogeneous nucleation could occur on any surface accessible to the solute molecules and could include seed, vessel, probe or particulate impurity surfaces. Utilising this nucleation pathway, template-induced or surface-mediated nucleation approach is the process of probing and/ or controlling nucleation by introducing templates with specific properties as heterogeneous surfaces where nucleation could occur. Template-induced nucleation has been studied using different templates to gain insights into heterogeneous nucleation process and the factors affecting it. Templates may be highly ordered surfaces such as self-assembled monolayers (SAMs) or amorphous structures such as polymers. Irrespective of the type of template, template

surface properties such as surface chemistry and surface roughness are expected to play an important role in template-induced nucleation.

1.1. Research Objectives

The focus of this work is to elucidate the influence of template surface chemistry on nucleation of polymorphic forms and to develop molecular level understanding of template-induced nucleation. The specific aims of this thesis are:

- To establish the effects of surface chemistry on nucleation of different polymorphs in template-induced nucleation process.
- To study the influence of template-induced nucleation over a wide range of temperature and solute concentration to build Template-induced Polymorphic Domain (TiPoD) plots on templates with various surface chemistries.
- To investigate the influence of solvent on template-induced nucleation process and establish the effectiveness of the process in solvents with varying polarity.
- To model interactions at template-crystal interface to simulate the interaction energy between template surface and crystal facets. Correlate the simulated interaction energies with experimental observations so as to develop further understanding of template-induced crystallisation process.

1.2. Thesis outline

The structure of this thesis is as follows. Chapter 2 introduces the theoretical aspects of crystal nucleation and the factors affecting polymorphic

nucleation from solution. It also includes a review of published literature on template-induced crystallisation process. Chapter 3 provides details of the model compound (Carbamazepine), experimental procedures and characterisation methods. Chapter 4 describes the results from characterisation of template surfaces prepared for crystallisation experiments. Experimental results on template-induced crystallisation of carbamazepine polymorphs are provided in Chapter 5. The effects of supersaturation, temperature and solvent on template-induced polymorphic control are discussed along with the calculation for free energy advantage of template-induced nucleation process. Chapter 6 focuses on molecular modelling and simulation of template-induced crystallisation. The modelling methodology and results on simulation of interaction energy are detailed in this chapter. Chapter 7 provides a summary of the significant results obtained in this study and details the future scope of this work.

Chapter 2

Crystal Polymorphism and Template-Induced Nucleation

Crystallisation is the process of producing solid state crystalline product with long range molecular order either from liquid, gas or disordered solid state. It essentially involves generation of a nuclei and subsequent growth guided through molecular recognition. The molecular arrangement could however be dictated by the environmental conditions which influences both thermodynamics and kinetics of the process. Difference in molecular arrangement (polymorphism) could affect the quality of crystals by altering physicochemical properties such as solubility, compressibility, adhesion, density, melting point, etc. Hence, understanding polymorphism, its origin, implications and methods for control are essential aspects in utilising crystallisation as an effective purification and formulation unit operation. This chapter deals with the basic theory on polymorphism, kinetics and thermodynamics of polymorph crystallisation, and a brief review of studies on template-induced polymorphic crystallisation.

2.1. Polymorphism and its origin

Polymorphism is the phenomenon by which molecules form two or more crystalline phases which are chemically identical but differ in their molecular arrangement and/ or conformations of molecules in the crystal lattice (Grant, 1999). Crystal structures are characterised by three-dimensional symmetry with repetitive units termed as unit cells. Each unit cell contains all

structural features and symmetry elements that repeat in the crystal structure. Unit cells can be distinguished by three axial lengths (a, b, c) and inter-axial angles (α, β, γ), which helps to classify them into one of the seven primitive crystal systems. The internal symmetry of unit cell is expressed as a space group which enables a complete crystal lattice to be built from a single asymmetric unit (*Z'*) consisting of one or more molecules. Based on this, 230 space groups have been identified to describe all possible arrangement of identical objects in an infinite three-dimensional lattice. Polymorphic structures can be identified based on the differences in lattice structures and can be classified accordingly. However, different methods of polymorph classification exist and polymorphs may belong to more than one class.

2.1.1. Conformational polymorphs

Flexible molecules can form multiple conformations of the molecule and associate with each other in different orientations. Presence of different molecular conformations in different polymorphs results in conformational polymorphism. Common bonds such as C-C, C-N, C-O, etc. posses rotational flexibility and contribute to conformational polymorphs in common APIs. 5-Methyl-2-[(2-nitrophenyl)amino]-3-thiophenecarbonitrile, commonly known as ROY (for red, orange and yellow crystals) is a classic example of conformational polymorphism with each seven polymorphic forms having different conformation of molecule (Chen *et al.*, 2005a).

2.1.2. Configurational polymorphs

Configurational or packing polymorphs involve different configurations of the same molecule in identical conformations (Babu *et al.*, 2010). Form I and form II polymorphs of acetaminophen are examples of configurational

polymorphs. Though the molecular conformation of acetaminophen molecule in both forms are identical, form I has pleated sheets stacked along the b-axis of the crystal while form II comprises of parallel hydrogen-bonded sheets along the c-axis, thereby exhibiting better compaction behaviour (Heng, 2005).

2.1.3. Synthon polymorphs

Synthons are commonly stated as the supramolecular building blocks which form the basic molecular recognition unit of the crystal (Desiraju, 1995). Synthon polymorphs differ in their hydrogen-bonding pattern and hence often referred as hydrogen-bond polymorphs. Molecules such as sulfathiazole, isonicotinamide and tetrolic acid exhibits this form of polymorphism (Gelbrich *et al.*, 2008; Leiserowitz, 1976; Roy & Matzger, 2009).

2.1.4. Variable Z' polymorphs

This polymorphism arises due to the difference in the symmetry-independent molecules in the asymmetric unit cell. The molecular arrangement and hydrogen bonding pattern in these polymorphs are so similar that their classification as a separate polymorphic form is often debated (Karami *et al.*, 2006). Form 1 and form 2 polymorphs of pyrazinedioxide is an instance of polymorphism due to variation in *Z'* (Babu & Nangia, 2007).

2.2. Thermodynamics of polymorphism

The free energy of polymorphs varies due to the difference in molecular arrangements within their crystal structures. Consequently, a crystal structure with the least free energy is termed as the stable polymorph while the higher

order crystal forms are termed metastable. The free energy of solid phase structure is dependent on temperature and can be represented using Helmholtz energy (*A*) which can be expressed using the relationship

$$A = E - TS \qquad (2.1)$$

where *E* is the internal energy, *T* is the absolute temperature and *S* is the entropy (Bernstein, 2007). Since enthalpy values can be experimentally obtained, the relationship can also be written in terms of Gibbs free energy (*G*) in the following form

$$G = H - TS \qquad (2.2)$$

where *H* is the enthalpy. When temperature is equal to 0 K, the free energy of the phase is equal to enthalpy. Above absolute zero temperature, entropy of the system contributes to the free energy value. Difference in the entropy of the polymorph crystal structures lead to different correlations between free energy and temperature. This may lead to a transition in thermodynamic stability order at some temperature below melting point. If such a transition occurs, the polymorphic system is known as *enantiotropes*. Systems which do not exhibit such behaviour are termed *monotropes*. Schematic representation of energy-temperature (E–T) relationship in monotropic and enantiotropic polymorphic systems for a dimorphic (system with two polymorphs) is represented in Figure 2.1. As seen from the E–T plot, there exists a transition point between polymorphs in an enantiotropic system, above which the stable polymorph becomes the metastable and vice versa.

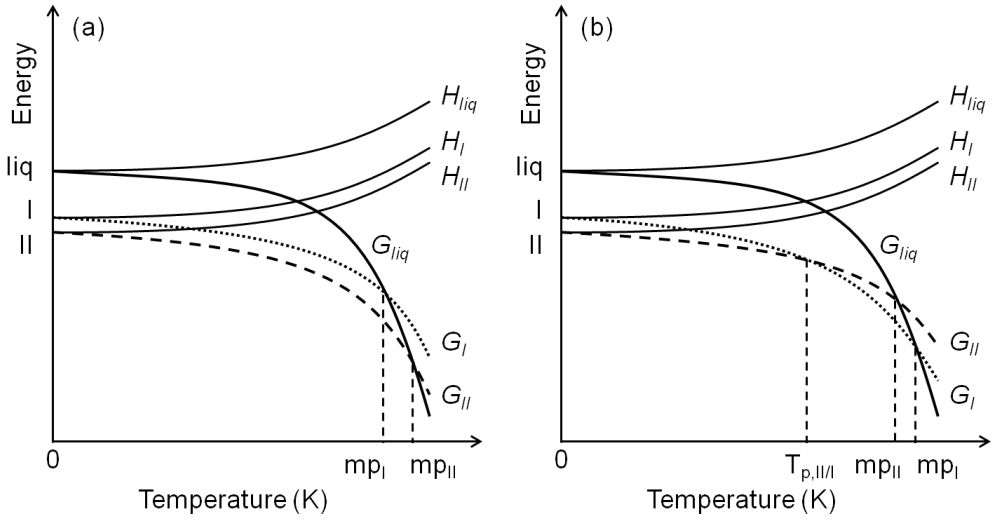

Figure 2.1. Energy-temperature (E-T) diagram for a dimorphic (a) monotropic and (b) enantiotropic polymorphic systems at constant pressure. *H*: enthalpy, *G*: Gibbs free energy, mp: melting point, T_p: transition point between two polymorphs.

Due to difficulties in obtaining exact E–T relationship for a polymorphic system, Burger and Ramberger (1979a, 1979b) proposed a series of rules to determine thermodynamic stability order of two polymorphs based on experimentally determinable values. Though exceptions could occur to each rule, such rules are commonly used in establishing thermodynamic stability order between polymorphs. The more relevant rules are briefly explained below.

Heat of transition rule. As per this rule, if an endothermic enthalpy of phase transition between polymorphs is observed at a specific temperature, there would be a transition point (T_p) below that temperature. Thus, the system would be enantiotropic. On the contrary, if an exothermic enthalpy of phase transition is observed, then the system is monotropic.

Heat of fusion rule. According to this rule, if the heat of fusion for the polymorph with higher melting point is lower, then the polymorphs are

enantiotropic. The rule is useful when the kinetics of transformation is very slow to be observed before melting and is based on the assumption that heat of transition can be approximated by the difference between the heats of fusion of polymorphs.

Density rule. The rule suggests that, if the higher melting polymorph has higher density they form monotropic system. This is based on the assumption that stable polymorph will have higher packing efficiency resulting in stronger intermolecular and van der Waals interactions. However, exceptions to this rule occur due to the influence of strong hydrogen bonds which compensate for close packing. For example, stable polymorphs of ritonavir and acetazolamide have lower density than metastable forms (Haisa *et al.*, 1974; Robertson & Ubbelohde, 1938).

Solubility rule. If the solubility of the higher melting polymorph is always lower than the lower melting polymorph, they form monotropic pair. However, if the solubility of higher melting crystal form is higher than the other form at any particular temperature, they are enantiotropes. The relationship arises since the solubility is directly proportional to the free energy and the stable form always has lower solubility, irrespective of the solvent used. Based on the solubility of a crystal polymorph, the free energy of dissolution (ΔG^{diss}) is expressed using the relationship

$$\Delta G^{diss} = \Delta H^{diss} - T\Delta S^{diss} = RT \ln (x) \qquad (2.3)$$

where ΔH^{diss} and ΔS^{diss} are the enthalpy and entropy of dissolution and x is the solubility of the polymorph expressed in mol fraction. This relationship is based on the approximation that the effect of small concentration variation on activity coefficient is negligible and that the activity is proportional to the

solubility. Plotting ln(x) versus (1/T) gives the Van't Hoff plot which can be used to find ΔH^{diss} and ΔS^{diss}.

2.3. Nucleation kinetics and polymorphism

While thermodynamics dictate the stability order of polymorphs, the occurrence of polymorphic forms during crystallisation is also controlled by the kinetics of nucleation and growth of crystals. Describing crystal nucleation with the analogy of chemical reaction kinetics (Figure 2.2), the rate of nucleation depends on the free energy difference between initial and final stages and the activation energy required for the process. Nucleation involves formation of prenucleation aggregates which upon reaching a critical size forms stable nuclei with some degree of molecular order. The solute molecules need not always order themselves into the lowest energy structure, but may form a structure with the least activation energy. This structure could further transform into more stable structure(s) through successive rearrangements. This is highlighted in the Ostwald's rule of stages which states that "when leaving a metastable state, a given chemical system does not seek out the most stable state, rather the nearest metastable one that can be reached without loss of free energy" (Ostwald, 1897). This rule implies that metastable polymorphs are most likely to appear first in a crystallisation process and subsequently transform into the most stable form, dictated by the transformation process. Although this behaviour is observed in many instances, it is not followed always due to a number of other influencing factors (Mattei & Li, 2011).

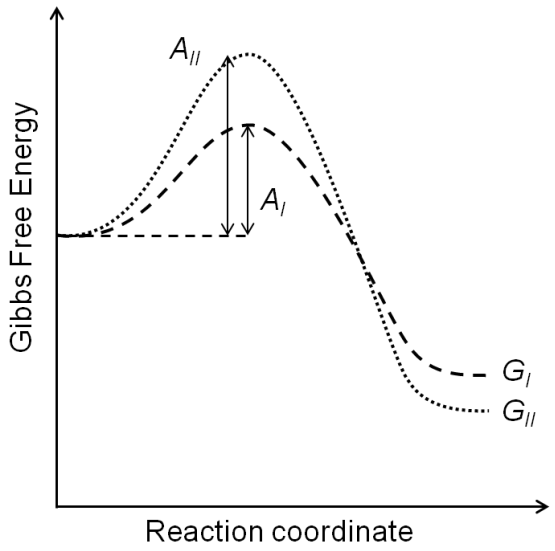

Figure 2.2. Free energy profile for crystallisation of polymorphs. *G*: Gibbs free energy, *A*: Activation energy for nucleation.

Formation of a stable nucleus is a prerequisite for the formation of a new crystal phase from solution. Nucleation involves formation of clusters of a new phase from the solution. Unless the size of the newly formed cluster is above a minimum threshold referred to as the critical radius, the cluster would be thermodynamically unstable and hence dissolve back into the solution. The rate of homogeneous primary nucleation can be given by an Arrhenius type equation,

$$J = A_n e^{-\frac{\Delta G_{crit}}{RT}} \qquad (2.4)$$

where A_n is the pre-exponential factor and ΔG_{crit} is the Gibbs free energy associated with the formation of a nucleus with critical radius. The activation energy barrier defined by the Arrhenius type equation signifies that though the free energy of the bulk crystal per molecules might be lower than that of the molecules in solution, the creation of a new interface between the crystal and the solution counters the energy drop to an extent. Until the free energy gain obtained from the ordering of the crystal structure is lower than the energy

requirement for the new surface generation, a stable crystal will not be formed. As a result, the surface area to volume ratio of the cluster is significant in determining the stability of the cluster. Gibbs free energy of a nucleus is a function of interfacial energy (γ_{SL}) and radius of nucleus (r). When the nucleus reaches critical radius (r_{crit}), ΔG_{crit} can be given by the following relationship.

$$\Delta G_{crit} = \frac{4\,\pi\,\gamma_{SL}\,r_{crit}^2}{3} \qquad (2.5)$$

The size of the critical cluster is notably sensitive to the supersaturation (σ) of the solution with a higher supersaturation reducing the critical size and thereby increasing the nucleation rate. With the assumptions that the nucleus is spherical and that the activity coefficient of the solute at equilibrium in solution and nucleus are the same, the relationship between r_{crit} and σ can be written as

$$r_{crit} = \frac{2\,\gamma_{SL}\,V_m}{k\,T\,\ln(\sigma)} \qquad (2.6)$$

where V_m is the molecular volume. Combining equations 2.4 – 2.6 and grouping the constants in the exponential terms into a single term (B), nucleation rate at constant temperature can be written as

$$J = A_n e^{\frac{B}{[\ln(\sigma)]^2}} \qquad (2.7)$$

The pre-exponential factor A_n is a function of solution concentration, solvent properties and temperature. From the above equations, it can be observed that temperature, supersaturation and the interfacial tension at the nucleus-solution interface are the major parameters that influence nucleation rate. At any given temperature, solution supersaturation is the foremost factor in determining the nucleation rate for a given compound in solution. As the

supersaturation increases, the critical radius decreases and thereby increases the nucleation rate. It is to be pointed out that interfacial tension of the stable polymorphic form would be higher than that of the metastable form, thereby resulting in larger critical radius and subsequent higher activation energy for the stable form nucleus at equal supersaturation for both polymorphs (Teychené & Biscans, 2008). However, due to the differences in the solubility between different polymorphs, the supersaturation with respect to the stable form would be higher than that of the metastable polymorph at any given solution concentration. As described by Cardew and Davey (1982) for a dimorphic system, these opposing factors can result in three possible nucleation behaviour of the solution as shown in Figure 2.3. Out of these three possibilities, two classes of behaviour can lead to situation where the nucleation rate of the polymorphs would be equal at some supersaturation values. At these instances, the thermodynamic, structural and kinetic factors are in delicate balance with each other, thereby allowing formation of both polymorphs at the same time, often termed as concomitant nucleation (Bernstein *et al.*, 1999). The actual polymorph composition at such a situation would be further guided by the stochastic nature of nucleation and growth kinetics of the polymorphs.

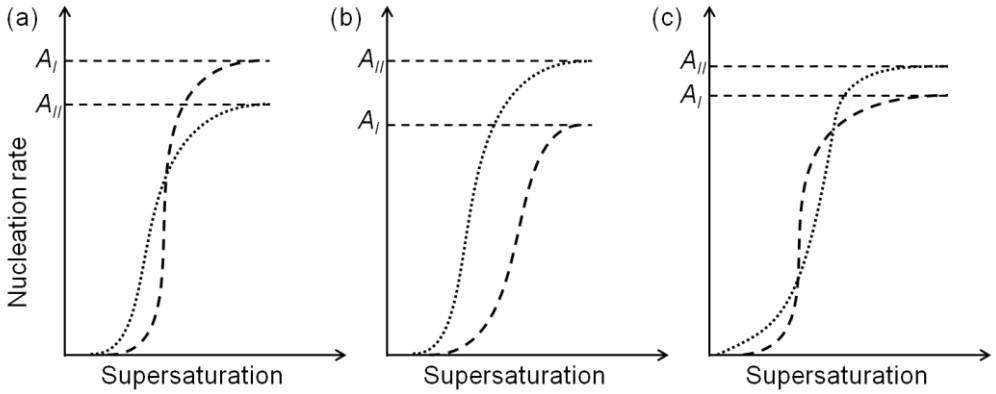

Figure 2.3. Three possible situations of nucleation rate changes in dimorphic systems. (form I is the stable and form II is metastable polymorph). (a) Nucleation rate of metastable form higher than that of stable form at high supersaturation, (b) stable form nucleation rate higher than that of metastable form at all supersaturations, (c) metastable form has higher nucleation rate only at an intermediate range of supersaturation (Cardew & Davey, 1982).

2.3.1. Classical and non-classical approaches on polymorph nucleation

The above equations and explanations are mostly based on the classical nucleation theory (CNT) which was initially developed for vapour condensation and later adapted for crystal nucleation from solution. Though widely recognised, value of the pre-exponential factor (A_n) predicted by CNT and determined experimentally are found to differ by a few order of magnitude (Erdemir *et al.*, 2009). The inherent assumptions involved in the CNT have been attributed to be a significant contributor to such a large error. Some of the erroneous assumptions are the following:

i. Critical nucleus is assumed to be a perfect sphere which has identical crystal packing and density to the final solid form.

ii. Growth of nucleus is assumed to take place by addition of one monomer at a time.

iii. Solution is assumed to be homogeneous with no concentration gradient or fluctuations.

iv. The nucleus–solution interface is assumed to be well defined, without considering the dependence of interfacial energy with the radius of crystal nucleus (capillary assumption) (Gebauer & Cölfen, 2011).

Other "non-classical" theories on crystal nucleation have been suggested to overcome these limitations of CNT (Davey *et al.*, 2013; Gavezzotti, 2007). One of the widely accepted models is the two-step theory of nucleation. This theory was put forward based on experimental evidences from macromolecular crystallisations and colloidal suspensions (Igarashi *et al.*, 1999; Savage & Dinsmore, 2009; Streets & Quake, 2010). Proof from model simulations and experimental observations in small organic molecule crystallisations also support this theory to a large extent (Savage & Dinsmore, 2009; Vekilov, 2010). As per two-step nucleation mechanism, nucleation is a multistep process with different activation energy barriers. The first step is the formation of dense liquid clusters with higher solute concentration. This is followed by the second step where a stable nucleus is formed inside the dense liquid cluster. The dense liquid droplets are highly disordered, but the stable nucleus formed inside has an ordered molecular structure. This implies that structural reorientation/ arrangement can occur after density fluctuation, as opposed to CNT where both structure fluctuation and density fluctuation occur simultaneously. The activation energy barrier for the individual steps in a two-step nucleation process is lower than that required for a CNT mechanism. This is schematically represented in Figure 2.4. The dense liquid cluster formed in

the first stage can be stable or metastable with respect to the solution as shown in the figure. It has been calculated that the energy barrier for cluster formation is lower than the energy barrier for molecular rearrangement within the liquid cluster (Filobelo *et al.*, 2005). Hence, it is often assumed that the second step is the rate limiting step in a two-step nucleation process (Erdemir *et al.*, 2009; Filobelo *et al.*, 2005). Through experimental observations in protein crystallisation by Vekilov and co-workers (2004), it is also concluded that large density-fluctuations or long-lifetime droplets are not essential for structure fluctuations that result in stable nuclei. Structure fluctuation in liquid clusters is a probability function and there exists density fluctuations with optimal size and density where the highest probability for the formation of stable nucleus occurs.

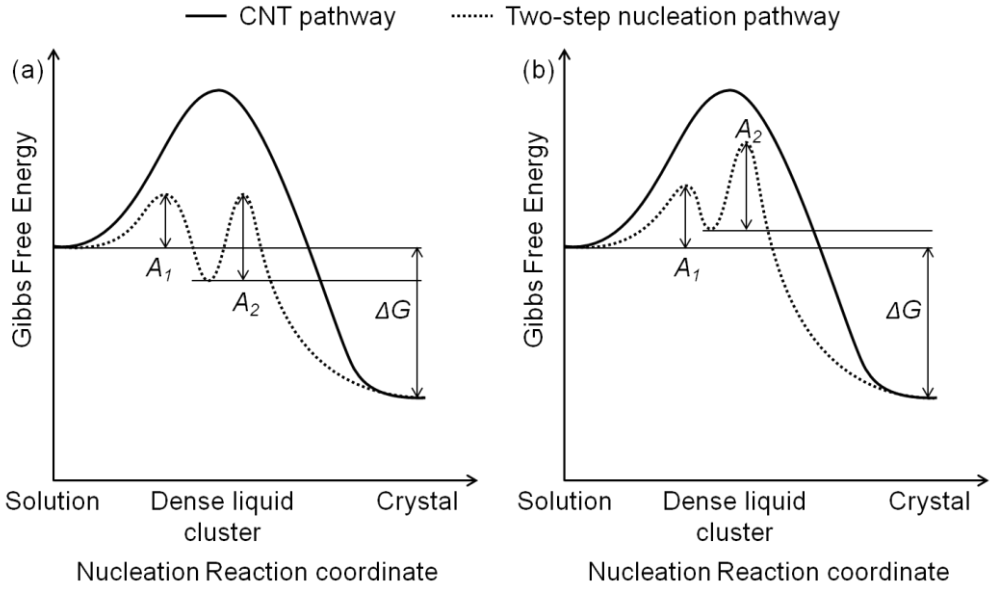

Figure 2.4. Free energy profiles for CNT and two-step nucleation mechanism wherein the dense liquid cluster is either (a) stable or (b) metastable with respect to the solution.

Although CNT is widely used for theoretical evaluation of nucleation kinetics even in polymorphic systems, it does not take into consideration the

molecular mechanisms underpinning polymorphic nucleation. While the growth units considered in CNT are primarily monomers, it is known that the solute–solute association occurs both in supersaturated and undersaturated solutions (Erdemir *et al.*, 2009). It has been revealed through spectroscopic studies that molecular recognition and association in solution is an essential step towards polymorph generation. Solute–solvent interactions are also found to promote specific patterns of solute conformations and dimer formation in many instances (Bernardes *et al.*, 2014; Davey *et al.*, 2013; Hamad *et al.*, 2006). Ageing or solution history is also known to influence nucleation of specific polymorphs, an effect that is not predicted by CNT due to the time-independent nucleation rate (Kuhs *et al.*, 2014; Nordström *et al.*, 2012). In this context, formation of dense liquid clusters and prenucleation aggregates that undergo molecular rearrangement as suggested by two-step nucleation mechanism appears to be more appropriate to explain polymorph specific nucleation. However, there exists some ambiguity in the nature of prenucleation and high-density liquid clusters with respect to their activation energy barrier and mechanism of cluster formation. Some of the other important issues that are yet to be answered in two-step nucleation theory include queries on molecular association within clusters, cluster size, shape and interaction between clusters (Davey *et al.*, 2002; Gebauer & Cölfen, 2011). Nevertheless, both theories suggest an exponential relationship between nucleation rate and supersaturation (the thermodynamic driving force). In the absence of a well established unique theory that is capable of explaining all phenomena associated with nucleation of polymorphs, inferences from both

classical and non-classical theories needs to be drawn appropriately with caution to gain insights into preferential nucleation of polymorph.

2.4. Effect of operating conditions on polymorph nucleation

2.4.1. Effect of supersaturation

Supersaturation is the thermodynamic driving force for crystallisation. Both nucleation and growth of crystals in solution is feasible only under supersaturated conditions. Supersaturation (σ) is a dimensionless factor and can be defined as the difference in the chemical potential of a solute in its supersaturated state (μ^{ss}) to its equilibrium state (μ^{eq}). The chemical potential can be correlated to the solute concentration using activity of the solute (a_{solute}). Supersaturation can hence be expressed using the following equation:

$$\ln(\sigma) = \mu^{ss} - \mu^{eq} = \ln\left(\frac{a_{solute}^{ss}}{a_{solute}^{eq}}\right) \approx ln\left(\frac{C^{ss}}{C^{eq}}\right) \qquad (2.8)$$

Thus, supersaturation $\sigma = C^{ss}/C^{eq}$, where C^{ss} and C^{eq} are solution concentrations at supersaturated and equilibrium conditions.

Supersaturation can be achieved through several methods depending on the method of crystallisation. Cooling, evaporation and addition of anti-solvent are some of the commonly used methods for supersaturation generation in crystallisation process. As explained in section 2.3 and in Figure 2.3, the kinetics of polymorph nucleation can be significantly affected by supersaturation. Depending on the supersaturation regime used and the relative nucleation kinetics, preferential nucleation of metastable or stable polymorphs or concomitant nucleation can take place. Moreover, supersaturation affects not only the nucleation rate, but also growth rate of crystals. Higher

supersaturation generally increases nucleation and growth rate of crystal polymorphs, though at different rates. It is reported that the polymorphic composition at lower supersaturation are dictated primarily by relative nucleation rates while relative crystal growth rate of polymorphs is the determining factor at higher supersaturations (Datta & Grant, 2005).

The method and rate of supersaturation generation has also been observed to regulate polymorphic outcome of crystallisation. This occurs due to the existence of metastable zone width and induction time for nucleation. Metastable zone width is the maximum allowable supersaturation before nucleation of the solid phase. Even after achieving the supersaturated state, there exist a lag time before crystal nucleation occurs. This is termed as the induction time for crystallisation. Generally, fast supersaturation generation promotes nucleation of kinetically favoured polymorph while slow supersaturation generation favours thermodynamically favoured polymorph (Bernstein *et al.,* 1999). Rapid supersaturation generation methods such as crash cooling, anti-solvent addition and spray drying are hence adopted to produce metastable crystal forms.

2.4.2. Effect of temperature

Temperature has both thermodynamic and kinetic implications on polymorph crystallisation. Solubility of organic molecules in most instances increases with temperature. The stability order of polymorphs itself could be influenced by temperature as in the case of enantiotropic systems as explained in section 2.2. Apart from the nucleation kinetics, growth kinetics and transformation kinetics of crystal polymorphs are also affected by temperature. Rates of solution mediated transformation of polymorphs generally tend to

increase with increase in temperature due to higher solubility and molecular mobility. Therefore, pharmaceutical crystallisation processes are designed and controlled to avoid undesirable temperature variations that might affect polymorphic composition of the product. Specific temperature profiles are often used in conjunction with seeding to avoid uncontrolled nucleation and phase transformation with the additional objective of crystal size control (Cote *et al.*, 2009; Muller *et al.*, 2009; Parsons *et al.*, 2003).

2.4.3. Effect of solvent

Solvent plays a crucial role during solution crystallisation. Solvent–solute interaction is imperative in controlling nucleation and polymorphism over and above its effect on the growth of crystals from solution. Generally, the solvent affects crystal nucleation and growth in two ways (Du *et al.*, 2014). Firstly, the solvated solute molecules in solution have to be desolvated before they can aggregate to form a nucleus or to attach to a growing crystal face. Likewise, solvent molecules that are bound to the surface of a nucleus or a growing crystal facet have to be replaced by the solute molecules for integrating into the lattice structure. Both these steps are regulated by the strength of solvent-solute interactions which may include van der Waals and hydrogen bonding forces. Secondly, solvent also affects nucleation by means of its effect on solubility. Combing these two different factors, fast nucleation rates could be achieved in a solvent with high solubility along with moderate solute-solvent interactions (Gu *et al.*, 2001). Based on the CNT, interfacial energy (γ_{sl}) and critical radius (r_{crit}) of the nucleus are also affected by the solvent interactions, thereby altering nucleation rate (Yang *et al.*, 2014).

In the context of polymorphism, solvents influence polymorphic outcome through a combination of factors. Solvents affect the structure of prenucleation clusters or solute aggregates thus favouring nucleation of one polymorph over other. Modelling molecular aggregates of benzamide in polar solvent is reported to favour P1-type polymorph while non-polar environment favour P3-type polymorph (Ectors *et al.*, 2014). Similarly, experimental spectroscopic data has been used to explain preferential polymorph formation of dihydroxybenzoic acid (Davey *et al.*, 2001). In toluene, molecular aggregation of dihydroxybenzoic acid is limited to dimer formation through carboxylic acid functionality similar to form 1 polymorph while chloroform favours supramolecular species similar to chain motif found in form 2 polymorph. As a result, pure form 1 is obtained from toluene and pure form 2 from chloroform. Solvents can also dictate the type of solute interactions that occur during aggregation process. It is reported that carbamazepine dimmers formed in solvents with different polarity possess different hydrogen-bonding patterns between solute molecules while in solution (Hunter *et al.*, 2012). In addition to doctoring solute–solute interaction, recent studies also suggests that solvent molecules form an integral part of the high-density liquid cluster formed prior to nucleation (Bernardes *et al.*, 2014).

Solvents could also result in formation of solvates which are solute crystal structures with solvent molecules incorporated into the crystal lattice. Though solvents do not alter the thermodynamic relationship between polymorphs (Khoshkhoo & Anwar, 1993), if solvate structures are present, they exhibit their own thermodynamic relationship with other polymorphs and

alter solid state content depending on crystallisation conditions (Kitamura, 2004).

When the nucleation rates of polymorphic forms are similar, the relative growth rates of crystal polymorphs could play an important role in determining solid state composition. A polymorph with higher growth rate will dominate over the slower growing crystals and consume the supersaturation further slowing down the growth of other polymorph crystals. However, if the crystallisation process is not interrupted, composition of the stable polymorph will increase over time through solution mediated polymorphic transformation process. The rate of this transformation is also dictated by the solvent. Similar to the effect on nucleation, solvents with high solubility and medium solvent–solute interactions result in faster transformation kinetics (Gu *et al.*, 2001).

Solvent properties such as hydrogen-bonding capacity, dielectric constants, polarity and dipole moment are important factors in regulating solvent-solute interactions which influence both nucleation as well as crystal growth of polymorphs (Aitipamula & Nangia, 2012; Wan *et al.*, 2014). Solvent density and viscosity could affect molecular diffusion and transfer of solute molecules into the crystal lattice. These factors influence nucleation, growth and transformation rate of polymorphs. Hence, selection of a suitable solvent or solvent mixture is highly essential for ensuring polymorph purity in crystallisation.

2.4.4. Other factors

Polymorphism is affected by a number of other factors that can potentially influence both thermodynamics and kinetics of nucleation and

growth of crystals. pH and ionic strength of the solution can play a significant role in polymorph selective crystallisation. Glycine, when crystallised from aqueous solution within the pH range of 3.8 – 8.9 produces the α polymorph while at pH below and above this range results in γ form crystals (Towler *et al.*, 2004). Presence of additives and impurities in solution is also known to alter the appearance of crystal polymorphs (Poornachary *et al.*, 2007). In rare instances, additives have even been reported to produce new polymorphs of 1,3,5-trinitrobenzene which are not obtained in their absence (Thallapally *et al.*, 2004). Trace amount of impurities can prevent nucleation and/ or solution mediated transformation of polymorphs by preferential attachment to specific crystal facets or through interaction with solute molecules (Davey *et al.*, 2013; Poornachary *et al.*, 2012).

Agitation is another operating parameter that is stated to affect polymorphic crystallisation. Crystal structures with shear sensitive planes are postulated to be more sensitive to agitation rate than other polymorphs (Liu *et al.*, 2014). Agitation rate is also found to affect the rate of crystal nucleation and solution mediated polymorphic transformation through its influence on solute transport (Gu *et al.*, 2001; Kitamura, 2004). Evidences suggest that external source of energy in the form of ultrasound (sonocrystallisation) or laser also affect nucleation of polymorphs. Louhi-Kultanen *et al*. (2006) found that sonocrystallisation is effective in altering the relative composition of α, β and γ polymorphs of glycine. Likewise, Sun *et al* .(2006) demonstrated that nonphotochemical laser-induced nucleation using linear, circular and elliptically polarised light can nucleate specific polymorphs of glycine. However, the molecular mechanism behind the influence of such factors on

polymorphism is not fully understood. Templates or heterogeneous nucleating surfaces with or without confinement effects are other external factors that are investigated to control nucleation of specific polymorphs. Further discussion on this topic follows in section 2.7.

2.5. Impact of polymorphism on pharmaceutical product development

Variations in solid state structure can affect a myriad of product qualities such as chemical (reactivity, photochemical activity), physical (density, hygroscopicity, refractive index, colour, particle morphology), kinetic (dissolution rate), thermodynamic (free energy, solubility, heat capacity, melting point), surface (surface free energy, adhesiveness) and mechanical (compactability, flowability, tensile strength, hardness) properties (Lee *et al.*, 2011). Effect of some of these properties on pharmaceutical product development is explained in this section.

2.5.1. Stability

Solid form stability and bioavailability are often pointed out to be the key attributes in the development of a quality drug product (Lee *et al.*, 2011). During the development of the solid form of a new drug or pharmaceutical excipient, considerable effort is taken to identify the most stable crystalline polymorph. The stable form is generally chosen for further development due to concerns on product stability. However, in exceptional circumstances where the stable form solubility is too low for adequate bioavailability or when fast dissolution is required for rapid action or due to processing difficulties associated with stable crystal form, a metastable crystal form could be chosen for product development (Singhal & Curatolo, 2004). Developing metastable

polymorphs for a product is more challenging than stable form development due to the inherent instability of the solid form. Impact of stresses arising from both processing and environmental conditions on phase transformation has to be studied in detail and care must be taken to avoid any detrimental stress not only within processing steps but also in the product supply chain (Myrdal & Jozwiakowski, 2008).

Chemical stability or reactivity is also affected by polymorphs due to the difference in intermolecular interactions and can impact the life time of the product. In case of photolytic degradation, metastable polymorph has been demonstrated to be more prone to such degradation, thereby limiting storage and exposure options (De Villiers *et al.*, 1992).

2.5.2. Bioavailability

Bioavailability of a drug is affected by its solubility and dissolution rate in the body. Due to difference in lattice free energy of polymorphs, they have different solubility as well as dissolution rates. Recall of rotigotine transdermal patches (for the treatment of Parkinson's disease and restless legs syndrome) in 2008 due to the appearance of 'snow-flake like' crystals within the patch is a recent example where the difference in bioavailability due to polymorphism affected product quality (Chaudhuri, 2008). Another case of polymorphism affecting bioavailability is reported for chloramphenicol palmitate where only form B is biologically active while stable form A is biologically inactive (Maeda *et al.*, 1980).

2.5.3. Processability

Mechanical properties such as elasticity, hardness, yield pressure, and density are dependent on the lattice structure of crystals and hence differ

between polymorphs. Surface properties and the resulting cohesive/ adhesive nature of particles are also different for different polymorphs. These mechanical properties along with the morphology of the particles influence processability or manufacturability of the product. Flowability and compactability are important particle attributes that can aid easy manufacturing of the final product. Crystal structures with slip planes are expected to exhibit higher plasticity and therefore better tabletting properties. Consequently, sulfamerazine form I exhibits better compressability than form II due to the presence of slip plane (Sun & Grant, 2001). Impact of processes on polymorphism is also important in drug development. Process induced solid-state transformation can occur either between polymorphs or between polymorphs and solvates (Peterson *et al.*, 2003). Although important, differences in processability of polymorphs are considered only as secondary factors in comparison with stability and bioavailability (Lee *et al.*, 2011). Limitations in processability of crystal polymorphs are often overcome through selection of suitable excipients and processes which can assure quality of the final product (Gregory, 1995).

2.6. Polymorph screening

Polymorph screening is an essential component of early stage drug development to identify all possible solid state phases of the molecule so that the ideal solid form can then be selected for further development and drug approval processes. Polymorph screening requires high purity compounds to avoid impurities which might affect polymorphism, and also to evaluate the influence of additives on crystallisation (Yamano, 2011). A thorough polymorph screening generally involves a wide range of crystallisation

methods such as cooling, evaporative, and anti-solvent crystallisation from solution. Crystallisation from melt, vapour deposition, spray drying, and other processes such as vapour sorption, grinding, heating and compaction are also considered for generating new polymorphs (Lee *et al.*, 2011). Due to the influence of solvents on polymorphism and extensive usage of solvent-based crystallisation methods in pharmaceutical industry, polymorph screening is usually conducted from various solvents. Solvents and solvent mixtures covering a wide range of properties such as hydrogen-bonding capability, polarity, dipole moment and viscosity are used for screening purposes (Allesø *et al.*, 2008; Gu *et al.*, 2004).

A wide range of operation conditions such as supersaturation and temperature are essential in exploring all thermodynamic and kinetic situations that can lead to formation of different crystal polymorphs. Rate of supersaturation generation is also a factor that needs to be considered. In order to improve screening capability, high-throughput techniques that can run hundreds of parallel screens are developed and employed in the industry (Alvarez *et al.*, 2009; Morissette *et al.*, 2004). With further development of non-classical crystallisation methods using supercritical fluid, high pressure conditions, small-volume confinement, microfluidics, and laser-induced and template-mediated nucleation, some of these methods could also contribute towards comprehensive polymorphic screening process.

Computational methods for predicting polymorphic occurrence are being developed to complement experimental screening methods and to make the screening process more efficient. Several global optimization methods for generating all possible conformations and packing arrangements of a given

molecule are utilised for generating polymorph crystal structures (Cross *et al.*, 2002; Gavezzotti, 2005; Payne *et al.*, 1999). However, computational methods are prone to overestimation of probable polymorphic structures if accurate kinetic and thermodynamic parameters are not included (Davey, 2003; Price, 2008). Even with such limitations, results from computational predictions can aid in optimal design of experiments to explore unknown polymorphic structures (Arlin *et al.*, 2011; Hulme *et al.*, 2007).

2.7. Heterogeneous nucleation templates

In a typical crystallisation process, by and large crystals are expected to form via heterogeneous nucleation pathway (Price *et al.*, 2005). In this mechanism, nucleation occurs on foreign particles or surfaces which may or may not be chemically identical to the nucleated material. The probability of homogeneous nucleation at low or medium supersaturation is limited due to the high energy penalty associated with the formation of a surface between the growing nucleus and solution. The energy requirement for the creation of new interface counters the favourable volume free energy of the nucleus until a critical radius is attained. In the case of heterogeneous nucleation, the critical radius of the nucleus could be reduced due to the reduction in interfacial area of the nucleus with the solution as well as favourable surface interaction with another solid phase. This reduces both the critical radius and activation energy barrier required for the formation of a stable nucleus and thus improves the probability of heterogeneous nucleation (Ward, 2001). In a typical crystallisation system, many foreign surfaces can act as templates where heterogeneous nucleation occurs. Some of them include the surface of crystallisation vessel, stirrer, probes, and minor particulate impurities.

Due to the difficulties in controlling heterogeneous nucleation, a common approach used for the control polymorphism is seeding. Seeding involves addition of small crystals of the required polymorph into the supersaturated solution to grow more of the same polymorph. Thereby, seeding attempt to avoid heterogeneous nucleation while allowing crystal growth, although some extent of secondary nucleation may occur during the process. Chemical purity and polymorph purity of the seed crystals are essential to ensure success of seeding process (Cimarosti *et al.*, 2010). Generally, while seeding is performed, primary nucleation is avoided by maintaining supersaturated solution within metastable zone (Lee *et al.*, 2011). Control of final product quality is achieved through design parameters such as seed loading, temperature cycling, etc. However, a few instances where seeding is not able to control polymorphism due to cross-nucleation is also known. In cross-nucleation, seeds of one crystal form promote nucleation of other crystal forms resulting in the production of a polymorph mixture (Chen *et al.*, 2005b; Yu, 2003).

Due to the wide array of surfaces that can potentially cause heterogeneous nucleation in common crystallisation methods, it is difficult to study and control factors affecting such nucleation. To overcome this difficulty, template-induced nucleation approach has been developed to systematically study nucleation on template surfaces with known properties. Research on template-induced nucleation of organic crystals gained significant momentum in the past decade. Use of templates for control of crystal morphology, polymorphism and crystal size has been reported in literature (Hiremath *et al.*, 2005; Lee *et al.*, 2005; Lee *et al.*, 2002). Templates such as

self-assembled monolayers, other crystalline substrates, polymer substrates, colloidal interfaces and functionalised silica have all been used for nucleation control of crystal polymorphs. Such templates aim to utilise the advantage of heterogeneous nucleation while providing tools to alter surface properties of nucleating surface. Different surface properties of the templates can influence the heterogeneous nucleation of crystals. Broadly, these include two dimensional lattice structure and surface topography/ morphology of template, and surface chemistry which in turn regulate the surface energy of the template. These factors manipulate the interactions between the heterogeneous surface and solute molecules or molecular clusters that form the crystal nucleus (Diao *et al.*, 2011c). Although direct experimental observation of template–nucleus interaction is rather difficult to achieve with the present day characterisation techniques, the impact of template on nucleation and growth of crystal polymorphs can be reasoned in an inferential manner based on the crystals that form on the templates. With additional inputs from molecular modelling, different types of heterogeneous nucleation templates have been developed and reported to control crystal nucleation and polymorphism.

Heterogeneous templates have also been used for producing crystal structures that are not obtained in the absence of such templates. Bucar *et al.* (2013) reported the formation of stable form I polymorph of (caffine)·(benzoic acid) cocrystal using designed heteronuclear seeds. Previous attempts to produce this polymorph through other well established techniques had failed consistently for about sixty years until heteronuclear seeds were introduced. This example highlights the prominence of heterogeneous templates in promoting nucleation of different polymorphs.

This section will provide a review of various types of templates that are used for controlling nucleation of organic molecular crystals.

2.7.1. Self-Assembled Monolayer (SAM) templates

Preliminary work on oriented growth of organic crystal on a Langmuir monolayer was embarked by Landau *et al.* (1985) with crystallisation of glycine over amino acid monolayers. Glycine was reported to crystallise with [110] facet attached to chiral *R* amino-acid monolayer and with $[0\bar{1}0]$ face on *S* amino-acid monolayers. However, such monolayer templates had limited scope for scale up since the organic surfaces were neither homogeneous nor well defined (Aizenberg *et al.*, 1999). In comparison, alkanethiols forms well defined monolayers with highly ordered molecular structure on metal substrates (Vericat *et al.*, 2010). Thiol-based SAMs on gold surface are the most widely used ordered monolayer templates for crystallisation studies. These types of templates have the advantage of fast surface modification which can be conducted under mild conditions. In this surface modification, ordered monolayer is formed due to the specificity of thiol group with gold resulting in strong gold-sulfur bonds (Schreiber, 2000).

2.7.1.1. Driving force for nucleation control on SAM templates

Two-dimensional (2D) molecular order in the monolayer aids solute aggregation on the template surface through epitaxial relationship. In epitaxial growth, the 2D molecular order and geometry on the template surface guides further ordered molecular arrangement of solute molecules with similar lattice structure. This ultimately leads to the transfer of structural information of the template to three-dimensional crystal structure. However, an absolute lattice symmetry is not required for epitaxial nucleation; even low symmetry

relationship with certain degree of lattice mismatch between template and nucleating structure can still lead to epitaxial nucleation (Ward, 2001). The lattice parameters of alkanethiol SAMs can be controlled by choosing appropriate thiol-metal combinations and different lattice geometries can be used to nucleate crystals with specific crystallographic orientation. Highly selective and oriented growth of malonic and succinic acid on different SAM templates have been reported to occur primarily based on epitaxial relationship between the nucleating plane and the template layer (Pokroy *et al.*, 2009). Similarly, SAMs formed using chiral molecules (molecules with identical chemical composition, but with non-superimposable mirror structure) have been observed to selectively nucleate crystals of racemic drug valine with enantiomeric excess or even pure enantiomer based on crystallisation conditions (Singh & Myerson, 2010). Apart from epitaxial relationship, the ordered molecular structure on SAM templates also influences direction depended molecular interactions such as hydrogen-bonding. Alkyl chain length parity of molecules that form SAM is stated to affect face selective growth of carbamazepine crystals due to the difference in possible bond angle variations (Dabros & Thalladi, 2007). The concept of chemical epitaxy whereby complimentary chemical groups are presented along with geometric lattice matching is proposed to be the most appropriate criteria for the selection of suitable SAM surfaces for preferential nucleation of crystals (Hiremath *et al.*, 2004).

SAM templates have been used for controlling nucleation of polymorphs under various conditions. SAM templates with analogous functional groups has been reported to be effective in nucleating and stabilising metastable

polymorph of glutamic acid along with oriented crystal growth (Dressler & Mastai, 2007). Different siloxane based SAM surfaces were found to preferentially nucleate kinetic polymorphs leading to selective nucleation of four polymorphs of *m*-nitrophenyl urea based on specific interfacial interactions at template-crystal interface (Capacci-Daniel *et al.*, 2010). Epitaxy, complimentary functional group interactions and dipole moment interactions between template and nucleating crystal facets form the driving force for nucleation of specific polymorphs on SAM templates (Hiremath *et al.*, 2005). This view is also supported through molecular modelling study of selective crystallisation of tolbutamide polymorphs on SAM (Zhang *et al.*, 2011).

2.7.1.2. High-throughput method with patterned SAMs

A specific application of SAM templates in crystallisation studies is the use of patterned template surfaces. A patterned surface contains islands with different SAM templates formed via sequential deposition of template molecules through specifically designed meshes. As a result, the template comprises of islands with different surface properties. The island size typically varies in the range of 100–1000 μm. Patterned SAM templates facilitate large number of crystallisation experiments on the same substrate thereby saving time and material while providing statistical accuracy (Singh *et al.*, 2011). On a typical SAM template crystallisation, the chemical and physical surface features are of primary importance. However, evaporative crystallisation of glycine polymorphs on patterned SAM templates has shown that other operating conditions such as supersaturation generation rate, pattern island size, shape, etc. are important aspects which can regulate nucleation kinetics

on patterned SAM arrays (Lee *et al.*, 2006). Nonetheless, patterned SAM templates present significant opportunity in incorporating template effect on high-throughput screening for crystal polymorphs.

2.7.2. Crystal substrates

Crystalline substrates have been used as templates for crystallisation of pure single crystals of inorganic substances for various optoelectronic applications for a few decades. Polymorphs of organic semiconductors have also been crystallised through this method, extending the possibility for small organic molecule crystallisation (Trabattoni *et al.*, 2013). Though not commonly used in pharmaceutical crystallisation, the methodology has been experimented for crystallisation of organic molecules and to attain specific polymorphic control. Recently, a new polymorph (form V) of pharmaceutical drug carbamazepine was crystallised by using form II dihydro-carbamazepine crystal as template (Arlin *et al.*, 2011). The occurrence of new polymorph was predicted with the help of molecular modelling and the template crystal was chosen based on the lattice arrangement of the predicted form (epitaxial relationship). Another instance where the crystal surface of one polymorph acts as a template for nucleation of another form has been reported in case of sulfathiazole. Form IV sulfathiazole facets provide a template for nucleation and growth of form II crystals through epitaxial interactions (Munroe *et al.*, 2011). Similar behaviour has also been studied in the case of $_{L}$-glutamic acid. Experimental and modelling data showed that preferential binding of crystal facets with large number of hydrogen bonds occur between α and β polymorphic forms of glutamic acid (Hammond *et al.*, 2007). Although some of these examples are not caused by intentional templating, fundamental

understanding from these work has been used in developing crystalline silica and mica templates for template-induced crystallisation studies (Campbell *et al.*, 2013).

2.7.3. Polymer templates

Polymers provide templates without crystalline order due to the inherent amorphous nature of their molecular structure. Nevertheless, a wide array of polymers with varied chemical composition are easily available and can be promptly modified to create required surface features, making them good candidates for template-induced crystallisation. Polymers have been shown to facilitate growth of single crystals through heterogeneous nucleation (M. D. Lang *et al.*, 2002; Price *et al.*, 2005; Sudha *et al.*, 2014). Unlike SAM or crystalline templates, designing polymers as templates do not require prior knowledge of precise lattice structure. The chemical functionality and surface features of the template are more important for polymer heteronuclei (Di Profio *et al.*, 2012). Diverse groups of polymers classified based on functional groups, chemical composition, and network structures have been utilised to study their ability to control polymorphic crystallisation of acetaminophen and aspirin (Diao *et al.*, 2011c; M. D. Lang *et al.*, 2002). Similarly, library of polymer templates used with high-throughput screening method was used by Price *et al.* (2005) for producing polymorphs of pharmaceutical compounds such as carbamazepine, acetaminophen, sulfamethoxazole and ROY.

2.7.4. Other heterogeneous templates

Crystallisation within confined spaces is another area of interest in controlling nucleation and growth of crystal forms. Rigid nanoporous materials as well as soft polymer-gel matrices have been used as templates to

control nucleation. Porous glass and aluminum oxide templates with ordered pore structure have been shown to result in selective nucleation of acetaminophen polymorphs (Graubner *et al.*, 2013). The structure of pores in templates is suggested to impact both the thermodynamics and kinetics of nucleation of polymorphs. By regulating the pore size of glass particles in the order of critical radius of nucleus, it was shown that polymorphs of anthranilic acid and ROY could be preferentially crystallised (Ha *et al.*, 2004). Similarly, crystallisation of mefenamic acid polymorph on geometrically imprinted polymer substrates with different pore shape revealed that the shape of the confining pores can assist selective polymorph nucleation through angular matching with the nucleated crystal (López-Mejías *et al.*, 2013). Soft confinement in polymer gels also regulate crystal nucleation in ways similar to the rigid porous material, along with the added features of mesh like network and choice of manipulating solute-gel interaction through selection of suitable polymer chemistry (Diao *et al.*, 2011a). Crystallisation of aspirin and acetaminophen within polymer gels has been controlled by tuning the gel microstructure and chemistry (Diao *et al.*, 2011b). Other templates such as emulsion droplets and electrochemically tunable surfaces are also reported in literature to control nucleation of organic crystals (Kwokal & Roberts, 2014; Ueno *et al.*, 2003).

Irrespective of the templates investigated, interfacial interaction between template surface and nucleating crystal facet is pointed out to be the primary decisive factor in selective nucleation of crystal polymorphs on templates. These interactions could be epitaxial, polar moments, hydrogen-bonds or electrostatics depending on the nature of template and crystal surfaces.

2.8. Summary

Controlling the nucleation of crystal polymorphs is an important aspect of successful crystallisation process. Polymorphic crystallisation is guided by a delicate interplay of thermodynamic and kinetic factors influencing crystal nucleation and growth. Different strategies are used to manipulate these factors and to crystallise the desired polymorphs. Template-induced nucleation is one such strategy for controlling polymorphism which utilises the advantages offered by heterogeneous nucleation pathway. Experimental and molecular modelling studies on the mechanism of template-induced crystal nucleation would be helpful in improving fundamental understanding of the process and in developing novel templates for controlling polymorphism for a wide range of molecules.

Chapter 3

Experimental Methodology

This chapter introduces the model compound and templates used for template-induced nucleation study. Method of crystallisation, template production and characterisation methods used for surface analysis and polymorph determination are also detailed.

3.1. Model compound

Carbamazepine (CBZ) is a pharmaceutical API with anticonvulsant and mood stabilising effect, used in the treatment of epilepsy and bipolar disorder. CBZ is also known under names carbamazepen, amizepin and 5*H*-Dibenz[*b*,*f*]azepine-5-carboxamide. It is marketed under several brand names such as Tegretol, Epitol, Calepsin and Carbatrol. The chemical structure of CBZ is provided in Figure 3.1.

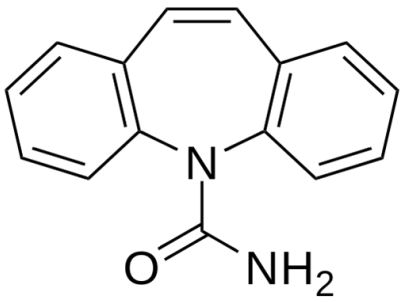

Figure 3.1. Carbamazepine molecular structure

CBZ has 5 known anhydrous polymorphs, hydrate and several other solvate structures. Of the five anhydrous forms, only four of them are commonly observed and reported. Formation of a fifth polymorph (form V) has been reported only through crystallisation via vapour deposition (reverse

sublimation) on form II crystal of analogous molecule 10,11-dihydroxycarbamazepine (Arlin *et al.,* 2011). Henceforth, further discussion on CBZ polymorphs is limited to the widely studied first four polymorphs. The first CBZ crystal structure was reported in primitive monoclinic cell (*P*-monoclinic - form III), followed by trigonal (form II), *C*-centered monoclinic (*C*-monoclinic – form IV) and triclinic (form I) polymorphs (Himes *et al.,* 1981; M. Lang *et al.,* 2002; Lowes *et al.,* 1987; Reboul *et al.,* 1981). There has been some ambiguity on the nomenclature of CBZ polymorphs in literature due to different naming systems used by different researchers. Some of the different reported nomenclature for CBZ polymorphs is provided in Table 3.1. In this thesis, nomenclature suggested by Grzesiak *et al.* will be followed (Grzesiak *et al.*, 2003).

Triclinic	**Trigonal**	**P-Monoclinic**	**C-Monoclinic**	**References**
III	II	I		a
α		β		b
γ	α	β		c
C3	C2	C1		d
I		III	II	e
I	II	III	IV	f *

a - (Otsuka *et al.*, 1999; Yoshihashi *et al.*, 2002); b - (Kogan *et al.*, 2007; Lefebvre *et al.*, 1986); c - (Edwards *et al.*, 2001; Fernandes *et al.*, 2007; Florence *et al.*, 2006); d - (Pohlmann *et al.*, 1975); e - (Rustichelli *et al.*, 2000; Tian *et al.*, 2006); f - (Cruz Cabeza *et al.*, 2006; Grzesiak *et al.*, 2003; M. Lang *et al.*, 2002). * Nomenclature used in this thesis.

Table 3.1. Nomenclature of CBZ polymorphs in literature

The molecular arrangement and crystallographic data of CBZ polymorphs are provided in Figure 3.2 and Table 3.2 respectively. It can be

observed from Figure 3.2 that the molecular structure of polymorphs I, II, III and IV are all based on hydrogen bonded dimer motifs showing configurational polymorphism. CBZ molecule has limited conformational flexibility and hence the molecular conformation in form I-IV polymorphs are very close to the gas phase optimised conformation (Florence *et al.*, 2006). Form III is the most stable form at room temperature, but exhibits enantiotropic relationship with form I, with transition temperature in the range of 70 – 80 °C (Upadhyay *et al.*, 2012). Based on lattice energy calculations and computational structural optimization study, the relative stability of CBZ polymorphs at 0 K was predicted to be in the order form III > I > IV > II (Florence *et al.*, 2006). However, another study by Cruz Cabeza *et al*. (2006) has argued that the stability of CBZ polymorphs at 0 K follows the order III ≈ IV > I > II based on a different computational method. In either case, disagreement prevails only in the relative stability of form IV with the rest of them in the order III > I > II.

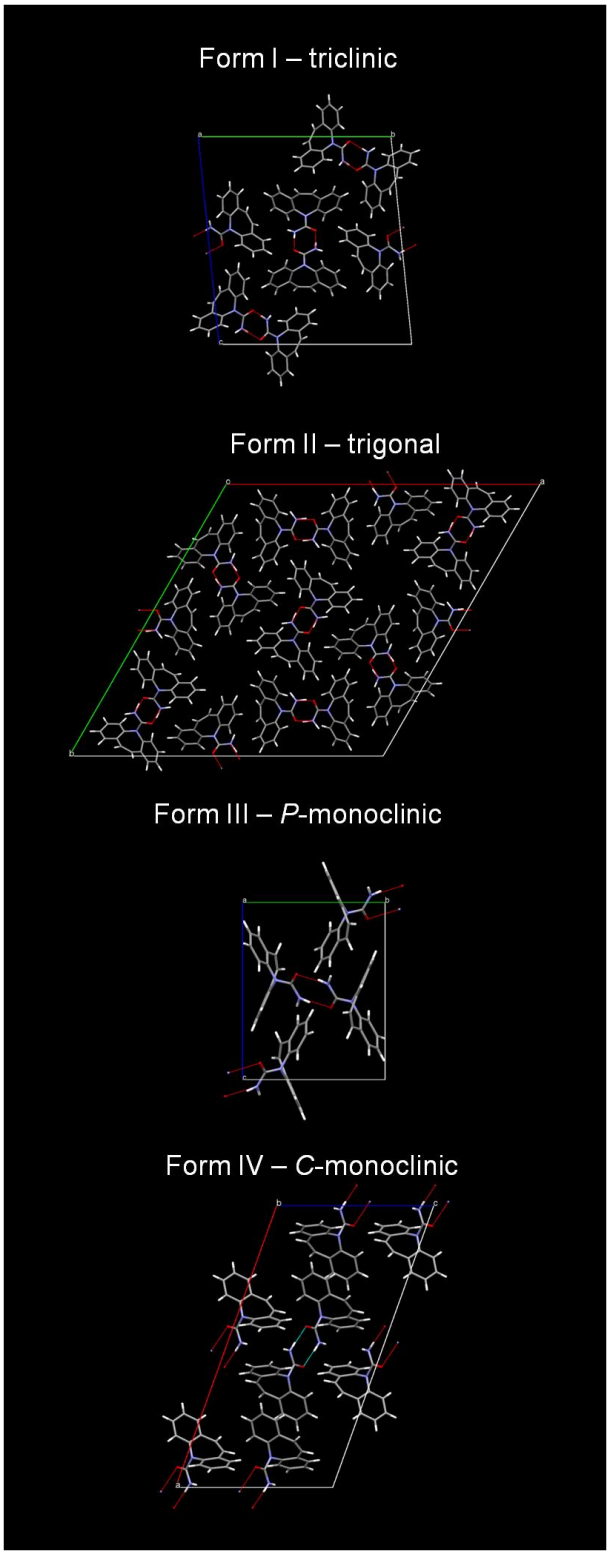

Figure 3.2. Unit cells of four CBZ polymorphs; form I and III viewed along a-axis, form II along c-axis and form IV along b axis (images produced using Materials Studio Visualizer). The red dotted lines in the structure represent hydrogen bonds. Colour scheme: grey = carbon, white = hydrogen, red = oxygen, purple = nitrogen.

	Form I	**Form II**	**Form III**	**Form IV**
Space group	$P\bar{1}$	$R\bar{3}$	$P2_1/n$	$C2/c$
Unit cell dimensions	a = 5.17 Å b = 20.57 Å c = 22.25 Å	a = 35.45 Å b = 35.45 Å c = 5.25 Å	a = 7.53 Å b = 11.15 Å c = 13.92 Å	a = 26.61 Å b = 6.93 Å c = 13.96 Å
Unit cell angles (deg)	α = 84.1 β = 88.0 γ = 85.2	α = 90.0 β = 90.0 γ = 120.0	α = 90.0 β = 92.94 γ = 90.0	α = 90.0 β = 109.7 γ = 90.0
Molecules per unit cell (Z)	8	18	4	8
Crystal habit*	Flat needles	Needles with hexagonal cross section	Prismatic	Plate
Calculated density (g/cm^3)	1.34	1.24	1.35	1.30
CCDC reference	CBMZPN11	CBMZPN03	CBMZPN02	CBMZPN12

Table 3.2. Crystallographic data for CBZ polymorphs (*crystal habit is based on literature)s

Different experimental procedures have been employed by several researchers to produce pure polymorphic forms of CBZ. Being the polymorph with the highest melting point, pure form I is easily produced from melt crystallisation or by holding any of other CBZ crystal forms above 165 °C for a few hours (Upadhyay *et al.*, 2012). Form I can also be produced through crystallisation from solution above 80 °C (Sypek *et al.*, 2012). Form II is obtained through fast crystallisation (rapid supersaturation generation) methods. Cooling crystallisation from toluene is also reported to produce pure form II (Harris *et al.*, 2005). Form III polymorph is produced via cooling or evaporative crystallisation from solvents such as ethanol or iso-propanol (Grzesiak *et al.*, 2003). Form IV polymorph is obtained through evaporative crystallisation from methanol in the presence of hydroxypropyl cellulose or by drying dihydrate form over phosphorous pentoxide at ambient temperature

(Harris *et al.*, 2005; M. Lang *et al.*, 2002). In either case, form IV is obtained only in the presence of additives in crystallising solution. Well characterised polymorphic forms, established crystallisation methods, presence of multiple polymorphic forms which crystallise from same and different solvents make CBZ a suitable model compound for studying template-induced nucleation process.

3.2. Template for crystallisation

Glass surfaces functionalised with alkylsilanes were selected as templates for crystallisation experiments. Silanisation is a well established technique for functionalisation of surface with hydrolysable functional groups (Cras *et al.*, 1999). Glass or silica surfaces when cleaned and hydroxylated exhibit hydroxyl functional groups on the surface. The alkylsilanes with ethoxy or methoxy functional groups react with the hydroxyl groups on the surface and form siloxane bonds, thereby forming chemisorbed layer on such surfaces. This occurs through a two stage reaction. The alkoxy groups of silanes are first hydrolysed by surface water on hydrated glass, followed by the condensation of silanes on to glass surface. Thermal curing after silanisation ensures cross linking of silanes. The schematic representation of the functionalisation reaction and the final structure of cured silane layer are provided in **Figure** 3.3. Different methods for silanisation procedure on glass/ silica surface involving elevated or room temperature from organic, aqueous or vapour phase deposition has been reported (Halliwell & Cass, 2001). In ideal situation, each trialkoxysilane molecule can result in one or two attachments with the glass surface based on availability of surface hydroxyl groups and their spacing. Upon thermal treatment after surface attachment, the

unreacted silanol groups in adjacent silanes can cross link with each other, thereby forming a strong surface-attached layer.

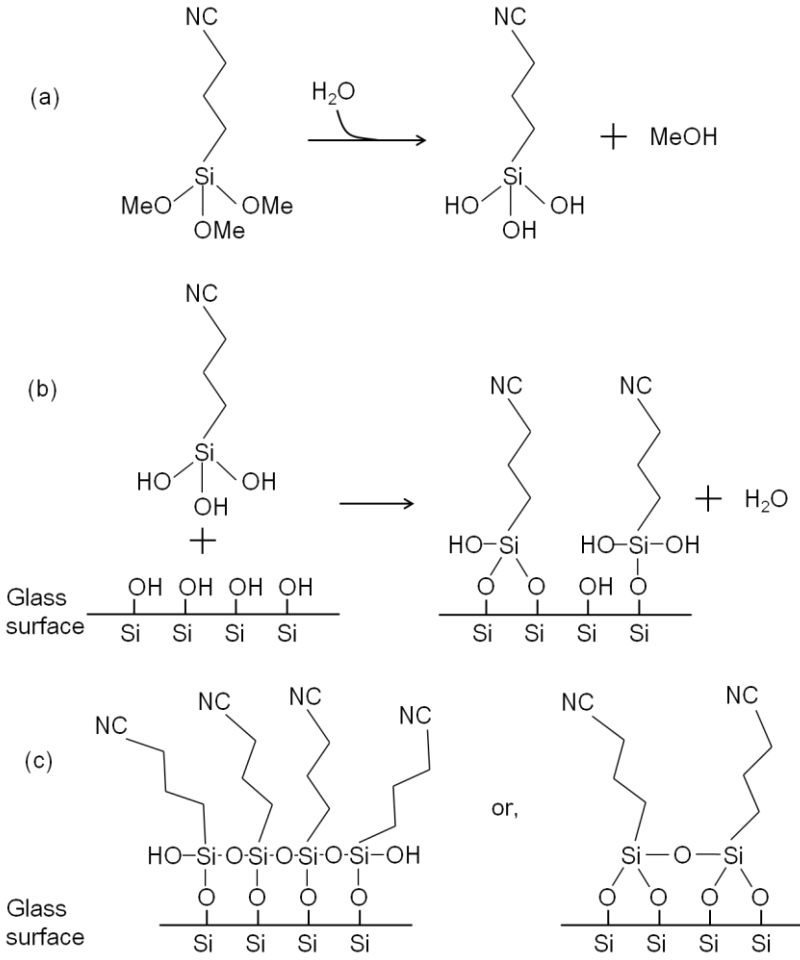

Figure 3.3. Schematic representations of silanisation reaction and final silane structure. a) hydrolysation of alkoxy silane; b) condensation reaction on glass surface; c) ideal structures of silane on glass surface with silanes linked through one or two siloxane linkages to glass.

3.3. Materials

CBZ used for crystallisation experiments at different stages of work were sourced from three suppliers – Sigma-Aldrich, Apollo Scientific and Junda Pharmaceutical Co. Ltd. However, only recrystallised CBZ was used for crystallisation and solubility studies. Ethanol (EtOH), iso-propanol (IPA), toluene (TOL), acetonitrile (ACN) and methanol (MeOH) used for

crystallisation were analytical grade (AnalR NORMAPUR®) reagents procured from VWR Internaltional. Silanes used for the functionalisation were purchased from Sigma-Aldrich and used as received. The silanes are 3-cyanopropyl triethoxy silane (cyano silane), 3-mercaptopropyl trimethoxy silane (mercapto silane) and 3-trifluoropropyl trimethoxy silane (fluoro silane). Structures of the silanes are provided in Figure 3.4.

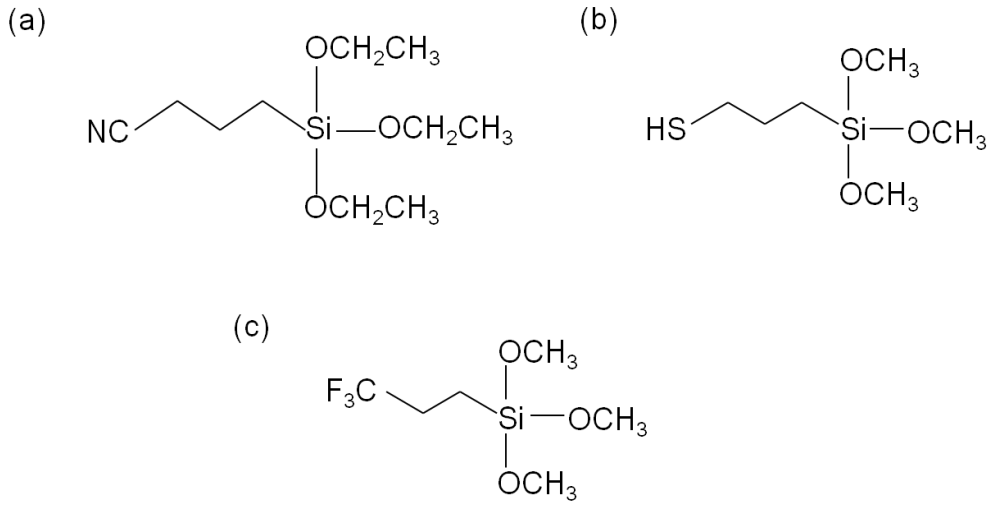

Figure 3.4. Chemical structure of silanes used for surface functionalisation. a) cyano silane, b) mercapto silane, c) fluoro silane.

3.4. Experimental methods

3.4.1. Crystallisation experiments

Crystallisation of CBZ was conducted in functionalised glass vials maintained at required temperature. Initial supersaturation for crystallisation was generated by dissolving required amount of solute in solvent by stirring at higher temperature. This was followed by natural cooling to the crystallisation temperature without stirring. Recrystallised CBZ was used for preparing supersaturated solution to avoid effects of trace impurities present in purchased CBZ. Supersaturated solution was added into glass vials through

0.22 μm filter to avoid particulate impurities. The vials were hermetically sealed to avoid evaporation of solvent. Temperature was maintained at 15, 20 or 25 °C by regulating the temperature of the incubator in which the glass vials were placed for crystallisation.

The inner surface of glass vials form an interface with the crystallising solution and hence act as the template surface for crystallisation. Therefore, the whole inner surface of each vial was functionalised to avoid the effect of multiple surfaces or interfaces in contact with crystallising solution. Ideally, the solution would be in contact with only two interfaces – one with the functionalised vial surface and with the solvent saturated air above the solution in the sealed vial. Functionalised glass cover slips were also used as template surfaces in certain instances to facilitate removal of crystals while attached to surface. In the case of glass cover slips, the templates were placed at the bottom of vials or crystallisation dishes into which the supersaturated solution was poured. The functionalisation method used for both vials and cover slips are the same and is explained in next section.

3.4.2. Template functionalisation

Prior to silanisation, the glass surfaces were cleaned and pretreated to form hydroxyl surface groups to enhance silanisation efficiency. Cleaning involves repeated washing of vials or cover slips with de-ionised water (DI water) and ethanol to remove dust and other organic contaminants from the surface. Surfaces are further cleaned overnight with 5 N nitric acid. This removes any covalently bonded surface impurities and readies the template for hydration process. Acid content from the surface is removed by washing with copious amount of DI water, followed by hydration in boiling water for 4 – 6

hours. During hydration, the surface groups of glass are hydroxylated resulting in silanol (Si – OH) groups. Expression of hydroxyl content on template surface is essential for successful silanisation process (Cras *et al.*, 1999). However, excess water content on surface can inhibit silanisation process and hence vials and cover slips are dried at room temperature after hydration process. All templates including control surfaces (clean glass cover slips) undergo these pretreatment steps while other templates are further functionalised through silanisation process. Liquid phase silanisation is carried out in toluene with 1% silane content. The silanisation solution is poured into the vials and left overnight at room temperature. For cover slips, they are dipped into a silanising solution inside Corning® silanisation jar. Individual slots for each cover slip ensure full surface exposure to solution. After silanisation, the solution is poured out and the vials/ cover slips are washed with toluene and ethanol to remove any excess silane from surface. Templates are then subjected to heat treatment at 80 – 100 °C for 20 – 24 hours to complete surface attachment and cross linking of silanes.

3.4.3. Solubility measurement

Solubilities of form II and form III CBZ crystals in ethanol were measured using the Crystalline system (Avantium, The Netherlands). The apparatus works on the principle of 'clear point' measurement, the temperature at which a suspension with a known concentration of solid turns into a clear solution upon heating. In the case of stable form III polymorph, the clear point temperatures of a slurry suspension of CBZ were determined at various heating rates. By extrapolating the data to zero heating rate, the actual dissolution temperature that is independent of the heating rate was determined.

Solubility of form II CBZ was determined using an adapted bracketing method. In this method, multiple vials with solution samples saturated with a known quantity of the stable crystal form were first prepared and held at 0.25 °C (±0.1 °C) temperature intervals. 5 mg of form II crystals was added to each of the equilibrated solutions. If the initial solution concentration was below the solubility of the metastable form at that particular temperature, the added crystals fully dissolved (typically within 2 – 3 minutes). On the other hand, if the solution concentration was above the solubility limit, the added crystals did not dissolve fully and the excess solid underwent solution mediated transformation to the stable form over a period of time. Among the multiple solution samples, the lowest temperature at which the added form II crystals dissolved completely corresponded to the saturation temperature with respect to the metastable form.

3.5. Characterisation techniques

Crystal growth and polymorphic form of crystals were confirmed using optical microscopy and X-ray diffraction (XRD) techniques. Face indexing of form III CBZ crystal was performed using single crystal XRD analysis. The template surfaces were characterised using contact angle analysis, X-ray photoelectron spectroscopy (XPS) and ellipsometry. The characterisation methods used for these techniques are described in this section.

3.5.1. Optical microscopy

Crystal habit was observed using optical polarized light microscope (Olympus, BX51) and handheld digital USB optical microscope (Veho, VMS-004D). Images from the polarised light microscope were recorded using Soft

Imaging System's *Analysis* software and those from USB optical microscope was captured using Veho's *MicroCapture* software.

3.5.2. X-ray diffraction

Powder X-ray diffraction (PXRD) was used for confirming polymorphs of CBZ. Analysis was performed with a PANalytical X'Pert PRO diffractometer with nickel-filtered Cu α radiation operated at 40 kV and 40 mA. The samples were scanned from 3° to 60° 2θ using a step size of 0.01°.

3.5.3. Single crystal XRD

Crystal face indexing was conducted using Agilent Xcalibur 3E diffractometer at room temperature using graphite monochromatised Mo K α radiation (λ = 0.71073 Å). The crystal facets were indexed with the data analyzed using Agilent Technologies' *CrysAlisPro* software system.

3.5.4. Contact angle goniometry

A Krüss Drop Shape Analyser DSA 10 (Krüss GmbH) was used for the dynamic sessile drop contact angle measurement. Advancing contact angle of three probe liquids (water, formamide, and diiodomethane) were measured at ambient conditions. The shape of the droplet was fitted using the tangent method to obtain the contact angle using the *Drop Shape Analysis* software (DSA version 1.0). A minimum of 5 droplets on 3 different samples of the same surface chemistry were measured. Surface energy of the template surface was then calculated using both Owens-Wendt method and Acid Base calculations proposed by van Oss, Chaudhury and Good (vOCG) (Owens & Wendt, 1969; C. J. Van Oss *et al.*, 1988).

3.5.5. X-ray photoelectron spectroscopy (XPS)

3.5.5.1. Principle of XPS

XPS is a spectroscopic technique that measures elemental composition on a surface based on photoelectric effect. It is also called as Electron Spectroscopy for Chemical Analysis (ESCA). In XPS measurement, X-rays are used to irradiate the sample surface, causing core level electrons from surface atoms with bonding energy lower than the incident X-ray to be emitted. The kinetic energy and number of electrons emitted from the sample are measured and analysed to form the spectrum which consists of electron current density against electron energy. Since the binding energy of emitted electrons is characteristic to each elemental state, the presence of specific elemental states on the surface can be determined from the kinetic energy of emitted electrons using the following relationship.

$$E_B = hv - E_K - \phi \qquad (3.1)$$

where, E_B is the electron binding energy, hv is the energy of the photon (X-ray), E_K is the kinetic energy of the emitted electron and ϕ is the work function of the spectrometer.

With the sensitivity factors applicable to each element, the peak area for each binding energy can be used to find the relative composition of each elemental state. Due to limitations in exciting and capturing electrons from inside the sample, only surface molecules (up to a depth of about 10 nm) are sensitive to this measurement. However, it has to be noted that this technique is not sensitive to hydrogen or helium.

3.5.5.2. Experiment setup

XPS spectra were obtained on all functionalized glass cover slips using a ThermoFisher Scientific Theta Probe X-ray Photoelectron Spectrometer (ThermoFisher Scientific Inc.) with a twin anode AlKα X-ray source ($h\nu$ = 1486.6 eV) at 15 kV x 20 mA (300 W). Survey spectra were collected at pass energy of 100 eV while using 20 eV for high resolution spectra. After removal of the non-linear (Shirley) background, high resolution core level spectra were used for the quantification of the functional end groups present on the surface. Gaussian – Lorentzian product function was used for peak fitting. The high resolution data was fitted using the *Avantage* software (Thermo VG Scientific). The software incorporates sensitivity factors and corrects for the electron energy analyzer transmission function. The sample for analysis is placed on the sample holder which is pushed into the chamber which is maintained at ultra high vacuum (10^{-8} – 10^{-9} mbar) during spectra collection. The X-ray beam when focussed on the template surface has a spatial resolution of about 800 × 600 μm.

3.5.6. Ellipsometry

3.5.6.1. Principle of Ellipsometry

Ellipsometry is an optical characterisation technique that correlates changes in polarisation of light due to interactions (reflection, absorption, transmission and scattering) with a material to the optical properties and thickness of the medium with which the interaction occurred. Polarisation change, constituting amplitude ratio and phase difference, of light reflected or transmitted by a single or multilayered material primarily depend on its refractive index and thickness. By measuring the polarisation change of

reflected light to an incident light of known state (typically linearly polarised light) at different incident angles, refractive index and thickness of the layer(s) can be calculated through parameter optimization and data fitting to a model system. Ellipsometry has also been used to measure roughness, crystalline nature of thin films and doping composition of single or multilayer composites. The sensitivity of the technique for measuring multilayer composites relies on the variation in refractive index between layers. With adequate experiment setup and model development, ellipsometry is suggested to be capable of providing information on molecular layers thinner than the wavelength of the probing light itself, down to atomic length scales (Arwin, 2000).

3.5.6.2. Experiment setup

Ellipsometry is performed to measure the thickness of silane layer formed on template surfaces as a result of silanisation process. However, since the refractive indices of glass and silane layer are very close, this affects the sensitivity of thickness measurement on glass templates. This was overcome by using silicon substrate which has a refractive index of 3.42, significantly different than that of the silane layer (1.45) (Tokumitsu *et al.*, 2002). Silicon wafer produces an oxide layer (SiO_2) on surface through oxidation. The silicon wafer acts similar to a glass surface during silanisation due to the chemical composition of the surface oxide layer. The Si [100] facet is subjected to same silanisation process as explained before and ellipsometry is conducted on this surface. Measurement was conducted on *VASE*® (J. A. Woollam Co., Inc.) ellipsometer and the data was acquired and analysed with the integrated

software *WVASE32*®. The refractive index ($n(\lambda)$) of the silane layer is modelled as a Cauchy layer following the relationship,

$$n(\lambda) = An + \frac{Bn}{\lambda^2} \qquad (3.2)$$

with An and Bn values fixed at 1.45 and 0.01 respectively. Both the oxide layer and silane layer are considered as part of Cauchy layer. The thickness of Cauchy layer is found out through data fitting and silane layer thickness is calculated by subtracting the oxide layer thickness from total thickness. Variable angle of incidence and spectroscopic measurement can optimise the determination of sample parameters. Hence, wavelength range of 900 – 1600 nm and five different incidence angles ranging from 65° to 75° at steps of 2.5° were used to measure polarisation phase change.

Chapter 4

Template Preparation and Characterisation

Functionalised template surfaces were prepared using silanisation procedure and characterised using multiple techniques to confirm functionalisation and surface properties. Based on an initial screening of templates with different surface chemistries for polymorph crystallisation, three functionalised templates were selected for further crystallisation experiments. The functional head groups on the selected templates were cyano (nitrile, -CN), mercapto (thiol, C-SH) and tri-fluoro (-CF_3). (The structure of silane molecules used for these functional groups are provided in Figure 3.4. Henceforth, the three templates would be referred to as cyano, mercapto and fluoro templates. The results from the characterisation of the prepared templates are detailed in this chapter.

Functionalised glass cover slips were characterised using contact angle analysis, X-ray photoelectron spectroscopy (XPS) and ellipsometry. XPS spectra were used to confirm the presence of surface functional groups formed through silanisation while contact angle analysis provided surface energy of the templates in addition to confirmation of functionalisation. The thickness of the functionalisation layer grafted on the template surface was analysed using ellipsometry. Thereby combining the techniques, the surface chemistry, surface energy and thickness of the functionalisation layer on template surface were determined.

4.1. XPS analysis

The surface chemistry of the templates is quantified through XPS analysis on functionalised glass cover slips. XPS is highly surface-sensitive and provides quantitative data on the chemical state of atoms on surface. When the surface is irradiated using X-rays with energy hv, electrons with binding energy (E_B) lesser than the incident rays will be ejected as described by photoelectric effect. The kinetic energy (E_K) of the ejected electrons and the number of ejected electrons are measured using the detector. Using conservation of energy law, the energy of incident photon can be expressed as the sum of spectrometer work function, binding energy and kinetic energy of the ejected electron. Binding energies of the detected electrons are calculated from this relationship (equation 3.1). Electron binding energy of core shell electron of an atom is characteristic to it's chemical state. Hence, the chemical functional groups and their relative amount on surface can be quantified based on the number of electrons with specific binding energy ejected from the surface. The binding energies for chemical states of different atoms relevant to this study are provided in Table 4.1.

Atom (chemical state)	Functional group	Binding Energy (eV)
Carbon (C1s)	$C–H_x$ (methylene)	285.0
	C–Si	284.3
	C≡N, C–O	286.7
	C*–C≡N	286.1
	C–S	285.4
	$C–F_3$	292.6
	C*–C–F3	286.2
Silicon (Si2p)	Si–C	102.3
	Si=O	103.3
Oxygen (O1s)	Si–O–Si	532.5
	C–O–C	531.5
Nitrogen (N1s)	N≡C	399.7
Sulphur (S2p)	S–C	163.6
Fluorine (F1s)	F–C	688.8

Table 4.1. Binding energies of electrons from chemical states of different atoms. (* denotes the carbon atom for which the binding energy is stated)

XPS survey spectra of template surfaces were collected initially to establish the elements present on the surface. The survey spectra for three functionalised templates are provided in Figure 4.1. It can be observed that significant sodium peaks (Na_{1s} and Na_{Auger}) are observed in templates. Sodium peaks in the spectrum could arise from the interaction of X-rays with the glass beneath the functionalisation layer. Hence, contributions from sodium peaks are not taken into consideration for calculating atomic distribution of the functionalisation layer. High resolution spectra for peaks observed in survey

spectra were collected for quantitative analysis of surface functional groups. High resolution scans of relevant peaks on cyano, mercapto and fluoro templates are provided in **Figure** 4.2 to **Figure** 4.4.

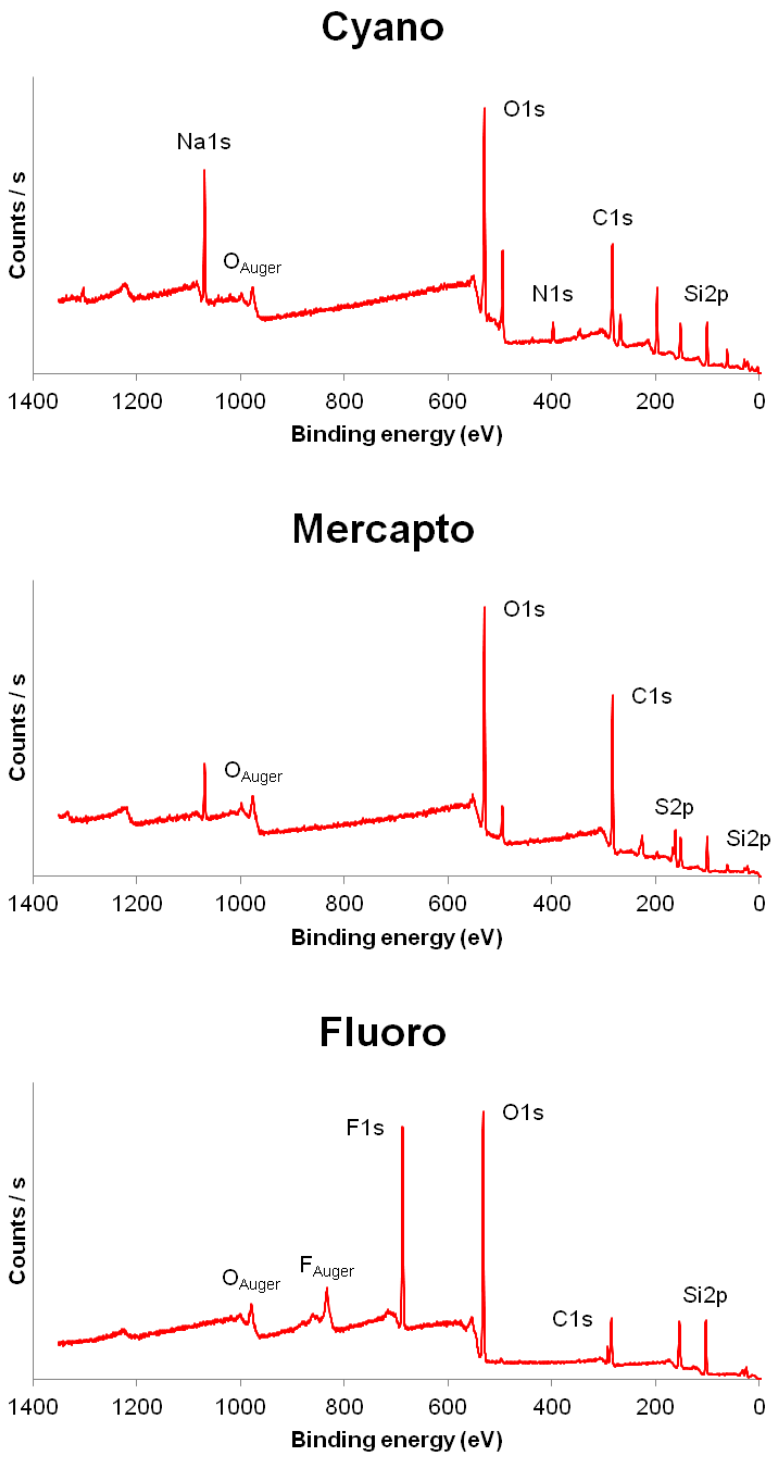

Figure 4.1. XPS survey spectra of functionalised tempaltes.

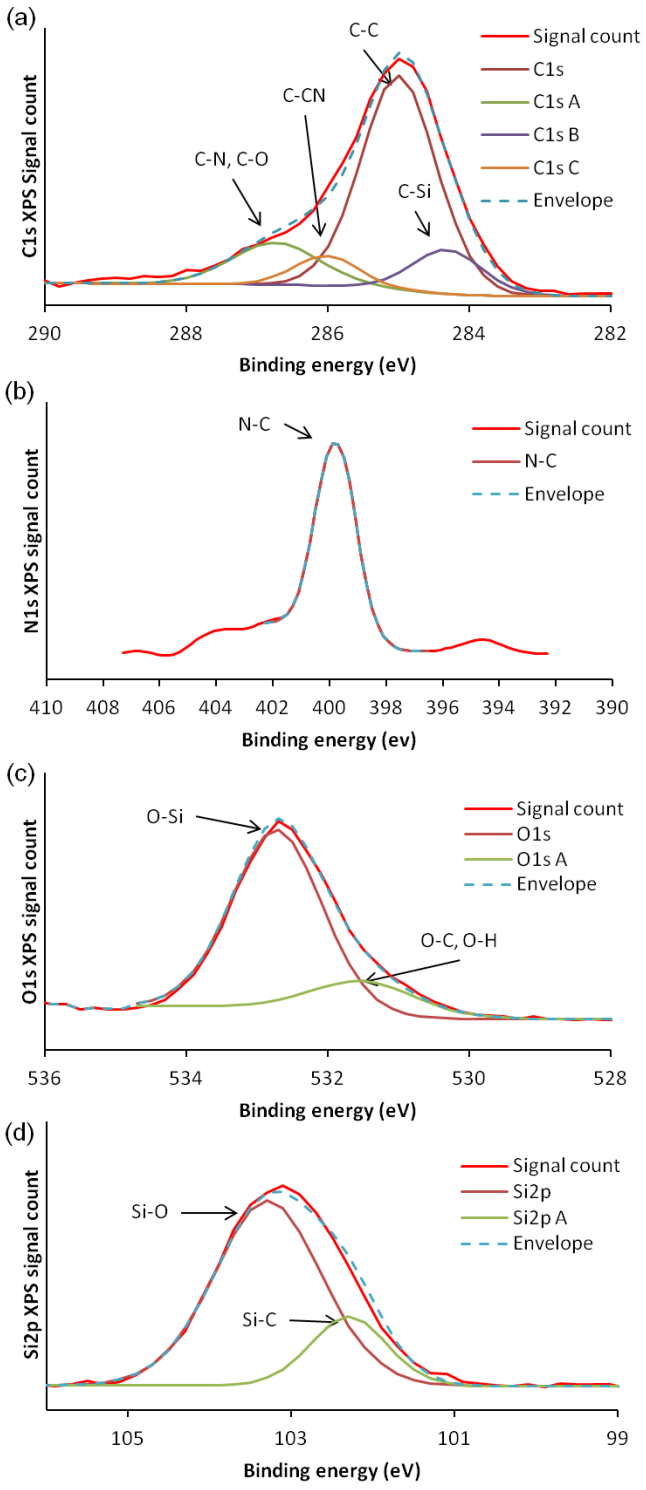

Figure 4.2. High resolution XPS spectra of a) C1s, b) N1s, c) O1s and d) Si2p peaks on cyano template.

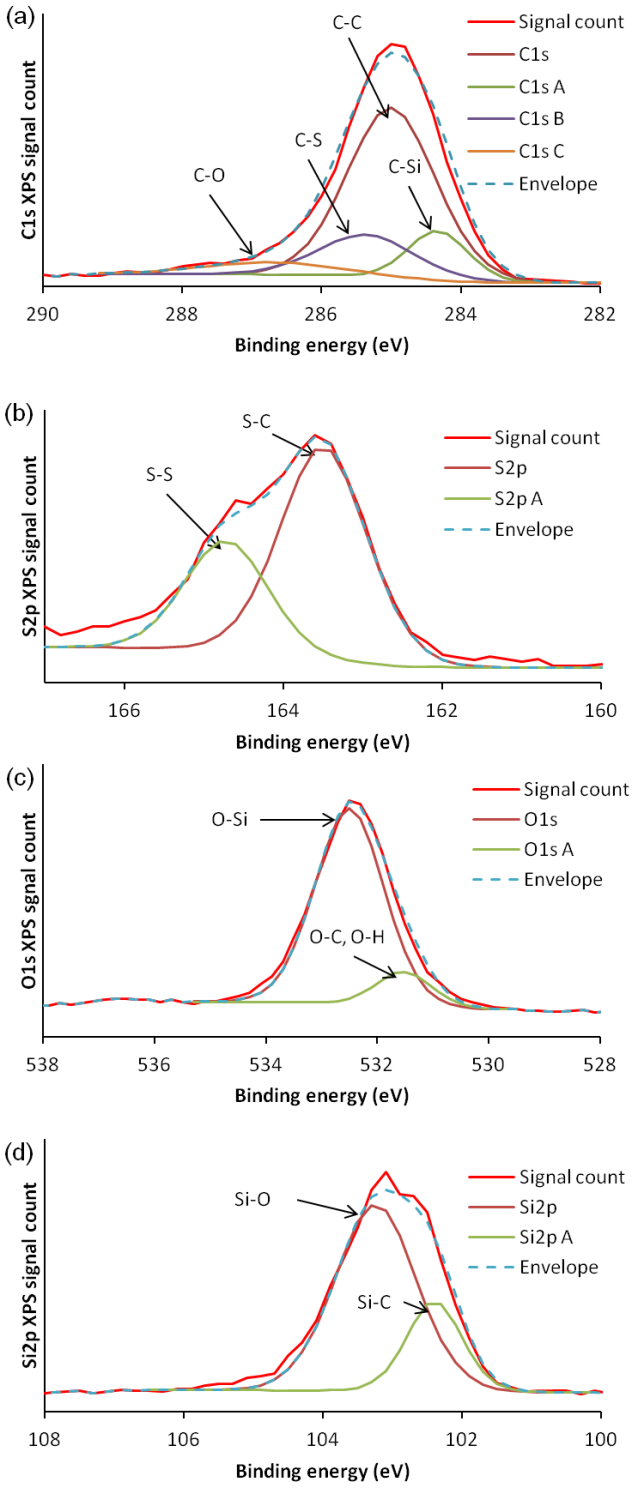

Figure 4.3. High resolution XPS spectra of a) C1s, b) S2p, c) O1s and d) Si2p peaks on mercapto template.

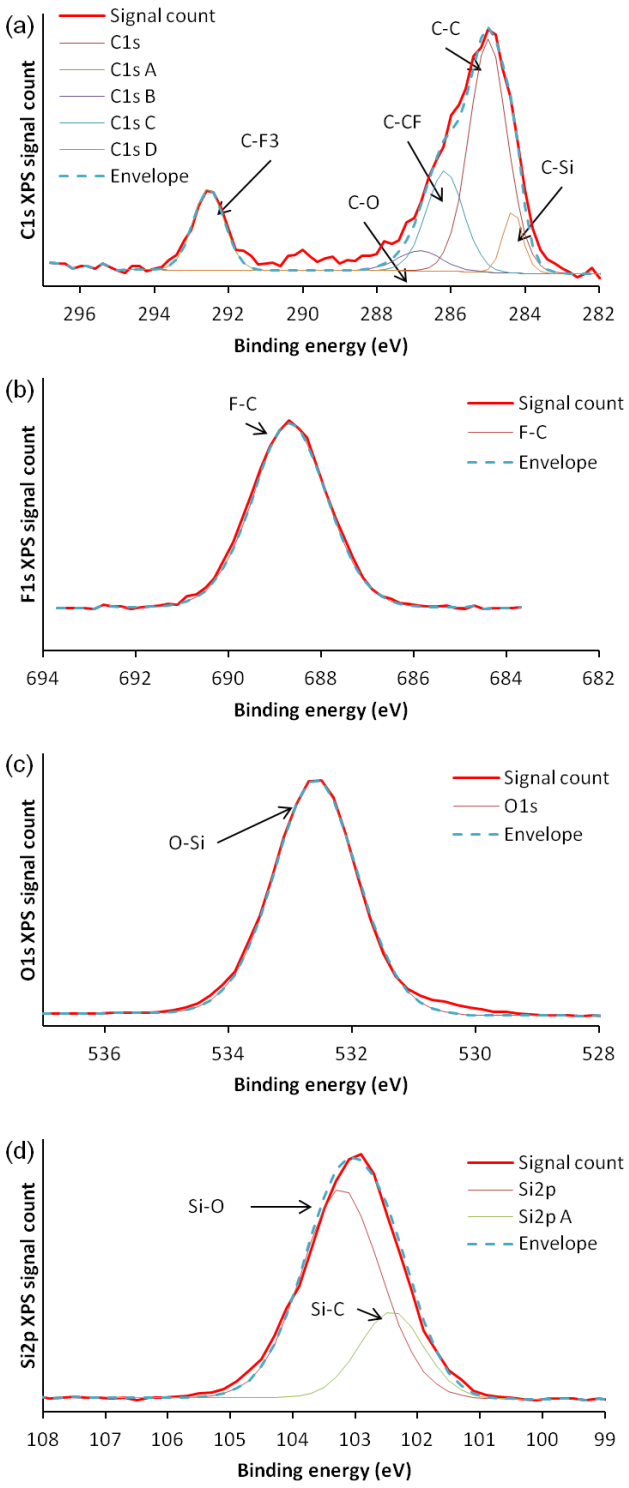

Figure 4.4. High resolution XPS spectra of a) C1s, b) F1s, c) O1s and d) Si2p peaks on fluoro template.

Deconvulated C1s high resolution spectrum on cyano template (Figure 4.2(a)) clearly indicates the presence of C≡N and C-CN bonds on surface with

binding energy peaks at 286.7 and 286.1 eV respectively. Other C1s peaks on cyano surface arise from C-C in the propyl chain and C-Si bond of silane molecules. The N1s peak on cyano template is a single sharp peak corresponding to the N≡C bond in the cyano functional group. Deconvulation of O1s and Si2p spectra shows the presence of multiple chemical states of oxygen and silicon atoms. Two distinct peaks for silicon on surface arise from the siloxane linkages (Si-O-Si) and Si-C bond with the propyl chain of silane molecule.

Similarly, C1s spectrum on mercapto template exhibits binding energy peak for C-S functional group at 285.4 eV along with other peaks corresponding to C-C, C-Si and C-O chemical states. On deconvulating S2p spectrum, it is observed that two peaks occur at 163. 6 eV and 164.8 eV. The peak at 163.6 eV corresponds to the S-C expected from the C-SH functional head group on silane molecule. However, the binding energy peak at 164.8 eV correlates to S-S (disulfide bond) functional group indicating polymerisation reaction of functional C-SH head groups on silanes attached to the surface. By comparing the relative area of S-C and S-S peaks, it is found that 30% of total mercapto functional head groups on silanes have undergone polymerisation to form disulfide bonds. O1s and Si2p spectra of mercapto template are similar to that of cyano template.

C1s spectrum of fluoro template stands out with the binding energy peak at 292.6 eV, characteristic for CF_3 functional group. Such a large shift in binding energy is caused due to the strong electronegative pull of the fluorine atoms attached to carbon (Ferraria *et al.*, 2003). C1s spectrum also exhibits another peak at 286.2 eV corresponding to the carbon atom in the propyl chain

attached to the CF_3 head group. The strong electronegative environment created by the three fluorine atoms is responsible for this chemical shift on the secondary carbon atom. However, unique peak in F1s spectrum indicates a single environment for all fluorine atoms in fluoro template.

The XPS spectra analysis confirms surface functionalisation with binding energy peaks corresponding to different functional groups on each template surface. The atomic composition of templates calculated based on the peak area for each atom is provided in Table 4.2. It is to be noted that the atomic composition of silicon and oxygen is higher than that expected in silanes due to the contribution from glass layer beneath the silane layer.

	Carbon (%)	**Oxygen (%)**	**Silicon (%)**	**Nitrogen (%)**	**Sulphur (%)**	**Fluorine (%)**
Cyano	45.0	35.4	16.3	3.3	-	-
Mercapto	54.3	30.1	10.2	-	5.4	-
Fluoro	31.3	38.1	17.9	-	-	12.7

Table 4.2. Atomic composition on functionalised template surfaces calculated from high resolution XPS spectra

4.2. Contact angle goniometry

Contact angle goniometry was performed on functionalised glass cover slips with three probe liquids. Glass cover slips were selected as sample substrates since flat surfaces enable more accurate contact angle measurement than curved surfaces (such as glass vials). Measurement of contact angle allows the calculation of surface energy of the templates which is a significant factor in determining template interaction with solution. Low surface energy is commonly associated with hydrophobic material with low wettability. Conversely, liquid spreads easily on surfaces with high surface energy.

Contact angle and solid surface energy is related through the Young equation, proposed by Thomas Young in 1805 (Young, 1805). Young equation is written as:

$$\gamma_{SV} = \gamma_{SL} + \gamma_{LV} \cos\theta \qquad (4.1)$$

where γ_{SV}, γ_{SL} and γ_{LV} are the solid-vapour, solid-liquid and liquid-vapour interfacial energies and θ is the contact angle of the liquid on solid surface. The relationship arises from the force balance of a probe liquid droplet on a surface as shown in Figure 4.5.

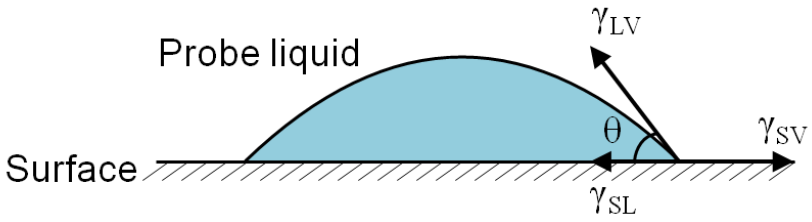

Figure 4.5. Contact angle of probe liquid on a surface.

The solid surface energy can be divided into a number of different components arising from specific type of intermolecular interactions (Fowkes, 1962). Several approaches such as Fowkes' method, Owens-Wendt method, Acid-Base calculations and variations for these methods have been proposed for constructing meaningful surface energy components from contact angle values (Zenkiewicz, 2007). Fowkes method assumes that the surface energy of solid is a sum of independent components and can be expressed as:

$$\gamma_{SV} = \gamma_{SV}^{d} + \gamma_{SV}^{h} + \gamma_{SV}^{p} + \gamma_{SV}^{i} + \gamma_{SV}^{m} \qquad (4.2)$$

where γ_{SV}^{d}, γ_{SV}^{h}, γ_{SV}^{p}, γ_{SV}^{i} and γ_{SV}^{m} are the surface energy components due to dispersive interactions, hydrogen bonding, dipole interactions, induction force and metallic interactions respectively. In the Fowkes approach, the dispersive component is solely due to London forces which exist for all molecules.

Owens and Wendt altered this approach by grouping non-bonding London, Debye and Keesom interaction into single dispersive component and the rest of the terms into one polar component (Owens & Wendt, 1969). Using Berthelot's principle, Owen's-Wendt method provides the following relationship:

$$\gamma_{SL} = \gamma_{SV} + \gamma_{LV} - 2\sqrt{\gamma_{SV}^{d}\gamma_{LV}^{d}} - 2\sqrt{\gamma_{SV}^{p}\gamma_{LV}^{p}} \quad (4.3)$$

By combining Young's equation with equation 4.3, solid surface energy and contact angle are related by the equation,

$$\frac{(1+cos\theta)\gamma_{LV}}{2\sqrt{\gamma_{LV}^{d}}} = \sqrt{\gamma_{SV}^{p}} \times \sqrt{\frac{\gamma_{LV}^{p}}{\gamma_{LV}^{d}}} + \sqrt{\gamma_{SV}^{d}} \quad (4.4)$$

When $\frac{(1+cos\theta)\gamma_{LV}}{2\sqrt{\gamma_{LV}^{d}}}$ is plotted against $\sqrt{\frac{\gamma_{LV}^{p}}{\gamma_{LV}^{d}}}$, square of the intercept provides the solid dispersive energy and square of the slope provides polar surface energy of the solid phase.

Another approach in determining components of surface energy was proposed by van Oss, Chaudhury and Good by dividing surface energy in long range interactions involving Lifshitz-van der Waals component (γ^{LW}) (consisting of London, Keesom and Debye interactions) and short range interactions termed acid-base component (γ^{AB}) (Carel J. Van Oss *et al.*, 1988; Van Oss *et al.*, 1986). Acid-base component is further divided into acidic (γ^{+}) and basic (γ^{-}) constituents and related by the equation,

$$\gamma^{AB} = 2\sqrt{\gamma^{+}\gamma^{-}} \quad (4.5)$$

The interfacial interactions can then be written as,

$$\gamma_{SL} = \gamma_{SV} + \gamma_{LV} - 2\sqrt{\gamma_{SV}^{LW}\gamma_{LV}^{LW}} - 2\sqrt{\gamma_{SV}^{+}\gamma_{LV}^{-}} - 2\sqrt{\gamma_{SV}^{-}\gamma_{LV}^{+}} \quad (4.6)$$

By combining equation 4.6 with Young's equation, the surface energy and contact angle relationship as per acid-base approach can be written as,

$$\gamma_{LV}(1 + cos\theta) = 2\sqrt{\gamma_{SV}^{LW}\gamma_{LV}^{LW}} + 2\sqrt{\gamma_{SV}^{+}\gamma_{LV}^{-}} + 2\sqrt{\gamma_{SV}^{-}\gamma_{LV}^{+}} \qquad (4.7)$$

If contact angle of three probe liquids with at least two having polar components are known, surface energy of a solid surface can be calculated using both Owens-Wendt (OW) and acid-base (vOCG) approaches. The surface tensions of probe liquids required for these calculations are provided in Table 4.3. Advancing contact angle of the probe liquids on template surfaces are provided in Table 4.4.

Solvent	**vOCG approach**				**OW approach**		
	γ_{LV}^{LW}	γ_{LV}^{+}	γ_{LV}^{-}	γ_{LV}	γ_{LV}^{d}	γ_{LV}^{p}	γ_{LV}
Water	26.2	48.5	11.1	72.8	21.8	51.0	72.8
Diiodomethane	50.8	0.0	0.0	50.8	50.8	0.0	50.8
Formamide	35.5	11.3	11.3	58.0	39.0	19.0	58.0

Table 4.3. Surface energy values of probe liquids in mJ/m^2.[vOCG approach solvent energy values (Della Volpe *et al.*, 2004), OW approach solvent energy values (Volpe & Siboni, 1997)]

	Cyano	**Mercapto**	**Fluoro**
Water	55.2 ± 1.7	74.9 ± 2.7	96.4 ± 3.2
Diiodomethane	35.3 ± 3.4	36.4 ± 2.2	74.3 ± 2.4
Formamide	38.8 ± 2.1	58.1 ± 1.3	83.0 ± 1.8

Table 4.4. Advancing contact angle (°) of probe liquids on template surfaces.

Advancing contact angles of probe liquids on templates were utilised to calculate surface energy of templates using both OW and vOCG approaches. Surface energy values computed through both methods are provided in Table 4.5. Surface energy values reveal that, among the three template chemistries, cyano functional group results in surfaces with the highest energy while fluoro functional groups results in least surface energy. Dispersive surface energy component of cyano and mercapto functionalised templates calculated through OW method are similar with a negligible difference of 0.4 mJ/m^2. Similar result is also observed in the Lifshitz-van der Waals component in vOCG method which represents dispersive interaction. However, the polar surface energy component (OW method) of mercapto template is about a third of cyano template which results in lower total surface energy for mercapto template compared to cyano template. In comparison with cyano template, the total surface energy of fluoro template is less than half. The dispersive component of fluoro surface is about half that of both cyano and mercapto templates. However, the polar component of fluoro surface is comparable with that of mercapto template. The trends are similar irrespective of the calculation methods employed in this study.

Functional head group	**OW approach**			**vOCG approach**			
	γ_S^d	γ_S^p	γ_S	γ_S^{LW}	γ_S^+	γ_S^-	γ_S
Cyano (-CN)	38.0	14.2	52.2	41.9	0.7	9.3	47.0
Mercapto (-SH)	37.6	5.0	42.6	41.4	0.0	3.7	41.4
Fluoro (-CF_3)	19.2	2.5	21.7	20.5	0.4	1.0	21.8

Table 4.5. Surface energy of templates calculated using Owens-Wendt (OW) approach and acid-base (vOCG) approach (values in mJ/m^2).

It is to be acknowledged that the contact angle values on the control templates (clean glass surface) were not used for calculating their surface energy value. The probe liquids, specifically water wets the control surface completely resulting in very low contact angle values below 8 °. The accuracy of the image fitting methodology used for establishing the contact angle values using the software used in this analysis is arguable. In addition, due to the very low contact angle of water, the needle used for liquid injection to the advancing droplet interferes with the droplet shape, thus further affecting the results. Hence the surface energy values of the control templates are not computed in this section. From available references, clean glass surfaces are expected to have hydroxyl groups on the surface and exhibit high surface energy value >70 mJ/m^2 as reported by Yongan Peter (2007) or 150-300 mJ/m^2 as reported by Fisher (1948), specifically high polar surface energy component.

Another aspect of the contact angle analysis that is to be discussed is the seemingly lower contact angle of fluoro functionalised template surface. Very high contact angle of water in the range of about 120 ° has been reported with fluorinated layer (Zisman, 1964). Low contact angle values could be attributed to patchy or incomplete surface coverage of the silane. Nonetheless, it is to be noted that such high values are reported in studies involving highly ordered SAMs with high fluorine content. However, the functional layer in our experiments consists of trifluoropropyl trimethoxy silane and the functionalised layer is not expected to be orderly packed when compared to that of SAM surfaces. Also, contact angle values in the range of 90 ° have been reported specifically with this silane (Owen & Williams, 1991;

Thomason, 2009). Hence it would be unable to conclude if the fluorinated surface layer is patchy from the obtained contact angle value.

To sum up the results of surface energy calculation from advancing contact angle data, the total surface energy of the template are in the order cyano > mercapto > fluoro. In case of dispersive component, the templates follow the order cyano ≈ mercapto > fluoro. For polar surface energy component, the order is cyano > mercapto ≈ fluoro.

4.3. Spectroscopic ellipsometry

Spectroscopic ellipsometry was used to find out the thickness of the silane layer attached to the template surface through functionalisation procedure. The technique measures the polarisation state of the light reflected from the template surface with thin silane layer. The polarisation state is characterised by two parameters: phase difference, Δ and amplitude component, Ψ. Δ and Ψ values of the reflected light were measured for five different angle of incidences (65°, 67.5°, 70°, 72.5° and 75°) in the wavelength range of 900-1600 nm[1]. The Δ and Ψ values are related to the optical constant (refractive index, n(λ)) and thickness of the layer through mathematical models. Based on initial guess values for refractive index and layer thickness, the best fitting model prediction with the least mean-squared error is found through iterative procedure. The optimised value for refractive index and layer thickness provide the properties of the surface layer.

[1] The optical fibre used in the instrument for coupling light beam between optical elements has strong absorption band around 1340-1450 nm. Hence, this wavelength region is avoided for the spectroscopic measurement (*WVASE32* User Guide).

The measured Δ and Ψ values as well as the best model predictions with the least mean-squared errors are plotted in Figure 4.6. Based on the best fitting models, the silane layer thickness is found to be 1.37 ± 0.03 nm. In comparison, the length of a stretched out silane molecule used in this study is about 7 Å. This leads to approximately 2 – 3 layers of silane molecules in the functionalised layer, depending on the molecular orientation on surface. Accordingly, the silane layer attached to the template surface through functionalisation method employed in this study is found to be consisting of multilayer silane molecules. A schematic representation of some of the physically possible configurations of cross-linked silanes is illustrated in Figure 4.7.

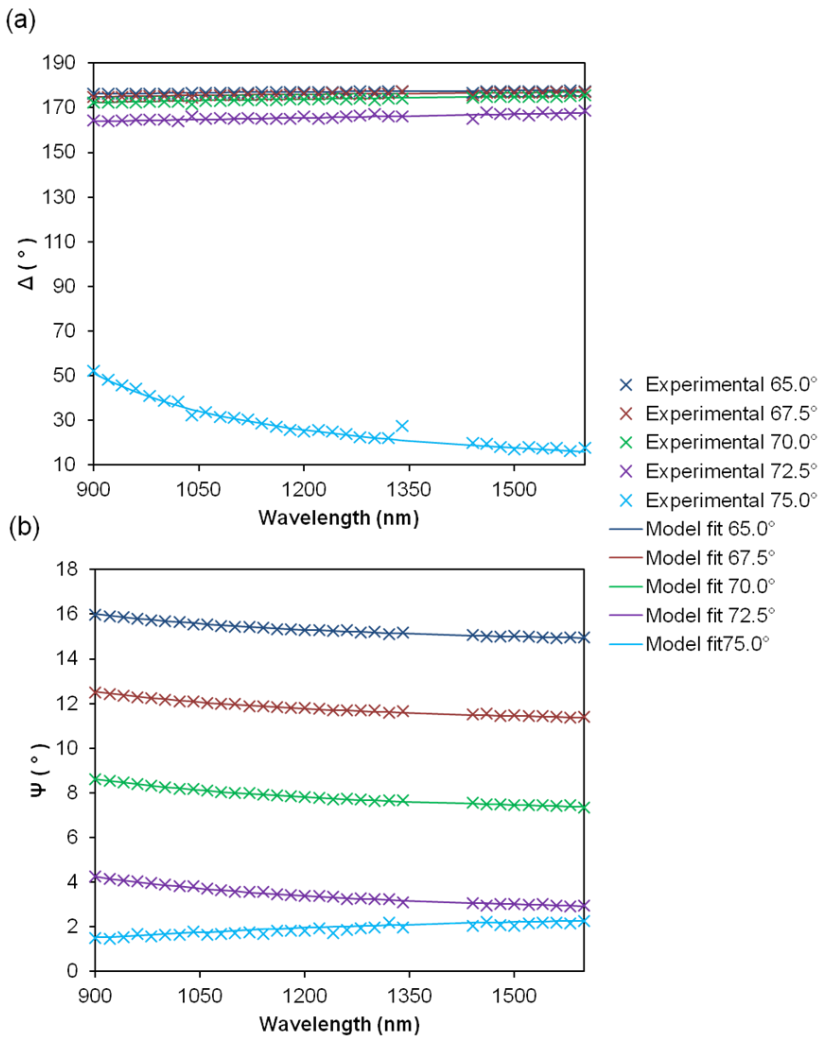

Figure 4.6. Experimental and model predicted data for spectroscopic ellipsometry for five incident angles

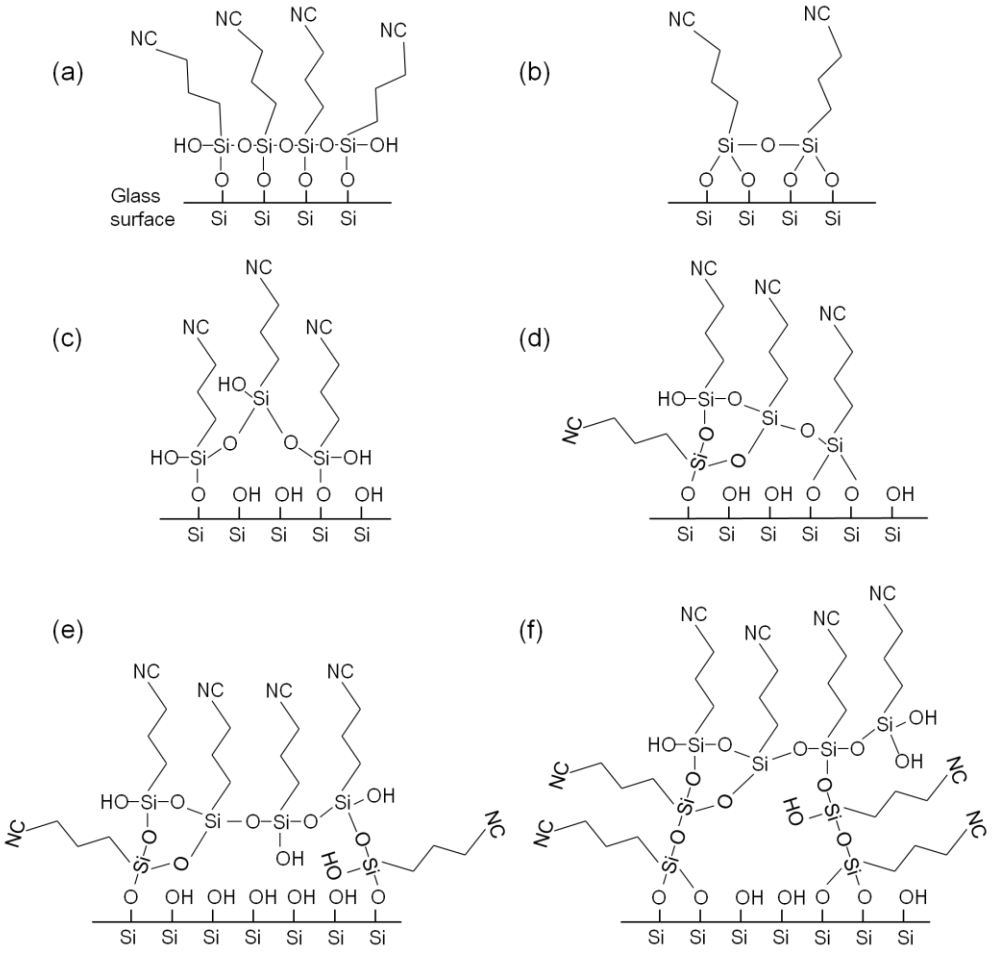

Figure 4.7. Schematic representation of cross-linked silane molecules on template surfaces, depicted using cyano silane; a) & b) represent uniform monolayer configuration, c-f) represents possible configurations that will lead to multilayer thickness of the functionalisation layer.

4.4. Summary

The results from template characterisation confirmed that the silanisation method used in this study was able to alter the surface properties of the glass substrates. XPS analysis established the changes in surface chemistry of the new templates depending on the silane used for functionalisation. Cyano, mercapto and fluoro templates exhibited the presence of respective functional groups as expected. However, XPS result also highlighted the disulfide cross linking that occurred in mercapto

functionalised templates. Almost a third of the silane head groups in mercapto template had undergone cross linking under the conditions used in this study. Changes to the surface energy of the templates caused due to difference in functional groups were studied using contact angle goniometry. The surface energy values revealed that the cyano functionalised templates had the highest total surface energy, followed by mercapto and fluoro templates respectively. Also, mercapto and fluoro templates have similar polar energy component. Spectroscopic ellipsometry showed that the surface layer formed through silanisation process has multilayer composition, with 2–3 monolayer thickness. Thus, surface characterisation results confirmed surface functionalisation and established the properties of the template surface.

Chapter 5

Template-induced Crystallisation

Template-induced crystallisation of CBZ polymorphs was initially conducted from ethanol solution. Crystallisations were performed in functionalised glass vials as well as in clean glass vials, the latter being the control experiments. Experiments were performed from various initial supersaturation values at three different temperatures. The functionalised vial surfaces acted as the templates for heterogeneous nucleation and the crystallisation was monitored using optical microscopy. CBZ crystal polymorphism was confirmed using X-ray diffraction. Template-induced nucleation was further conducted from different solvents to analyse the effect of solvents in the process. The results from these experiments are outlined and discussed in this chapter.

5.1. Identification of CBZ polymorphs

CBZ polymorphs are identified using the powder X-ray diffraction. Theoretical PXRD patterns of CBZ polymorphs are predicted using powder pattern prediction tool in *Reflex* module of *Materials Studio*. Crystallisation of CBZ from organic solvents used in this study only provided form II and form III crystals. Form II crystals were produced by fast cooling of saturated ethanol CBZ solution from 65 °C to 4 °C. Form II crystals were physically separated from form III crystals based on crystal morphology. Morphologically, form II crystals are needles with high aspect ratio while form III crystals are prismatic as shown in microscope images in Figure 5.1.

Pure form III crystals were prepared by cooling saturated ethanol solution of CBZ from 60 °C to room temperature (*ca*. 20 °C). Since form III CBZ is the most stable polymorph at these conditions, the solution was stirred for 2 hrs at room temperature to ensure form III purity through solution mediated transformation. The crystals of both forms were filtered, dried at 55 °C and powdered using mortar and pestle before XRD pattern of the powders were recorded. Theoretically predicted and measured PXRD patterns are provided in Figure 5.2.

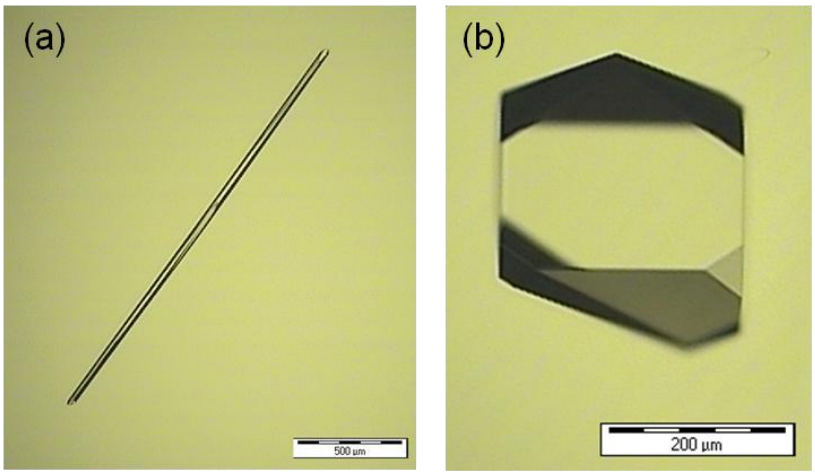

Figure 5.1. Crystal morphology of a) form II and b) form III CBZ crystals in ethanol.

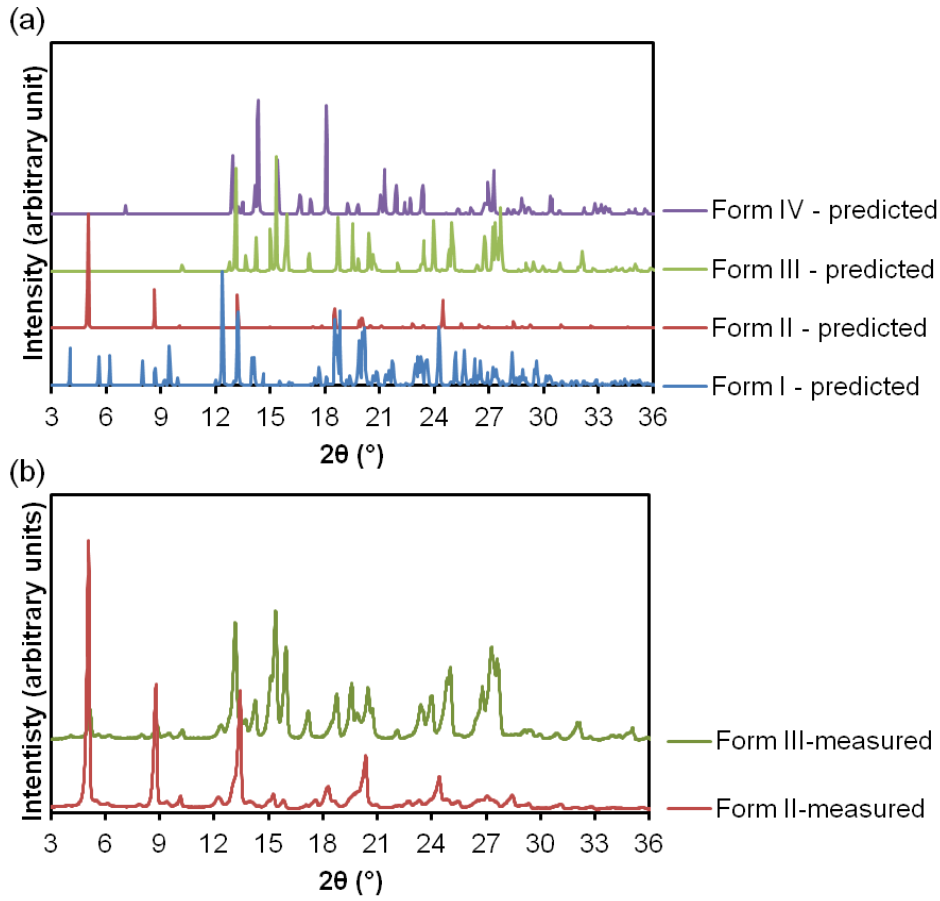

Figure 5.2. PXRD pattern of CBZ polymorphs; a) theoretical prediction for forms I-IV polymorphs, b) measured pattern for form II and form III polymorphs.

5.2. CBZ polymorph solubility

Crystal polymorphs exhibit different solubility in solvents due to differences in lattice free energy associated with polymorphic structures. Crystal solubility of the stable form can be found by allowing solvent to attain equilibrium with excess of solid crystals and measuring the solute concentration via methods such as gravimetric analysis, UV-vis spectroscopy, liquid chromatography, titration or solution density (O'Mahony *et al.*, 2013). Solubility could also be established by finding cloud point or clear point of solute-solvent mixture as used in this study (section 3.4.3). Cloud point in this

context refers to the condition at which the solid material first appears in a crystallising solution where the driving force is created by changing a variable such as temperature. Conversely, clear point refers to the condition at which the solid content disappears completely when the solution slurry is mixed continuously along with heating to dissolve the content. Since the solid content in solution is generally observed using light transmission measurements, at cloud point the transmissivity drops from 100 % while at clear point transmissivity reaches 100 %. However, cloud point and clear point depends on the rate of heating or cooling. Assuming linear dependency with rate of temperature change, the cloud and clear points at zero rate of heating can be determined by finding the values at different heating rates and extrapolating the results to zero heating rate. This approach is used in the present study to avoid the impact of heating rate in measuring clear point of CBZ form III in ethanol. The clear points of form III crystal slurry at different concentrations in ethanol for various heating rates and the resulting straight line curve used for solubility measurement is depicted in Figure 5.3.

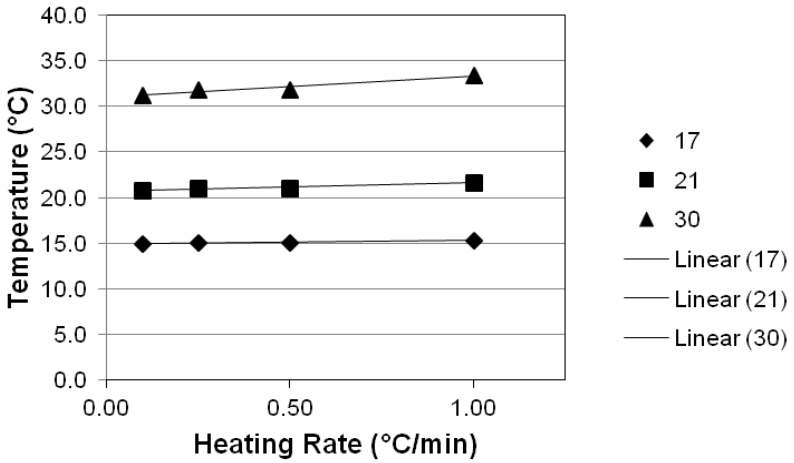

Figure 5.3: Clear points (°) of three concentrations (17, 21 and 30 mg/ml) of form III CBZ slurry in ethanol at four heating rates (1, 0.5, 0.25 and 0.1 °C/min)

Although solubility measurement of stable form crystals is routine and straightforward, solubility of metastable polymorphs are difficult to establish due to solution mediated polymorphic transformation of metastable polymorphs to stable polymorph (O'Mahony *et al.*, 2013). Modified bracketing method for clear point determination was adopted for form II solubility measurement. The procedure involved preparation of CBZ-ethanol solution with form III CBZ at concentration around the solubility of form III crystals. The required amount of CBZ form III crystals were added to 5 ml of solution in glass vials, stirred and heated to dissolve followed by cooling down to specific temperatures. A series of solutions with the same concentration is equilibrated at different temperatures (0.25 °C intervals) below the equilibrium temperature for form III crystals. After equilibration, a small amount (5 mg) of metastable form II was added to each vial. Depending on the solubility of form II crystals, the added crystals either dissolved in a few minutes or grew in the solution. The lowest temperature at which the crystals dissolved was taken as the equilibrium temperature for form II crystals at that concentration.

The solubility curves of forms II (metastable) and III (stable) CBZ polymorphs in ethanol are shown in Figure 5.4. Form III solubility measured in this work shows good agreement with previously reported data (O'Mahony *et al.*, 2013). In the temperature range from 8 to 32 °C, form II solubility is higher than form III solubility with a trend indicating monotropic relationship between the two polymorphs as suggested in literature (Grzesiak *et al.*, 2003). The average solubility ratio of form II and form III in this temperature range is found to be 1.1. This translates to a relatively small (~10%) deviation in the

supersaturation driving force for the two polymorphs in the concentration range used. Hence, in the ensuing sections, the supersaturation values are reported based on form III solubility.

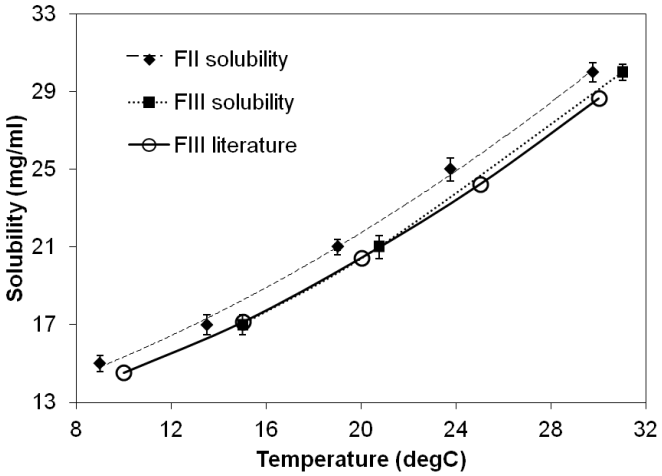

Figure 5.4. Solubility of CBZ polymorphs in ethanol.

Solubility of form III CBZ in acetonitrile, methanol and isopropanol are published in literature (Liu *et al.*, 2008; O'Mahony *et al.*, 2014). However, form III solubility in toluene is not reported and was hence measured. CBZ has very low solubility (<5mg/ml) in toluene and consequently the solubility measurement using transmissivity method described earlier is more prone to experimental errors. Conventional gravimetric technique was used to calculate the equilibrium solubility of form III CBZ in toluene. Pure form III crystals were equilibrated in toluene at specific temperatures in the presence of excess crystals. Fixed amount of clear supernatant liquid was then drawn into a pre-weighed vial and the weight of CBZ after solvent evaporation was measured. The measured solubility of form III CBZ in toluene is provided in Figure 5.5.

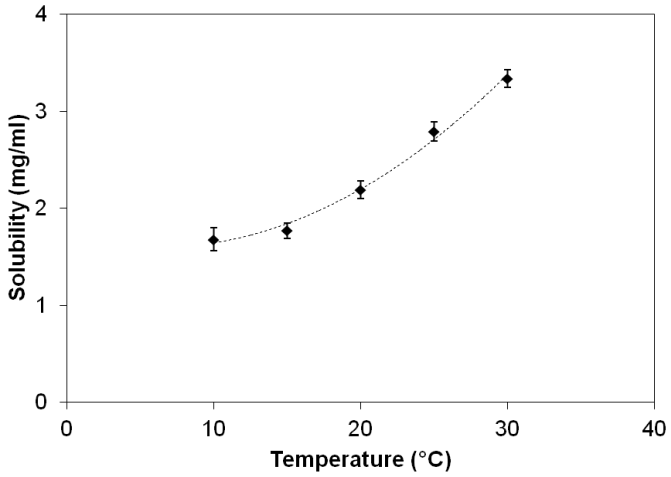

Figure 5.5. CBZ form III solubility in toluene.

5.3. Template-induced nucleation

Crystallisation of CBZ from ethanol (EtOH) was initially conducted in silanised glass vials with different surface chemistries exhibiting, amino (3-aminopropyl trimethoxy silane), cyano (3-cyanopropyl triethoxy silane), fluoro (3-trifluoropropyl trimethoxy silane and perfluorooctyl triethoxy silane), methyl (ethyl trimethoxy silane), mercapto (3-mercaptopropyl trimethoxy silane) and phenyl (triethoxyphenyl silane) functional head groups. In addition to the silanised vials, clean glass vials without silanes were also used for crystallisation as control substrates. However, initial screening results suggested that only templates with cyano, fluoro and mercapto functional head groups showed significant differences in polymorphic nucleation of CBZ under the conditions used. Hence, only templates with these three functional groups were used in further template induced crystallisation experiments as well as detailed template characterisations.[2] Supersaturation was generated by

[2] In case of fluoro template, only trifluoropropyl trimethoxy silane was used for template preparation since the perfluorooctyl triethoxy silane resulted in frequent self polymerisation and hampered the functionalisation procedure.

cooling EtOH-CBZ solution with 60 mg/ml concentration, dissolved at higher temperature (60–70 °C). The crystallisation temperature was maintained at 20 °C. Evaporation of solvent during crystallisation was prevented by sealing glass vials. Solvent evaporation at three phase contact line is known to nucleate metastable polymorphs and could interfere with the expected template-induced nucleation process (Capes & Cameron, 2007; Poornachary *et al.*, 2013). Crystal nucleation and growth in vials were monitored using handheld USB microscope and the time when the first crystals were observed was recorded. The time delay from the start of the crystallisation process to the observation of the first crystal is taken as the induction time of the experiment. Crystallisation in vials was found to be influenced by the surface chemistry of the vial in which crystallisation occurred. The influence was observed in terms of crystal polymorphism, induction time and number of crystals obtained. The results are discussed further in the following sections.

5.3.1. Template effect on Crystal polymorphism

In control vials, upon crystallisation from an initial concentration of 60 mg/ml, both form II and form III polymorphs were observed simultaneously, suggesting concomitant nucleation. Meanwhile, crystallisation in cyano functionalised vials resulted in form II crystals while mercapto and fluoro templates resulted in more of form III crystals than form II crystals. In control, mercapto and fluoro templates, the metastable form II crystals underwent solution mediated transformation into stable form III crystals within a time span of about 24 hours. However, in cyano functionalised templates the form II crystals did not undergo any apparent transformation to form III crystals in the same period. Form II crystals could be stabilised in solution in complete

absence of stable form nuclei arresting any possible solution mediated transformation. Lack of apparent transformation could also occur in case of too few form III crystals which will limit the overall solution mediated transformation rate. On cyano functionalised template, nucleation of form III could be limited as preferential nucleation of form II crystals occurs and their growth reduces the solution supersaturation, further reducing the thermodynamic driving force for form III nucleation. This could be the reason for form II stabilisation in cyano functionalised vials within the observed duration.

The results indicate that with the initial concentration used in this study, control vials with hydroxyl groups do not show preferential nucleation of either form II or form III crystal, resulting in concomitant nucleation at this supersaturation. However, cyano templates show strong preferential nucleation of form II crystals. Mercapto and fluoro templates on the other hand promote form III nucleation although form II nucleation is not completely suppressed. Images of early stage crystals and crystals growing in vials 24 hours from the start of crystallisation on different templates are shown in Figure 5.6 and Figure 5.7 respectively.

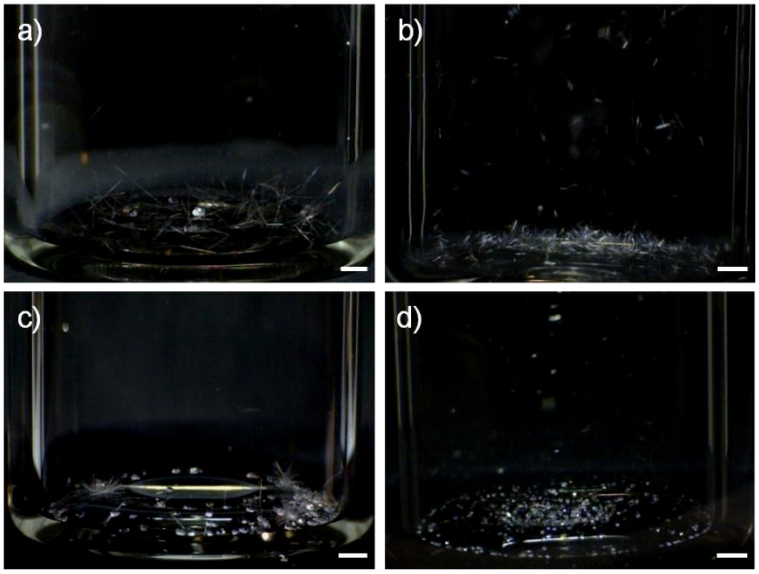

Figure 5.6: Images of crystals during early stages of crystallisation on a) control, b) cyano, c) fluoro and d) mercapto functionalised vials. Scale bars denote 1 mm.

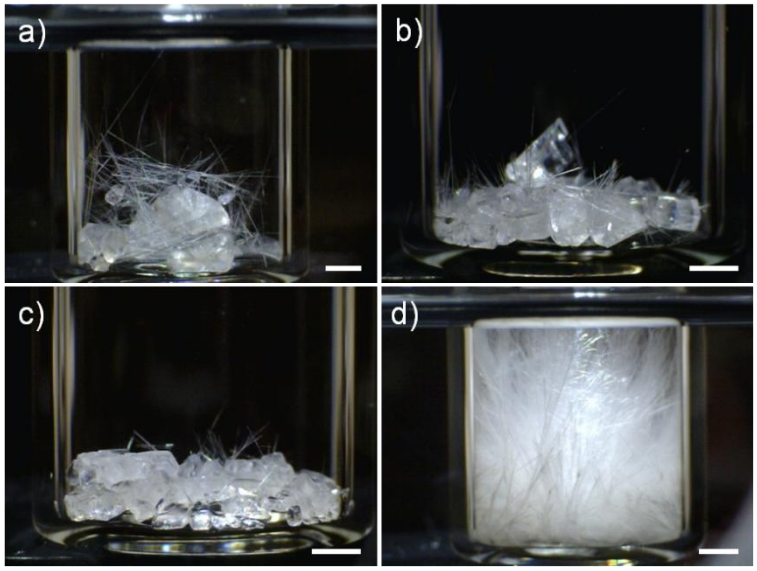

Figure 5.7. CBZ crystals grown from ethanol solution at 60 mg/ml initial concentration in a) control vial, b) mercapto, c) fluoro and d) cyano functionalised vials after 24 hours. Scale bars denote 1 mm.

Surface energy analysis of the template surfaces (chapter 4) has shown that the templates showed significant variation in total surface energy as well as polar surface energy components. Cyano functionalised templates have the

highest polar component while mercapto and fluoro templates showed similar low polar component. The similarity in the polymorph nucleation behaviour on mercapto and fluoro templates as well as the difference with that on cyano template points out that the polar surface energy component could be a decisive factor in preferential nucleation. If so, template-induced nucleation of form III crystals could be favoured by the low polarity of the template surface. On similar lines, it could be considered that the high polarity of cyano functionalised template could be the significant factor that results in preferential nucleation of form II on cyano templates. High polar interfacial energy component of polymer substrates have also been reported to promote oriented crystal growth of aspirin (Diao *et al.*, 2011c). However, surface polarity of the templates cannot be the single decisive factor that influences preferential nucleation of polymorphs. The control template which exhibited concomitant nucleation is more polar (Schakenraad *et al.*, 1986) than cyano template due to the presence of hydroxyl groups. Hence, along with the polarity variations, differences in the chemical nature of the functional groups on template surfaces such as their hydrogen bonding donor or acceptor properties and electronegativity, and the presence of surface charges could all play significant roles in preferential nucleation on templates. Nonetheless, impact of competing template–solute, template–solvent and solvent–solute interactions will have to be assessed for generating a complete picture of template-induced nucleation process.

5.3.2. Template effect on Induction time and Number of crystals

The time when the first crystals were observed in vials using optical microscope was recorded as the induction time. The size of the crystals

recorded for induction time measurements were typically less than 10 μm. Hence, the induction time reported here would include the nucleation induction time as well as the growth time for the stable nucleus to grow to the observed size. Even with this limitation, significant variation in induction time measurement is observed between control and functionalised vials. In control vials, the first crystals were observed after about 2 hours from the start of crystallisation. However, in functionalised vials, the average induction time was roughly in the range of 30 to 50 minutes, showing significant reduction in induction time compared to control vials. Smaller induction times in functionalised vials indicate favourable influence of functionalised silane layers on crystal nucleation.

Apart from polymorphism and induction time, the number of crystals observed in functionalised vials was also significantly different from that in control vials. Typically, only a few big form III crystals along with form II needles were observed in control vials. Meanwhile, large numbers of form II crystals were observed in cyano functionalised vials and similarly large numbers of form III crystals were observed in mercapto and fluoro vials (*cf.* Figure 5.7). Although no significant differences in induction time and number of crystals were observed between functionalised vials, they show pronounced disparity with control templates. These kinetic data thereby suggest that the silanised templates promote heterogeneous nucleation of CBZ crystals in comparison with control template.

5.3.3. Crystal orientation on templates – preferred orientation

Nucleation of crystals on SAM templates often exhibit selective interaction between specific facets of the crystal and template, resulting in

preferred orientation of crystals (Chadwick *et al.*, 2012). Similar orientation effects could also occur on silane based templates depending on relative interactions with particular crystal facets. Preferred orientation of crystals on template surface can be probed by capturing X-ray diffraction (XRD) pattern of crystals while attached to the surface. Such XRD pattern will exhibit high intensity diffraction peaks corresponding to the dominant crystal planes parallel to the template surface (Urbelis & Swift, 2014). Furthermore, glass templates could be directly used for XRD measurement as their amorphous structure does not interfere with the crystal diffraction pattern. To verify preferred orientation of CBZ crystals on the templates, XRD pattern of form II and form III as-grown crystals were obtained while adhering to the template surfaces. The XRD patterns are shown in Figure 5.8. Form III CBZ grown on mercapto and fluoro templates exhibited strong peaks at 2θ values of 15.7° and 15.2°, corresponding to (010) and $(11\bar{1})$ crystal planes respectively. The significance of these facets in crystal morphology is discussed later in section 6.1.4.

On cyano functionalised templates, form II needles were observed to grow perpendicular to the template surface as shown in Figure 5.9. The orientation suggests a selective interaction between the crystal facet perpendicular to the fast growing *c*-axis of form II crystal and template surface. However, XRD pattern of form II CBZ on cyano template exhibited strong peaks at 8.7° and 12.1° correlated to (100) and $(2\bar{1}0)$ facets, both parallel to the c-axis. This observation could be due to the fact that the crystals stick together and fall over with residual solution when the templates are removed from the crystallising solution. This cause the long axis of the needle

shaped form II crystals to lie parallel to the surface. Therefore, the preferred orientation effect caused due to acicular morphology of form II is highly significant as observed in the X-ray diffractogram. As a result, any preferred orientation effect due to the template-induced crystallization of form II could not be confirmed through XRD analysis.

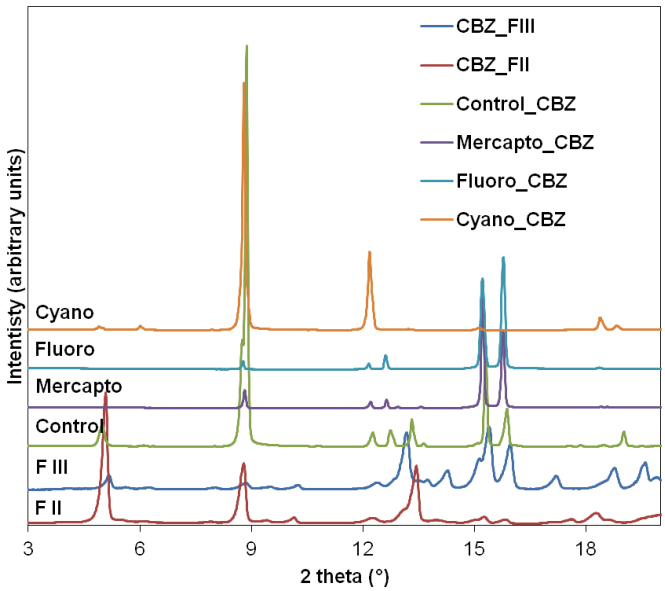

Figure 5.8. XRD pattern of crystals attached to template surface in comparison with the powder pattern of form II and form III polymorphs.

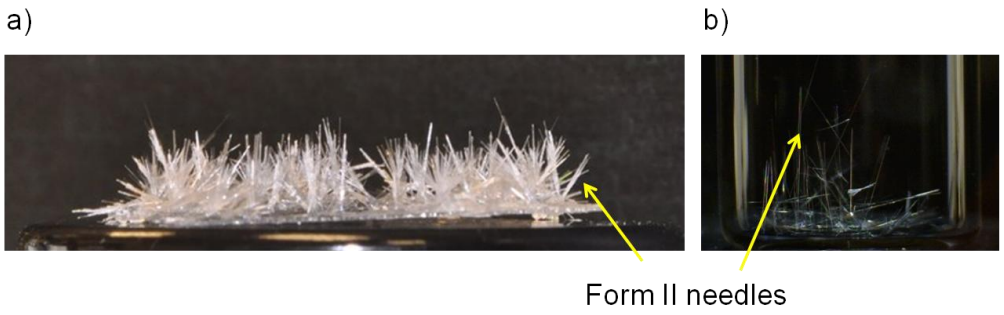

Figure 5.9. Form II crystals growing perpendicular on cyano functionalised a) glass cover slip and b) glass vial.

5.4. Effect of supersaturation and temperature on template-induced nucleation

Above results show that template chemistry affect polymorph nucleation. Similar observation has also been reported in case of polymer heteronuclei (Curcio *et al.*, 2014; Lopez-Mejias *et al.*, 2009). However, effect of solute concentration and temperature on template-induced nucleation phenomena has not been studied thoroughly. Towards this pursuit, CBZ crystallisation from ethanol is conducted at various supersaturations and temperatures with and without the presence of functionalised template surfaces. The results can then provide insight into the applicability of template-induced nucleation process within wider regions of crystallisation phase diagram.

The polymorphic outcome for template-induced crystallization of CBZ from ethanol solutions at various temperature and solute concentrations are presented with the help of a template-induced polymorphic domain (TiPoD) plot as shown in Figure 5.10. The TiPoD plot captures the difference in polymorph nucleation with variations in solution concentration, temperature and template chemistry. In TiPoD, the concentration-temperature plot is divided into regions or domains based on the polymorphic form that nucleated first as observed through optical microscope. However, care has to be taken in interpreting the domains as the domain boundaries are not strictly compartmentalised. Stochastic nature of nucleation and fine balance between thermodynamics and kinetics could play significant roles along the domain boundaries.

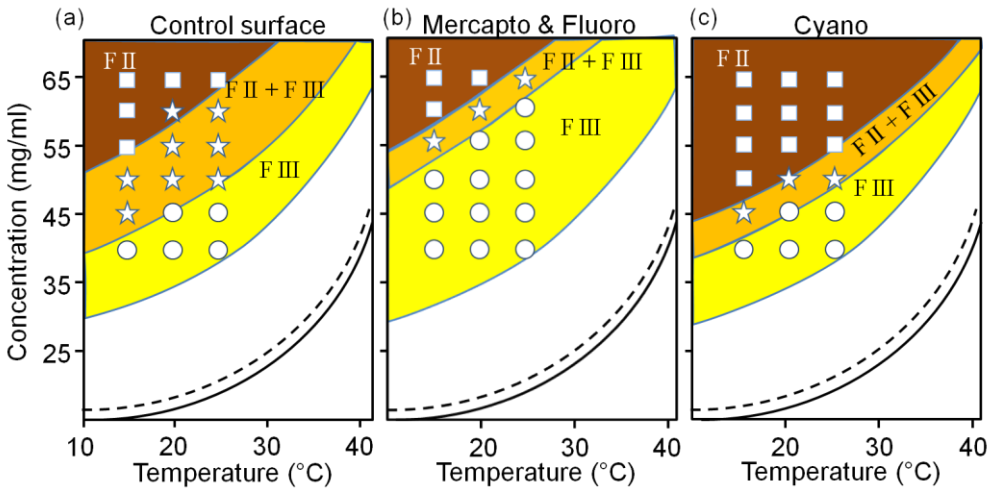

Figure 5.10. Template-induced Polymorphic Domain (TiPoD) plot for CBZ crystallisation from ethanol on a) control surface, b) mercapto and fluro and c) cyano functionalised surfaces. The continuous and broken lines at the bottom of the plots represent form III and form II solubility respectively.

From TiPoD in Figure 5.10, it can be observed that at any particular temperature, as the initial supersaturation is increased, the kinetically stable form II nucleates preferentially over form III. At lower supersaturations, nucleation of the thermodynamically stable form III crystals is dominant. At an intermediate range of supersaturation, concomitant nucleation of both polymorphic forms occurs. These observations are in-line with the expected and reported behaviour for nucleation of CBZ polymorphs (Florence *et al.*, 2006; Teychené & Biscans, 2008).

However, supersolubility regions in which the stable and metastable polymorphs crystallised were altered on using the template substrates. At 15 °C, concomitant nucleation of form II and form III CBZ occurred in control vials in the initial concentration range from 45 to 50 mg/ml (supersaturation ($\sigma = C^{ss}/C^{eq}$) range of 2.6–2.9). In contrast, at the same solute concentration and temperature, mercapto and fluoro surfaces predominantly nucleated form

III CBZ while cyano functionalised surfaces nucleated form II crystals. At 20 °C and 25 °C respectively, crystallisation from solutions with initial concentrations in the range of 50 – 60 mg/ml resulted in concomitant nucleation of form II and form III polymorphs on the control surface. Under these solution conditions, templates with mercapto and fluoro functional groups led to preferential nucleation of form III crystals while cyano functionalised surfaces favoured nucleation of form II crystals. The effect of templates on polymorph selection was significant within a supersaturation range of 2.0 to 3.2, slightly beyond the regime where concomitant nucleation was observed. Outside this supersaturation range, little impact was observed on the nucleation behaviour with varying surface chemistry. The concentration region where the template surface influenced the nucleation of CBZ crystal polymorphs can be noted from the changes in polymorphic occurrence domain area on the TiPoD plot.

5.5. Free energy advantage of template-induced polymorph nucleation

It is observed that templates with specific surface chemistry are able to selectively nucleate particular polymorphs over a range of concentration and temperature. This proposes a difference in the nucleation free energy for polymorphs on different templates. When nucleation of pure form II crystals are considered at 20 °C, from the TiPoD plot in Figure 5.10 it can be observed that the control surface results in pure form II nucleation at 65 mg/ml. However, cyano surface is seen to promote form II nucleation and pure form II is obtained at a lower concentration of 55 mg/ml. The free energy difference between the two crystallisation conditions on control (*co*) and functionalised

template (*t*) surfaces for obtaining pure form II crystals can be found using the relationship,

$$\Delta G_T^{co,t} = -R\,T \ln\left(\frac{C_T^{co}}{C_T^{t}}\right) \qquad (5.1)$$

where T is the temperature of crystallisation, and C_T^{co} and C_T^{t} stands for the solution concentration[3] which nucleates the required polymorphic form on control and functionalised template surfaces respectively. This relationship is used with the assumption that mole fraction ratio correspond to the activity ratio of the solute in solution (Parks *et al.*, 1934). Using the above relationship, an average free energy advantage of about 340 J/mol is available for form II nucleation on cyano template over the control surface in a temperature range of 15 to 25 °C. Similarly, based on the maximum concentration at which pure form III crystallization was obtained on control, mercapto and fluoro surfaces, an average free energy advantage of about 570 J/mol was calculated for the nucleation of form III crystals on mercapto and fluoro surfaces over the control surface in the same range of temperature.

The free energy calculation shows that templates offer specific free energy advantage for nucleation of specific polymorphs. The energy advantage could arise from specific molecular interactions between template surface and nucleating crystal. The lattice free energy difference between CBZ forms II and III is reported to be about 8 kJ/mol (Cruz Cabeza *et al.*, 2006). Although the calculated free energy advantage for nucleation of form II and form III polymorphs on cyano, and mercapto and fluoro templates is only 4–7

[3] The solution concentration used in this equation is in terms of mole fraction. In case of cyano template, concentration corresponds to the lowest concentration that results in pure form II crystallisation while on mercapto and fluoro templates this corresponds to the highest concentration that result in pure form III crystallisation.

% of the lattice free energy difference, experimental observations put forward that this contribution during nucleation stage towards stabilisation of preferred polymorph is significant.

5.6. Solvent effect

Solvent-solute interactions play a major role in crystal nucleation and growth. Conformation and aggregation of solute molecules in solution are solvent dependent (Yang *et al.*, 2014). In case of CBZ, solution phase NMR study suggested that dimerisation in polar solvents is mediated through aromatic interactions while non-polar solvents facilitates dimerisation through hydrogen bonding. As a result, CBZ dimmers expose amide groups in polar solvents and aromatic rings in non-polar solvent (Hunter *et al.*, 2012). In order to study the influence of solvents on template-induced selective nucleation of CBZ polymorphs, five different solvents with varying polarity were selected. Prior to template-induced nucleation studies, effect of solvent on CBZ polymorphism was studied by crystallisation of CBZ polymorphs from selected solvents in clean glass vials.

5.6.1. Effect of solvents on CBZ polymorph crystallisation

CBZ crystallisation was conducted from acetonitrile (ACN), methanol (MeOH), ethanol (EtOH), isopropyl alcohol (IPA) and toluene (TOL) in the descending order of their polarity index. The polarity index values are provided in Table 5.1. In agreement with published literature on CBZ crystallisation from organic solvents, within a supersaturation range of 1.3 – 4.0**,** crystallisation from MeOH, EtOH, IPA and ACN resulted in either pure form or mixture of form II and form III crystals (Grzesiak *et al.*, 2003). Lower

supersaturations (typically <2.5) resulted in nucleation of pure form III crystals while higher supersaturations (typically >3.0) resulted in form II nucleation. In the intermediate range of supersaturation, crystallisation resulted in concomitant nucleation of both form II and form III crystals. In contrast to other solvents, crystallisation from TOL resulted in nucleation of predominantly form II CBZ polymorphs due to the strong non-polar property of the solvent. This highlights the effect of solvent on prenucleation solute aggregates and the importance of solute-solvent interaction on nucleation (Hunter *et al.*, 2012). At low supersaturation, crystallisation from TOL results in nucleation of pure form II crystals. However, at very high supersaturation form III polymorphs are observed along with form II crystals. Figure 5.11 shows the image of crystals grown from different solvents at 15 °C. The behaviour of the CBZ crystallisation with varying temperature, supersaturation and solvent can be visually represented through the Polymorphic Domain (PoD) plots in Figure 5.12.

	Acetonitrile	Methanol	Ethanol	Isopropanol	Toluene
Polarity index	5.8	5.1	4.3	3.9	2.4

Table 5.1. Polarity index of solvents used for crystallisation (Snyder, 1974).

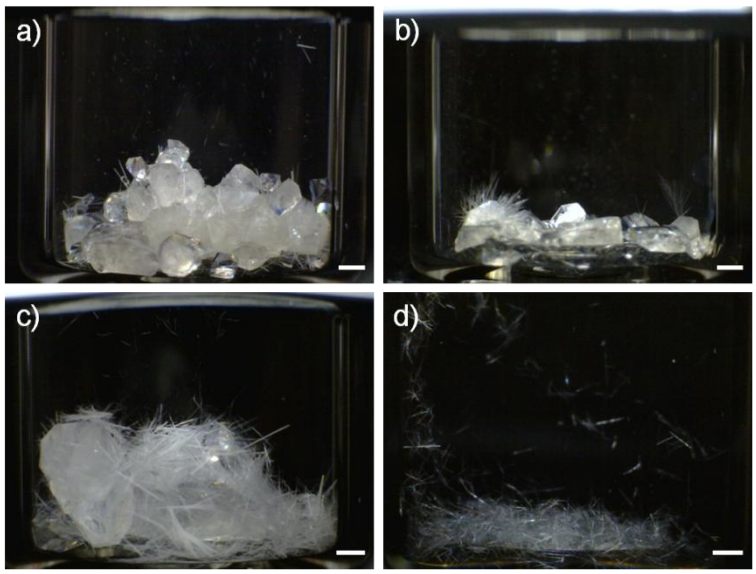

Figure 5.11. CBZ crystals in control vials grown from a) MeOH, b) IPA, c) ACN and d) TOL. The scale bars represent 1 mm

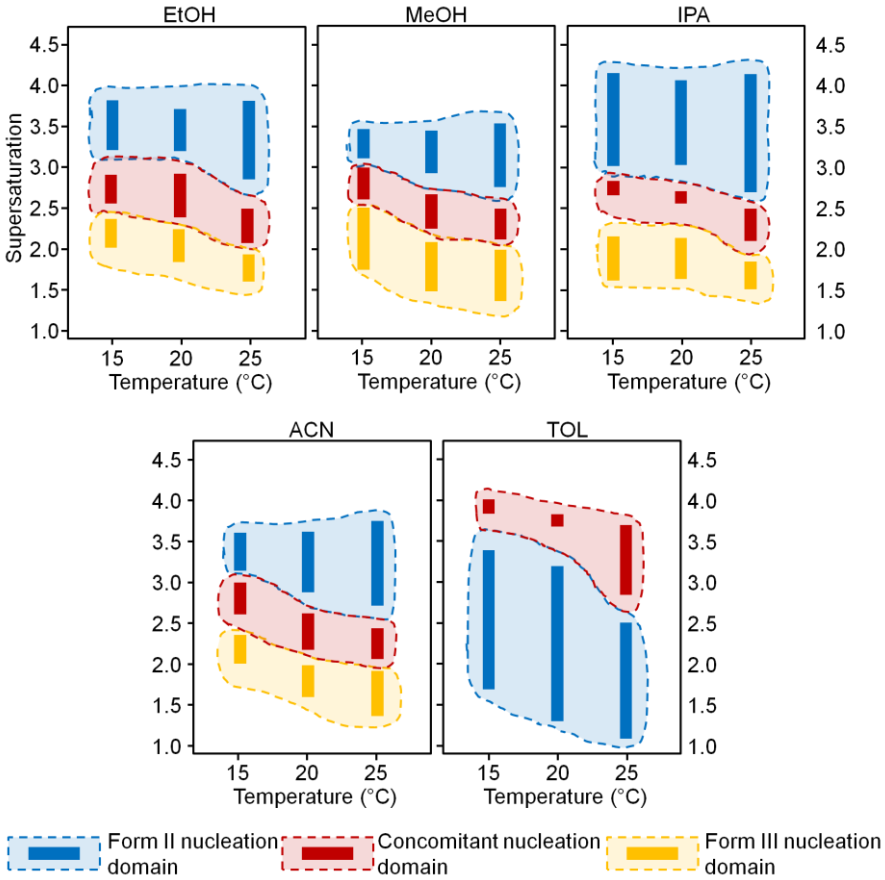

Figure 5.12. Polymorphic domain (PoD) for CBZ crystallisation from EtOH, MeOH, IPA, ACN and TOL solvents in terms of supersaturation vs temperature.

PoD plots for CBZ crystallisation from five solvents highlight the effect of solvent, temperature and concentration. It can be observed that MeOH, EtOH, IPA and ACN exhibit very similar behaviour in CBZ crystallisation with low concentrations resulting in stable form III crystals, high concentration resulting in pure form II crystals and intermediate concentration resulting in concomitant nucleation. The change in crystallisation behaviour in TOL is also evident from the occurrence domain due to the inversion of the form II and concomitant domain positions relative to other solvents.

5.6.2. Effect of solvents on template-induced nucleation

The nucleation of crystals is affected by the surface chemistry of the template (vials) used. In general, mercapto and fluoro templates enhanced crystallisation of form III polymorph while cyano functionalised templates promoted form II crystallisation. However, the influence of templates on crystallisation was dependent on solvent, temperature and supersaturation of the crystallising solution.

When crystallising from MeOH in control vials, CBZ formed pure form III crystals up to a concentration of 140 mg/ml at 15 and 20 °C, and up to 150 mg/ml at 25 °C. Under the influence of mercapto and fluro templates, crystallisation of pure form III polymorph was extended up to a concentration of 160 mg/ml at all three temperatures. On contrary, cyano functionalised templates resulted in pure form III crystallisation only below 110 mg/ml at 15 °C and below 120 mg/ml at both 20 and 25 °C. Under conditions probed in this study, crystallisation from methanol in control vials resulted in pure form II crystallisation only above 180, 190 and 200 mg/ml at 15, 20 and 25 °C respectively. Mercapto and fluoro templates did not alter form II nucleation at

15 and 25 °C. However, crystallisation in mercapto and fluoro vials at 190 mg/ml in 20 °C consistently resulted in concomitant nucleation as opposed to pure form II crystallisation in control vials. Although mercapto and fluoro functionalised vials did not have a significant effect on pure form II domain in methanol, cyano functionalised vials showed profound impact. At 15 °C, crystallisation above 140 mg/ml on cyano templates resulted in pure form II crystals. At 20 and 25 °C, only pure form II crystals were obtained above 150 mg/ml concentration. This is in sharp contrast to the control vials where a minimum concentration of 180 mg/ml was required to produce pure form II. In comparison with the control vials, the domain of concomitant nucleation of form II and form III crystals appeared to be narrower in all three functionalised vials. The result of varying polymorph outcome with template chemistry in methanol solution is presented through the TiPoD plot in Figure 5.13.a.

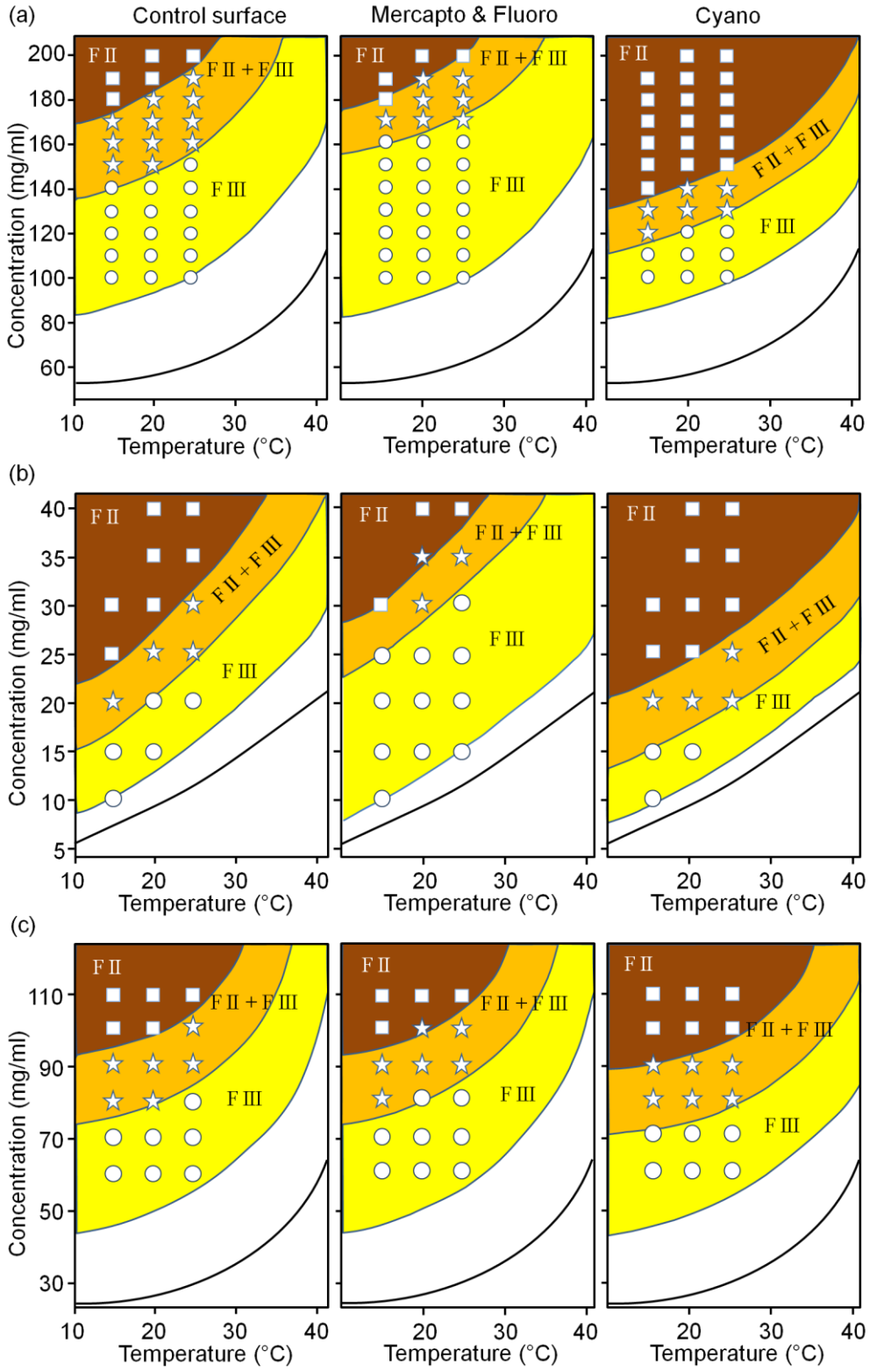

Figure 5.13. TiPoD plot for CBZ crystallisation from a) MeOH, b) IPA and c) ACN.

Template-induced crystallisation of CBZ from EtOH and IPA exhibited similar behaviour to that from methanol solution as described in the previous paragraph. The trend is notable in respective TiPoDs (Figure 5.10 and Figure 5.13.b) where mercapto and fluoro templates result in form III nucleation at even higher concentration than that observed in control vials and cyano template crystallising pure form II at concentrations lower than control vial. Thus, form III domain increased in the presence of mercapto and fluoro templates while form II domain increased in cyano template. In either case, domain where concomitant crystallisation occurred was narrowed in comparison with the control vial.

In case of ACN, templates were found to be less effective in controlling polymorph nucleation. Templates were found to alter polymorph production only on four (out of eighteen) experiment conditions (Figure 5.13.c). As mentioned before, CBZ crystallisation behaviour in TOL is different from the rest of the organic solvents used in this study. Apart from the fact that CBZ solubility is very low in TOL, crystallisation from the solvent resulted in form II CBZ crystals at low concentration range and concomitant nucleation at high supersaturation. However, templates were found to be effective in altering polymorph crystallisation in TOL. Mercapto and fluoro templates promoted form III nucleation at concentration above 6 mg/ml. At 20 and 25 °C with high concentration (8 mg/ml), it was observed that form III crystals appeared well ahead of form II crystals signifying the template-induced nucleation. On cyano functionalised templates, the domain of concomitant nucleation reduced with the expanding pure form II domain. The TiPoD plot for CBZ polymorphs in TOL is provided in Figure 5.14.

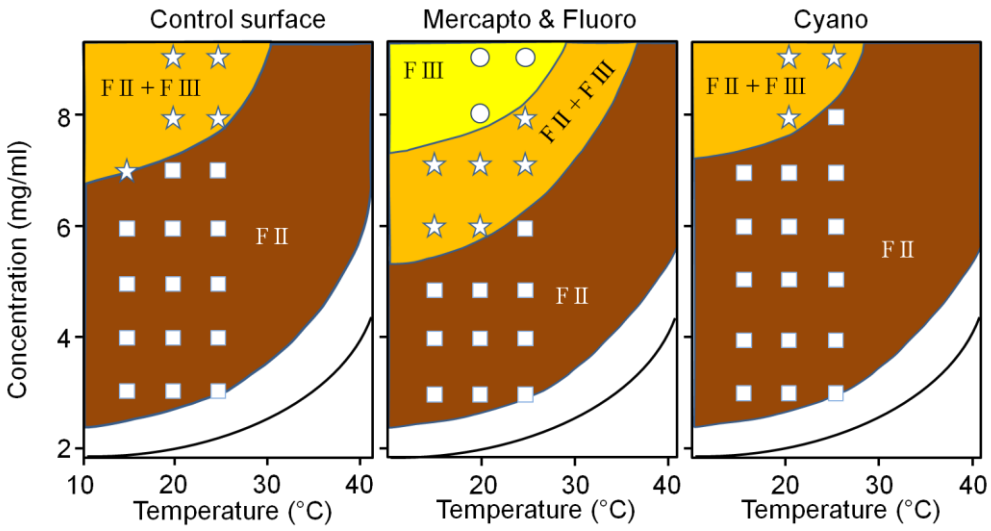

Figure 5.14. TiPoD for CBZ crystallisation from TOL.

From TiPoD plots in MeOH, EtOH and IPA, it can be concluded that the effect of templates on these three solvents are similar. The domain for form III nucleation is enlarged on using mercapto and fluoro templates while cyano templates boost form II nucleation domain. Since MeOH, EtOH and IPA exhibit moderate polarity and are alcohols, the results suggest that mechanism of template-induced nucleation in alcohol solvents are similar and remain effective. However TiPoD plot in highly polar ACN points out that templates used in this study are not significantly influential in ACN as observed in other solvents. The difference in nucleation behaviour of CBZ in TOL is highlighted by the major shift in domains of PoD plot. Nevertheless, the TiPoD plot in relatively non-polar TOL shows that the templates do exhibit their influence in TOL with form III nucleation domain appearing in mercapto and fluoro templates.

Solvents are known to guide the self-association of solute molecules through solute–solvent interactions. This in turn affects the nucleation rate of specific polymorphs and thus results in selective nucleation of polymorphs

based on supersaturation. Desolvation of solvent molecules from solute aggregates and nucleus interface is essential for the formation and growth of crystal nucleus. However, in presence of templates where heterogeneous nucleation occurs, the solute–template as well as solvent–template interactions play their role in altering nucleation kinetics. The solute–template interaction reduces the free energy barrier associated with the formation of critical nucleus. It has been suggested that in template-induced nucleation, the interfacial energy of the nucleus is reduced by a factor termed as the activity factor (ranging from 0 – 1) (Caridi *et al.*, 2014). This activity factor would include a balance between all interfacial energies, solute–template interactions and any lattice match between the crystal structure and template. The difference in template surface properties can decrease or increase the nucleation work for a stable nucleus and thereby modulate the nucleation rate. Similar to solvent–solute interactions, solvent–template interactions can result in solvent association with molecules at template–solution interface. Strong solvent association with the template surface can act as a barrier that prevents effective solute–template interaction.

From the experimental results, it is inferred that the effectiveness of template-induced nucleation mechanism changes with solvent polarity. In the most polar solvent used in this study (ACN), templates did not significantly alter the nucleation domains on TiPoD plots in comparison with other solvents. Reduced template activity in highly polar solvent could occur either due to strong solvent–solute or solvent–template interactions. However, since the nucleation behaviour of CBZ polymorphs in ACN did not show notable difference in comparison with other moderately polar solvents, it could be

assumed that the solvent–solute interaction as well as solute self association may not be significantly different between these solvents. This suggests that the difference in template-induced nucleation in these solvents could be due to variations in the solvent–template interactions. Highly polar solvent could be strongly associating with the polar components of the templates, thereby limiting solute–template interaction and reducing the template effect.

In case of TOL, the least polar solvent used, strong influence of solvent on solute association is evident from the inverted domain regions in PoD plots. TOL promotes nucleation of form II crystals due to this effect. However, in presence of mercapto and fluoro templates, form III nucleation is obtained in TOL. This shows that the solute–template interactions results in reduction in the activity factor for form III nucleation thereby increasing its nucleation rate. It also indicates that in case of low polar solvents the relative strength of solvent–template interaction is not as significant as in highly polar solvents, thus further aiding solute–template interaction.

5.7. Discussion

Experimental results on template-induced crystallisation provided in this chapter strongly suggest that the surface chemistry of the templates can alter polymorphic nucleation. Inferences from previous studies on solvent effect on polymorphism of CBZ could be utilised in understanding the influence of template surface chemistry in promoting preferential nucleation. Investigation of CBZ molecular self aggregation using NMR spectroscopy by Hunter *et al.* (2012) revealed that dimerisation of CBZ molecules in polar solvents is mediated through aromatic interactions while that in non-polar solvents occurred through hydrogen bond interactions. By drawing analogy to the

solvent effects on preferential nucleation of CBZ polymorphs, the role of functional groups on template-induced nucleation of specific CBZ crystal polymorphs can be envisaged. From a structural chemistry perspective, among the functionalised templates investigated in this study, the mercapto (–SH) head group can act as both acceptor and donor of hydrogen bond. On the other hand, both cyano (–CN) and fluoro ($–CF_3$) head groups can act as weak hydrogen bond acceptors. However, the results obtained from surface characterisation of the templates reveal that the cyano surface exhibited a much higher value of surface energy compared to the fluoro surface (Table 4.5). Moreover, the polar component of surface energy (arising from the basic component) for the cyano surface was determined to be significantly higher. These results indicate that the cyano template could act as a much stronger hydrogen bond acceptor and therefore — akin to a hydrogen bond acceptor solvent — promote nucleation of form II CBZ. Even as this molecular recognition perspective to explain the experimental observations is considered, it is to be noted that the thermodynamics and kinetics of homogeneous versus heterogeneous crystal nucleation could be significantly different.

Concomitant nucleation of polymorphs from the crystallising solution in the absence of templates indicates that the solute molecular assemblies that can lead to the formation of either polymorph are abundant in the solution phase. However, in the presence of specific templates the relative nucleation rate of polymorphs is altered, resulting in selective nucleation. This could be due to the alteration of either the kinetics or the thermodynamics of the nucleation of each polymorph. Myerson and co-workers have argued that template-induced nucleation is predominantly a kinetic process, without a

major change in nucleation thermodynamics (Curcio *et al.*, 2014; Diao *et al.*, 2011c; López-Mejías *et al.*, 2013). However, another school of study suggests that the thermodynamics for the creation of the stable nuclei is also altered during template-induced nucleation, thereby suggesting a thermodynamic effect of the templates on nucleation process (Caridi *et al.*, 2014; Kulkarni *et al.*, 2014). The free energy advantage for specific polymorphic nucleation (section 5.5) supports the latter view. However the solvent analogy of templates suggests that the templates could potentially affect kinetics as well. Thus, it could be proposed that template-induced polymorph selective nucleation affects both the kinetics and the thermodynamics of nucleation.

As discussed in section 2.7, template induced nucleation of different polymorphs of both organic and inorganic crystals have been reported in the literature. A major share of these reports has focused on utilising self assembled monolayers (SAMs) as templates (Singh *et al.*, 2011). SAM templates promote the nucleation of particular crystal forms predominantly through epitaxial relationship (Chadwick *et al.*, 2012; Mitchell *et al.*, 2001). On the other hand, polymer based templates lack any ordered molecular arrangements and hence promote nucleation through specific interaction of chemical functionalities and other template features such as porosity or surface topography (Diao *et al.*, 2011b; Price *et al.*, 2005). However, silanised templates used in this study lack precise molecular arrangement similar to SAMs although a small degree of molecular ordering on template surface is plausible. Unlike polymer templates, silanised templates in this study lack other characteristics such as porosity or specific surface topography. Such silanised templates have not been reported extensively for polymorphic

crystallisation in the literature. (Even though similar silanised glass/silica surfaces have been reported for template-induced crystallisation studies, they have been considered akin to SAMs with long range molecular order (Zhang *et al.*, 2011)) Similarly, to the best of my knowledge, it is for the first time that selective nucleation of concomitant polymorphs is reported using heterogeneous template. During concomitant nucleation, the relative kinetics and thermodynamics for the nucleation of both polymorphs are in a delicate balance that can be nudged either way for obtaining selective nucleation. The results from the template-induced nucleation of CBZ prove that heterogeneous templates can be used for altering concomitant nucleation. Likewise, a systematic study on the effect of solvents, temperature, and supersaturation in polymorph selective template-induced nucleation has not been reported. Template-induced Polymorphic Domain (TiPoD) plots were developed to capture the interrelationship between these factors that influence template-induced nucleation process. The PoD diagrams reveal that the effect of templates on polymorph selectivity is limited to a range of supersaturation at different temperatures. These diagrams help to highlight the variation in polymorphic nucleation occurring due to template-induced nucleation and limits within which effective utilisation of template induced nucleation could be achieved. The PoD plots in different solvents showed that solvent polarity affects the effectiveness of template-induced nucleation process. Experimental results suggest that solvents with medium or low polarity would be most effective in promoting solute-template interactions due to lower solvent-template interactions. This could be a useful guidance for selecting solvents for future studies on template-induced nucleation. Within the scope of the

present study, the TiPoD plots could be useful in anticipating the polymorphic outcome of a crystallisation experiment carried out at a particular solution condition under the influence of specific surface chemistry. Also, the approach of occurrence domain can be extended to develop design space diagrams that highlight the influence of variety of external factors that affect crystallisation. Furthermore, the PoD plots could highlight the operating regions in the crystallisation domain which could be implemented using process analytical technology (PAT) to achieve specific product quality through Quality-by-Design (QbD) approach.

The outcome of a crystallisation experiments are primarily affected by the combination of three factors – solution properties, process conditions and nucleation promoters (including templates, external stimulus such as ultrasonic waves, laser, etc.), each forming a corner of the 'crystallisation triangle' as depicted by Umang et al (2015). The process conditions include the scale of operation, hydrodynamics and, mass and thermal transport properties. Developing a versatile template-induced nucleation strategy would require analysis of TiPoD plots at different scale of crystallisation. The solution volume used in this study is in the range of 3–10 ml, which is higher than the volume used in many other reported studies on template-induced nucleation. Although the results from this scale of volume is promising, the lack of thorough knowledge on template-induced nucleation in conjunction with other process conditions such as hydrodynamics has to be addressed before any application for this approach can be designed.

5.8. Summary

Template-induced nucleation approach to control crystal polymorphism aim to provide engineered templates that can alter the nucleation kinetics and favour crystallisation of particular polymorphs. Template-induced nucleation of CBZ polymorphs on templates show that surface chemistry of the templates influences nucleation process and can result in selective nucleation of polymorphs. Cyano functionalised templates promoted nucleation of form II polymorphs while mercapto and fluoro templates favoured form III nucleation. Supersaturation, temperature and solvent of crystallisation influence template-induced nucleation process. The impact of templates on polymorph selective nucleation along with these factors was captured using Template-induced Polymorphic Domain (TiPoD) plots. The domain variations in TiPoD plots revealed that the template-induced nucleation mechanism was effective only within a range of supersaturation in the temperature range used. However, the free energy advantage of template-induced nucleation process calculated within that supersaturation range substantiates surface chemistry dependent polymorphic selectivity of templates. Crystallisation from solvents of varying polarity suggested that highly polar solvents could result in strong solvent–template interactions which hinders solute–template interaction and thereby suppresses template-induced nucleation pathway.

Chapter 6

Molecular Modelling

Computational molecular modelling is a valuable tool in understanding molecular level details of events which are experimentally observed in a macro-scale. Molecular modelling methods have been used in studying different aspects of crystallisation such as nucleation, growth, molecular conformation, effects of solvents and additives on crystallisation and many more (Poornachary *et al.,* 2012).

Different computational approaches for gaining mechanistic understanding of template-induced nucleation process have been reported in literature. Several molecular dynamics and Monte Carlo approaches have been reported to simulate nucleation of calcite on SAM templates (Freeman *et al.,* 2008; Quigley *et al.,* 2009). However, due to the large time scale difference between atomistic simulations (nanoseconds) and nucleation (minutes) (Harding *et al.,* 2014), most attempts for modelling template-induced crystallisation of organic molecules involve generating indirect inferences on nucleation event through understanding interfacial interactions between template and crystal facets. One of the most commonly reported approach in studying template-induced crystallisation where templates have ordered molecular arrangements (SAMs and other crystal substrates) is to search for epitaxial relationship between nucleating crystal and template surface using dedicated software such as GRACE (Geometric Real-space Analysis of Crystal Epitaxy) (Mitchell *et al.,* 2001) or EpiCalc (Hillier & Ward, 1996). Both software analyses degree of lattice matching between the different facets

of the required crystal form with a substrate lattice and rate the matching into different scores. A high degree of lattice matching is suggested to result in oriented growth of crystal on substrate. This method has been suggested to be the primary factor that influenced oriented growth of 1,3-bis(*m*-nitrophenyl)urea on SAM templates (Hiremath *et al.*, 2005). Another approach is to find the interaction energy between the template surface and crystal facet and to correlate this interaction energy to nucleation propensity of that template. Chadwick and co-workers (2012) studied preferential nucleation of acetaminophen crystals on $(0\bar{1}1)$ facet of α-lactose monohydrate and $(00\bar{1})$ facet of mannitol using this approach. Their results suggested that a combination of epitaxy and matching surface functionality would result in preferential crystal nucleation. A similar method for calculating the binding energy between template surfaces and crystal facets for rationalising template-induced nucleation of amino acids (α-glycine, $_{L}$-alanine and $_{DL}$-valine) was used by Lee *et al* (2002). The computed binding energy values showed good agreement with the nucleated crystallographic plane. Preferential nucleation of tolbutamide polymorphs on SAM templates has also shown significant correlation to calculated binding energies between SAM surfaces and crystal facets (Zhang *et al.*, 2011).

In this study, molecular modelling is used to calculate intermolecular interaction energy between crystal facets and template surfaces, which is a key factor in template-induced nucleation process and oriented growth of crystal polymorph. The detailed modelling procedures and the results are discussed in this chapter.

6.1. Crystal growth morphology

The external morphology of a crystal or crystal habit depends on the molecular structure of the solute, internal crystal structure and unit cell geometry, intermolecular interactions in the crystal structure, growth mechanism and other environmental factors such as solvent properties, supersaturation and presence of trace impurities or additives (Meenan *et al.*, 2002). Different computational approaches that simulate crystal morphology using geometrical rules and/or intermolecular interaction energies have been developed and applied for organic crystals. Two theoretical methods commonly used for crystal morphology prediction briefly discussed below.

6.1.1. Bravais–Friedel–Donnay–Harker (BFDH) method

The BFDH method for morphology prediction is based on geometry of the crystal lattice. It was developed from laws proposed by Bravais (1866), Friedel (1907) and Donnay and Harker (1937) and hence quoted together as BFDH law (Docherty *et al.*, 1991). The law can be summarized as "taking into account submultiples of the interplanar spacing d_{hkl} due to space-group symmetry, the most important crystallographic forms will have the greatest interplanar spacings". Accordingly, an *hkl* face with larger interplanar distance (d_{hkl}) than other faces will be morphologically more important than others in the final crystal morphology. Although helpful in creating a basic crystal morphology prediction tool based on crystallographic considerations, this method disregards other important information such as the bond type and intermolecular interactions that might affect crystal growth morphology.

6.1.2. Attachment energy model

Attachment energy (AE) model accounts for intermolecular interaction forces in crystal morphology prediction. It was proposed by Hartman and Bennema and follows the reasoning that the faces with the lowest attachment energies will be the slowest growing and therefore have the most morphological importance (Hartman & Bennema, 1980). Attachment energy is defined as the fraction of the total lattice energy which is released on the attachment of a new slice to the face of a growing crystal surface. This model is capable of providing good predicted models of vapour-grown crystals or when solvent molecules do not have strong interactions with the growing crystal in solution. However, stronger solvent interactions at the crystal growth front, higher supersaturation and other kinetic factors affecting crystal morphology can result in deviation from the morphology simulated using AE model.

6.1.3. Modelling CBZ crystal growth morphology

Both the BFDH and AE models implemented in *Morphology* module in Materials Studio (MS) (Accelrys Software Inc., Version 5.5) were used for morphology prediction of form II and form III CBZ polymorphs. Crystal structures of form II and form III polymorphs of CBZ were obtained from the Cambridge Crystallographic Data Centre (CCDC ref. codes CBMZPN03 and CBMZPN10, respectively). Geometry optimisations of the unit cell molecular structures of the polymorphs obtained from CCDC is first conducted to avoid large energy deviations of the structure latter in the calculations. The optimised crystal structures are then used to predict the crystal structures using both BFDH and AE models. In AE model, COMPASS force field (Sun, 1998)

was used for calculating the attachment energy of crystal facets. Based on the unit cell properties, both models generate a list of possible growth daces and their growth rates. Using this, a centre-to-face distance is assigned to each face and the crystal morphology is deduced from this information. The predicted crystal habits of CBZ are provided in Figure 6.1. It can be observed that form II crystal habit predicted using both the BFDH and AE models has an elongated acicular shape which is similar to the needle-like crystal habit observed experimentally (*cf.* Figure 5.1.a.). In contrast, the simulated crystal habit of form III polymorphs exhibits a prismatic bipyramidal shape and is generally in good agreement with the experimental habit (*cf.* Figure 5.1.b). Accuracy of the predicted form III crystal habit was further verified by comparing the predicted crystal shape with the morphologically important facets expressed in the experimental crystal habit. For this purpose, form III crystal facets were indexed and reported in the following section. The close similarity between the BFDH and AE predicted growth morphology suggests the absence of strong directionally oriented molecular interactions in both crystal forms (Docherty *et al.*, 1991).

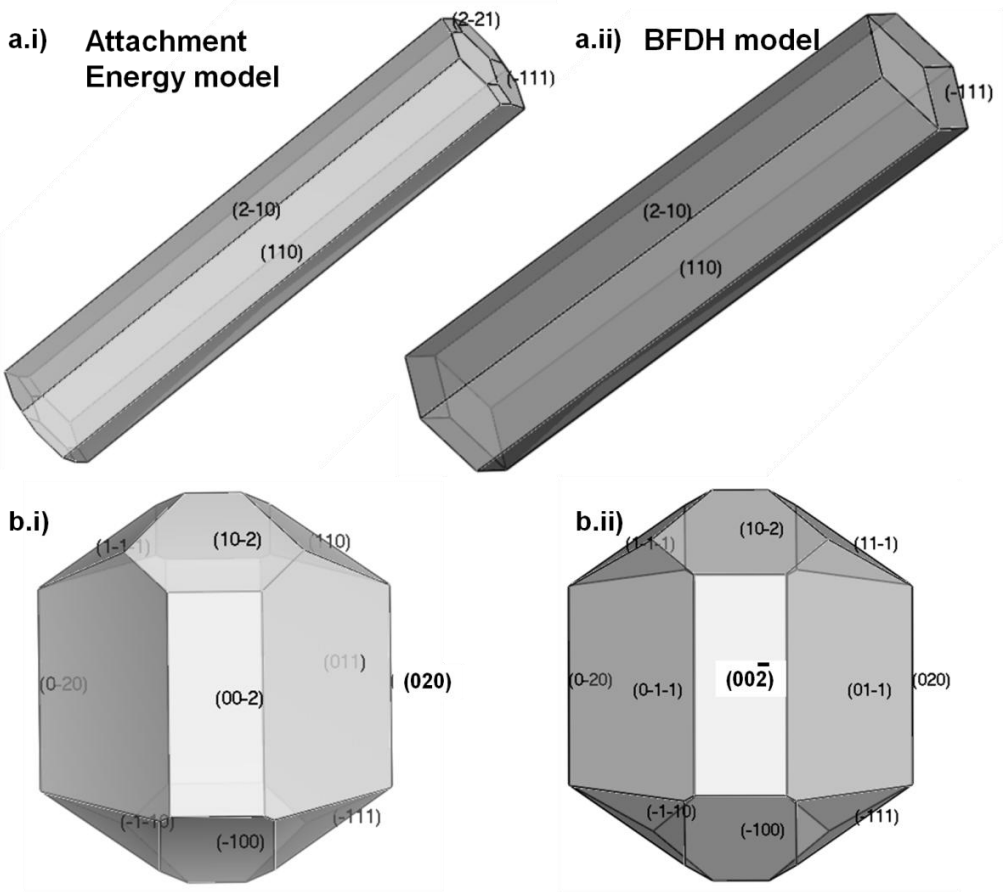

Figure 6.1. Predicted crystal growth morphology of CBZ polymorphs a) form II and b) form III using i) attachment energy and ii) BFDH models.

6.1.4. Crystal face indexing

Experimental face indexing of form III crystals revealed six unique facets as shown in Figure 6.2. The morphologically prominent facets are {101} which comprise about 40 % of the total crystal surface area. This is followed by {010} and {001} facets in decreasing morphological order, with approximately 30 % and 20 % contribution to the total surface area. {112} and {$\bar{1}$11} facets together contribute the rest 10 % of the total surface area.

By comparing the indexed facets of form III with the predicted crystal habit, it is observed that the predicted habit has several smaller facets which were not observed experimentally. This difference could be attributed to the

influence of solvent on the growth morphology which is not incorporated in the AE model.

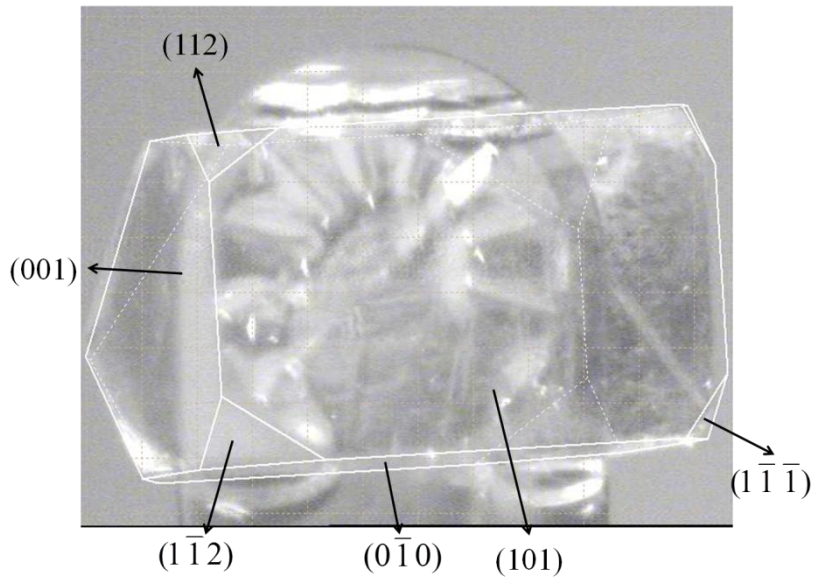

Figure 6.2. Form III crystal factes indexed using single crystal X-ray diffraction.

6.2. Interaction energy calculation

As discussed in chapter 2, molecular interaction at the template–crystal interface could significantly influence the nucleation of crystal polymorphs besides epitaxial relationship. In relating interaction energy between template surface and crystal facets to polymorphic nucleation, it is assumed that the molecular arrangement in the prenucleation solute aggregates or clusters that result in crystal nuclei exhibit a certain degree of similarity to the final crystal structure (Davey *et al.*, 2001; Mattei & Li, 2011; Sullivan *et al.*, 2014). The working hypothesis in these calculations is that if a template surface exhibits favourable interaction with a particular facet of a crystal polymorph, the template surface is most likely to guide heterogeneous nucleation of the specific crystal form with oriented growth from that facet interacting with the

template surface. The methodology adopted for calculation of the interaction energy and the insights obtained from the calculated energy values are explained in the ensuing sections.

6.2.1. Modelling methodology

The molecular models were built with template surfaces and crystal facets aligned close to each other within interactive distances. In developing a meaningful model whose interaction energy values can be used for experimental inferences, the following aspects were considered.

- While calculating average interaction energy between a crystal facet and the template surface, different possible orientations of the molecular cluster (prenucleation aggregate) on the template surface has to be taken into consideration. Hence, in the molecular model, the relative position of the crystal facet with respect to the template needs to be adaptable.
- The arrangement of molecules within the bulk of the cluster has to retain periodic structure as it is on a definite crystal facet. However, the molecules on the surface of the cluster which interact with the template surface molecules need to be relaxed for translational degree of freedom.
- Towards mimicking the physical process of formation of a small crystal nucleus on a large template surface, a two-dimensional flat template surface with periodic boundary conditions is built and a molecular cluster with dimensions small than the template is oriented over the template surface.
- The lattice dimensions of the periodic template have to be significantly bigger than the crystal cluster dimensions to avoid overlapping and interactions between the clusters. The model should also be able to

handle different orientations of the cluster approaching the template surface.

The *Forcite* module in MS is a collection of molecular mechanics tools that can perform various calculations. This module was used to simulate the interactions between a silane monolayer and the CBZ molecular cluster formed by cleaving the (*hkl*) facets of form II and form III crystal polymorphs. The silane monolayer comprised of 10 × 6 matrix of silane molecules substituted on alternative Si atom sites on a quartz {100} face. Figure 6.3 shows the molecular arrangement of silane molecules modelled on the template surface. The Si atoms of the silane monolayer were constrained in all three planes so as to maintain the monolayer pattern during molecular dynamics (MD) simulation. This assumption is valid since the Si atoms in silane molecules are attached to the glass substrate through covalent bonds and hence have restricted mobility. The silane layer was modelled with (x,y) dimensions large enough to accommodate a crystal facet approaching the template surface in different orientations without overlapping of crystal clusters in adjacent periodic structures.

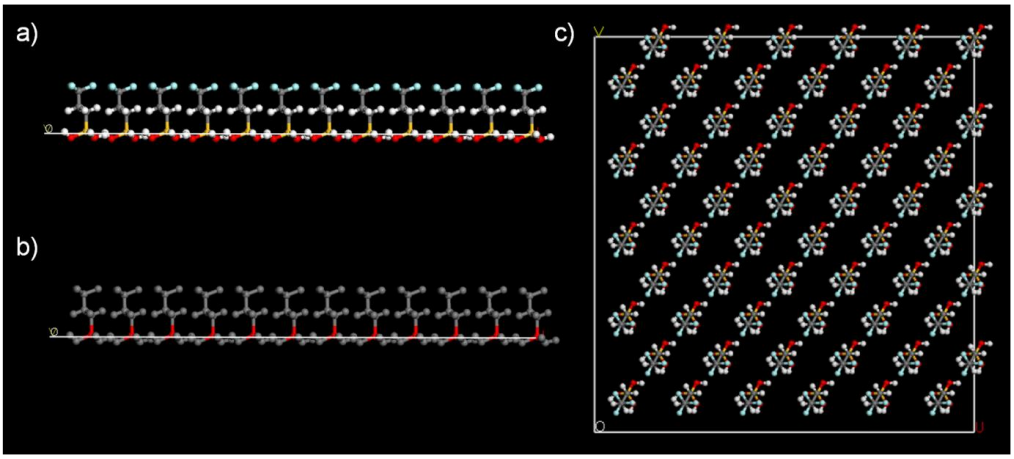

Figure 6.3. A molecular model of silane monolayer with fluoro functional head groups before MD simulation; a) side view, b) side view highlighting constrained Si atoms in red, c) top view. Colour scheme in (a) & (c): grey = carbon, white = hydrogen, red = oxygen, cyan = fluorine, yellow = silicon. Colour scheme in (b): grey = unconstrained atoms, red = constrained atoms.

Initially, the morphologically important facets were cleaved from the crystal structure of CBZ polymorphs and molecular clusters were built as motion groups with a minimum dimension of 25 Å × 25 Å. Defining motion groups helped in optimizing the facet orientation on a silane layer without losing spatial arrangement of CBZ molecules in the cluster. MS regards the atoms or molecules in a motion group as a collection of particles that can be translated or rotated such that the symmetry of molecules or atoms within the motion group is preserved during optimisation. In this way, the molecular arrangement in the cluster could be preserved to be similar to that of the crystal polymorph while at the same time allowing relaxation of surface molecules on the template for interfacial interaction. The (*hkl*) facets were then positioned over the silane layer and Quench simulations were performed. Quench methodology utilises both molecular dynamics and geometry optimisation calculations to find the low energy structures. During Quench,

the periodic or non-periodic molecular structures first undergo molecular dynamics simulation, generating an optimised trajectory which reduces the overall energy of the system. Further energy minimisation of the generated trajectory occurs via geometry optimisation. Here, MD simulations generate several initial configurations of the facet clusters for energy minimisation and thus different facet orientations on the silane monolayer can be sampled. During Quench simulations, MD was performed for 1 ps with a time step of 1 fs. The dynamics trajectory was captured at every 100 steps and geometry optimisation was performed on these trajectories. A snapshot of the orientation of the motion group, comprising of CBZ molecules, on the template surface is depicted in Figure 6.4. COMPASS forcefield (Sun, 1998) was used for the energy expression of both CBZ and silane structures based on published literature (Konkel & Myerson, 2011; Prohens *et al.*, 2013; Zhang *et al.*, 2011). Atomic charge sets defined with the forcefield were used without modification. Electrostatic and van der Waals forces were summed using Ewald summation method. MD simulation was performed with NVT ensemble at 293 K for 1 ps with a time step of 1 fs. Geometry optimisation of the crystal facet cluster–silane monolayer system was performed at every 100 steps of dynamics using Smart algorithm with medium quality[4] implemented in *Forcite*. After the Quench simulations, interaction energy between the silane monolayer and a crystal facet cluster was calculated using the relation:

[4] The Smart algorithm in MS is a cascade of the numerical methods - steepest descent, Newton Raphson and quasi-Newton (BFGS variant) for the iterative energy minimisation of the structure. The convergence criteria between iterations in a medium quality geometry optimization in MS are defined as the following: Energy = 0.001 kcal/mol, Max. force = 0.5 kcal/mol/Å, Max. stress = 0.5 GPa and Max. displacement = 0.015 (Å)

Interaction energy = Total energy of the system – (Energy of the silane monolayer + Energy of the crystal facet cluster)

Likewise, interaction energy on the control surface is computed by substituting the silane monolayer with hydroxyl functional groups. The lowest interaction energies from simulation runs (n=3) were in turn used to interpret specific interactions between the silane monolayer and crystal polymorph. It is assumed that the effect of solvation on the interactions between the crystal facet and template surface is relatively similar in the case of control and functionalised surfaces and hence is not taken into account in the simulation. The implications of this assumption are discussed in the next section.

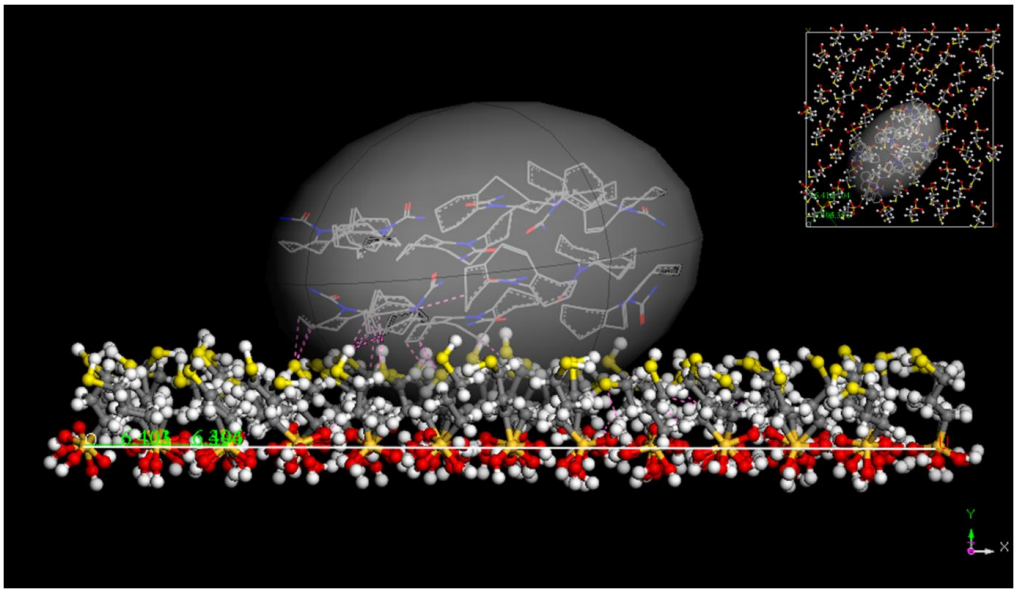

Figure 6.4. Motion group extracted from $\{2\bar{2}1\}$ facet of form II CBZ crystal oriented on mercapto silane template surface. Inset: top view of the molecular arrangement as observed along the b-axis.

6.2.2. Results and discussion

Quench simulation for interaction between each unique facet of both form II and form III CBZ crystals with four template monolayers (control, mercapto, fluoro and cyano templates) were performed. Each Quench cycle

consisting of MD simulation followed by geometry optimisation resulted in 11 facet orientations on the template surface. An example of the different cluster orientations on silane surface obtained from a single Quench cycle is shown in Figure 6.5. Different cluster orientations on silane monolayers provide a sample of the large number of probable facet orientations on template. The total energies of each of these local minimum energy configurations were calculated and the configurations with the lowest total energy from each quench cycle were selected for interaction energy calculations. The values of interaction energy between prominent facets of both form II and form III crystals and the template surfaces are provided in Figure 6.6. A negative value for the interaction energy relates to favourable template-crystal cluster interaction, with the strength of intermolecular interactions being proportional to the absolute value. Conversely, a positive value of interaction energy corresponds to unfavourable interaction between crystal facet and the template. Note that herein the inferences are obtained by comparing the values of interaction energy for different crystal orientations on the template surface on a relative basis rather than direct comparison of the absolute values.

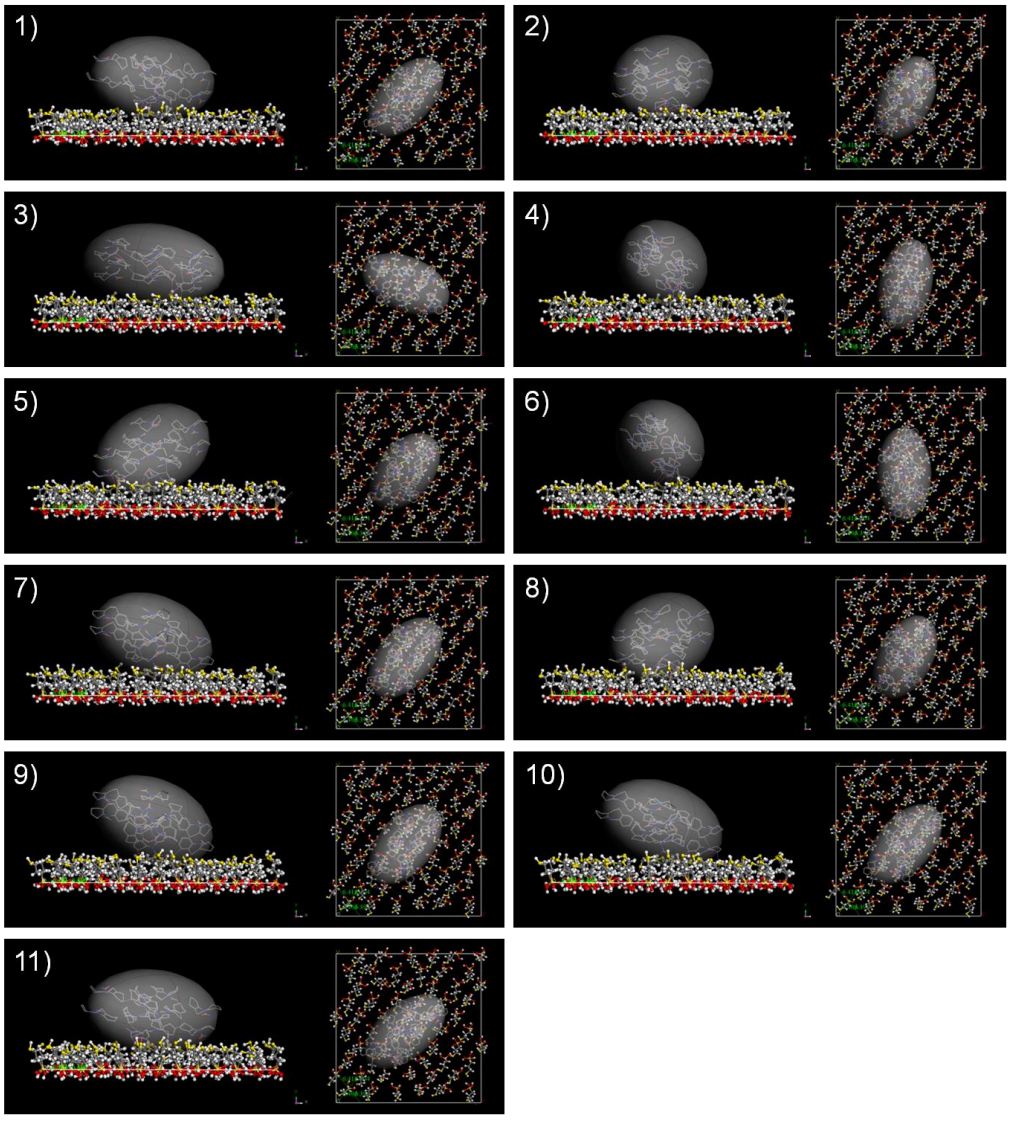

Figure 6.5. Snapshots of different orientations of $\{1\bar{1}\bar{1}\}$ facet of form II crystal on mercapto template produced through a single Quench simulation cycle. Each configuration is formed through the geometry optimisation of the frames generated through MD simulation separated by time interval of 100 fs. These molecular configurations are subsequently used for interaction energy calculation.

Resulting from the above calculations and analysis, from Figure 6.6b, both the mercapto and fluoro functionalised surfaces have significant favourable interactions with, {010} and $\{\bar{1}11\}$ facets of form III crystal. At the same time, both these templates exhibit unfavourable interactions with the

dominant facets of form II crystal (Figure 6.6a). In contrast, cyano functionalised template exhibits strong favourable interaction with form II facets along with significantly unfavourable interaction with, {101} and $\{1\bar{1}2\}$ facets of form III. In comparison, the control (hydroxyl) surface exhibits somewhat favourable interaction with form II facets and highly favourable interaction with {010} facet of form III.

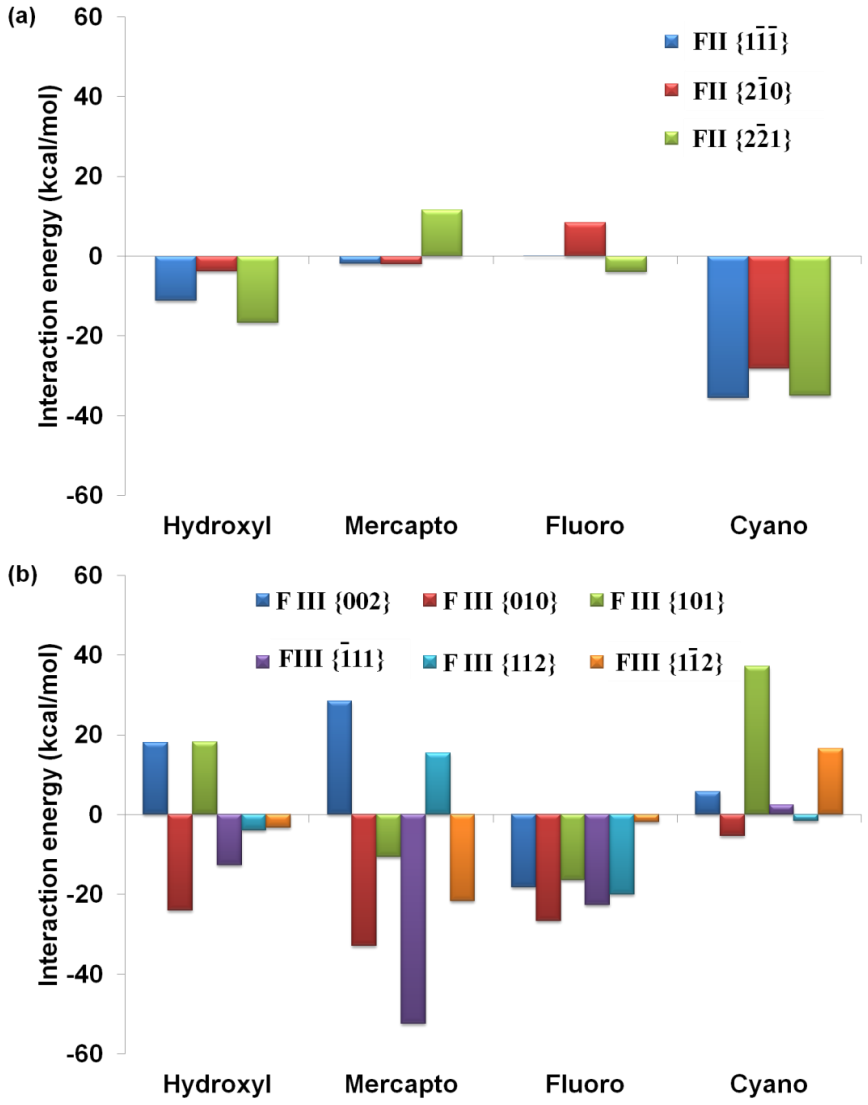

Figure 6.6. Interaction energy values of (a) form II CBZ crystal facets and (b) form III CBZ crystal facets with template surfaces.

By comparing the calculated values of interaction energies, it can be inferred that the control surface has favourable interactions with both form II

and form III crystal facets. On the other hand, mercapto and fluoro functionalised surfaces do not show significant interaction with form II facets while exhibiting strong favourable interactions with form III facets. The combined effects of these subtle intermolecular interactions could lead to predominant nucleation of form III crystals on mercapto and fluoro surfaces respectively. Similarly, the synergistic effects of favourable and unfavourable interaction of cyano functionalised template towards form II and form III facets respectively can induce selective nucleation of form II crystals.

The modelling results suggest that the morphologically significant facets of form III crystals favour interactions with mercapto and fluoro functional layers than cyano functional layer. The inverse is true for form II crystal facets which favour cyano template layer. Although the absolute values of interaction energies calculated in this analysis may not be definite, the results reveal the relative preference for cluster–template interactions. Favourable cluster–template interactions can reduce the activity factor (section 5.6.2) for heterogeneous nucleation and thereby increase the nucleation rate that particular polymorph. Conversely, unfavourable interactions between cluster and template layer can reduce the heterogeneous nucleation rate of corresponding polymorph on that template. When a template surface increases the nucleation rate of one polymorph while decreasing the same for other polymorphs, selective nucleation of the former polymorph would occur on that template. This is the synergistic effect observed in the strong preference of cyano functionalised templates towards nucleating form II crystals. Thus, calculated interaction energies between crystal facets and template layers are

able to capture the preferential polymorphic nucleation achieved through template-induced nucleation process.

Experimental results have suggested that solvents influence template-induced nucleation process through solvent–solute and solvent–template interactions. However, this impact of solvents was neglected in the present modelling study. When template-induced crystallisation is conducted from solution, solute interaction with template would need to overcome the solvation effect of solvents with solute and template surface. The strength of these interactions is predominantly determined by the polarity of the solvent as well as the template features such as surface energy and surface charge. Different solvents have been reported to crystallise different polymorphs based on the difference in the interaction with solute molecules. This could either be due to the difference in the interactions with crystal facets (Khoshkhoo & Anwar, 1993) or due to the difference in molecular interactions such as hydrogen bonding pattern between solvent and solute molecules (Du *et al.*, 2014; Hunter *et al.*, 2012). Similar difference in the solvent-template interaction could also be foreseen based on the difference in the molecular interactions at the interface. Polar solvents are expected to have high preference to bind to templates that exhibit polar surface groups. Such interaction could provide an additional obstacle for the solute to interact with the template, thereby reducing the template effect.

Although interaction energy calculations through the modelling approach presented in this study is able to account for preferential nucleation, the assumption of uniform solvent-template and solvent-solute interactions could lead to erroneous conclusions. Likewise, the effect of solution

supersaturation and temperature are also neglected in the present modelling approach as the focus of this work is to capture the effect of template-chemistry on template-induced nucleation. Given its limitations, the modelling results presented in this chapter is intended only to provide a qualitative approximation on the likelihood of crystal-template interaction in the absence of solvent that can lead to template-nucleation of the crystal. Hence, the relative interaction energy values calculated through this approach would be valid only for vapour phase crystal deposition on template or in solution phase crystallisation under conditions when the solvent-solute and solvent-template interactions are negligible or weak, which could possibly occur in non-polar solvents interact with polar template surfaces and solute aggregates. Template-induced nucleation would be significant only when the template–solute interaction energies are more favourable than solvent–solute and solvent–template interaction energies. The solvent effect could be incorporated into the present modelling approach either by introducing solvents along with the cluster and silane monolayer or through independent calculation of solvent–cluster interactions and solvent–template interactions. The latter approach would be preferable as it allows for the calculation of specific solvent-facet interaction energies which have been reported to be a strong influencing factor in determining the solvent effect on polymorphism (Khoshkhoo & Anwar, 1993; Lovette & Doherty, 2013; Yang *et al.*, 2014). Hence, more rigorous calculations would be needed to incorporate the solvent interactions in the present modelling approach. This would provide solvent specific crystal-template interaction energies which could aid in developing templates for specific polymorphic nucleation.

6.2.3. Summary

The molecular modelling results corroborate the experimental observations on preferential nucleation of form III CBZ on mercapto and fluoro templates and form II polymorph on cyano template. The variation in interaction energy between the template surface and different facets of the same crystal polymorph could be attributed to the heterogeneous nature of the crystal surfaces (Ho *et al.*, 2009; Modi *et al.*, 2014). The differences in surface functional groups and molecular spacing could influence intermolecular interactions at the template-nucleating crystal interface. Nevertheless, an epitaxial relationship between the template and crystal facet is not anticipated due to the characteristics of the functionalised templates used in this study (Lee *et al.*, 2014). Retrospectively, differences in the dipole moments, hydrogen bonding potentials, and polarity of both the crystal facet and template surfaces is reasoned to cause preferential nucleation of CBZ crystal polymorphs. One or more of these aspects can be effective in altering the thermodynamic (free energy barrier for crystal nucleation) and kinetic factors (molecular self assembling) that affect nucleation and crystal growth. Although solvents were not incorporated in the present modelling approach, the interaction energy associated with preferential nucleation of CBZ crystal polymorphs qualitatively correlates to the free energy advantage for template-induced nucleation derived from the TiPoD analysis (section 5.5). The impact of solvents in template-induced nucleation is a crucial factor that needs to be studied further by calculating solvent-template and solvent-solute interactions. With further development, the modelling approach could be expanded for the

prediction of preferential nucleation propensity for various template chemistries in different solvents.

Chapter 7

Conclusions and Future work

7.1. Conclusions

The aim of this research was to investigate preferential nucleation of polymorphs using template-induced nucleation approach and to elucidate the effect of surface chemistry in preferential nucleation of crystal polymorphs from solution. The major outcomes from this research project are summarised below.

7.1.1. Template chemistry and polymorph nucleation – development of TiPoD plots

Nucleation of CBZ polymorphs from ethanol solution was found to be influenced by the surface chemistry of the templates used to induce heterogeneous nucleation. When clean glass surfaces (control) were used as templates for crystallisation, concomitant nucleation of form II and form III CBZ polymorphs occurred at intermediate concentrations. However, templates with cyano functional groups on the surface preferentially nucleated form II CBZ crystals. In contrast, template surfaces with mercapto and fluoro surface functional groups nucleated more of form III CBZ over form II polymorph. These effects were tracked by determining template-induced polymorphic domains (TiPoD) on a concentration–temperature phase diagram which showed marked differences based on the chemistry of the template surface. The TiPoD plot is a novel concept that clearly depicts the interrelationship between solution conditions and template surface chemistry on the

crystallisation outcome. The TiPoD plots highlighted that the template effect on polymorph nucleation is a significant factor only within a narrow range of supersaturation. Relative free energy advantage for template-induced crystallisation of polymorphs was calculated through analysis of the TiPoD plots. The calculated values of free energy enabled relative quantification of the propensity of templates in inducing preferential polymorph nucleation of the stable and metastable polymorphs. In addition, the scope of TiPoD plots in the present study includes the ability to anticipate the polymorphic results under crystallisation conditions even beyond those reported in this work. The scope of PoD plots could be further extended to study the interrelationships of other factors that govern crystallisation. It could aid systematic and comprehensive study of polymorphic crystallisation under the influence of different operational parameters. Though explained in the context of carbamazepine, a model compound, these aspects of template-induced polymorphic nucleation would be applicable to other compounds under similar conditions. Thus, the possibility of polymorph selective nucleation using templates of different surface chemistry is demonstrated.

7.1.2. Interaction energy calculation using molecular modelling

Towards gaining a mechanistic understanding of the template-induced nucleation process, interfacial interactions between the functional groups on the template surface and the crystal facets of CBZ polymorphs were simulated using molecular modelling. The computational results revealed significant dependency of the interaction energy values on the template surface chemistry. Cyano functionalised templates exhibited highly favourable interaction energy with form II crystal facets while having unfavourable

interaction energy with form III facets. On the other hand, mercapto and fluoro surfaces exhibited more favourable interactions with form III facets than form II facets. These results corroborated well with the experimental observations on preferential nucleation of form II crystals on cyano surface and of form III crystals on mercapto and fluoro surfaces. Thus, templates exhibiting favourable interaction with the dominant facets of a specific crystal polymorph were observed to promote nucleation of that particular polymorph. This modelling approach could aid in the prediction of preferential nucleation of different crystal polymorphs on template surfaces with different chemistries. However, it is to be taken into consideration that the present modelling methodology has neglected the effects of solvents, supersaturation and temperature on calculating interaction energy values. The methodology could be extended further for calculating the competitive interaction of solute and solvent molecules with the template surface and thus to predict template-induced nucleation propensity in different solvents. Nonetheless, the combination of the present modelling methodology and TiPoD plots helps to gain a better knowledge on template-induced nucleation process.

7.1.3. Solvent effect in template-induced nucleation

Solvent plays an important role during nucleation through solute–solvent interactions. These interactions can affect solute conformation and structure of prenucleation aggregates, thereby causing nucleation of specific polymorphs. However, solvent influence is often an aspect neglected in many template-induced nucleation studies. Experimental observations on crystallisation of CBZ polymorphs from various solvents revealed that the impact of template surface chemistry on polymorphic nucleation differs with the solvent polarity.

Templates were able to influence preferential nucleation in solvent with medium polarity such as ethanol, methanol and isopropyl alcohol. However, in a highly polar solvent (acetonitrile) the templates were not so effective in inducing polymorphic selectivity. In the case of a highly non-polar solvent toluene, which typically results in CBZ form II nucleation, mercapto and fluoro templates were effective in nucleating form III CBZ crystals, displaying the influence of template-induced nucleation. The results suggested that the solvent–template interactions were strong in highly polar solvent, thereby hindering solute–template interactions. The combined effects of template surface chemistry and solvent on the polymorphic nucleation behaviour was thus established by determining the TiPoD plots in different solvents. The differences in the nature of TiPoD plots in different solvents further highlights the importance of conducting comprehensive study on template-induced nucleation using different process parameters. This would then aid to choose solvents with the best domains or regimes for achieving polymorphic control through quality-by-design approach.

7.2. Future work

7.2.1. Quartz Crystal Microbalance for probing template-induced nucleation

Template-induced crystal nucleation process is essentially a surface phenomenon. This work has revealed that templates of different surface chemistry can induce nucleation of specific crystal polymorphs through interfacial interaction at the template surface. Accurate detection of nucleation event is a great challenge in crystallisation studies due to the extremely small size of nuclei and the spatially and temporally random nature of nucleation

(Jiang & ter Horst, 2010). Changes in solution properties such as turbidity, density, electrical conductivity, ultrasound velocity, absorption spectra, refraction index and thermal analysis have been used to make inferences on the nucleation event (Marciniak, 2002; Rabesiaka *et al.*, 2011). However, direct measurement of the surface interaction occurring at the time of heterogeneous nucleation poses significant hurdles over and above those associated with the nucleation event itself. Nonetheless, quartz crystal microbalance (QCM) technique can be used for probing the interactions at template surface while possibly detecting the nucleation event. The basic theory of QCM is discussed in Appendix – A.

Two features of QCM make it a highly desirable technique in studying template-induced nucleation process. The first feature is the very basic ability of QCM to detect minuscule changes in mass of adsorbed material and viscoelastic properties of the environment surrounding the resonator. The penetration depth of the probing shear waves in pure water at 20 °C is only about 2500 Å and hence the sensitivity of QCM measurements are limited to very close region from the quartz crystal surface (O'Sullivan & Guilbault, 1999). This is the second feature that makes it ideal to study template-induced nucleation as the region of interest is the events that occur at the interfacial region. The interaction forces at the template surface which influence crystal nucleation is also limited to the immediate proximity to the surface. Through surface treatment, the quartz sensor itself can be made to act as the template. This would provide real time information on changes to the solution properties occurring at the template interface. Changes to the solution molecular structure such as solute aggregation at surface and solute-template interaction

could be examined based on changes in resonant frequency, resistance and dissipation factor. Inferences on the relative strength of solute-template interaction can also be constructed through the analysis of dissipation factor.

QCM technique has been used for determining induction time and metastable zone width for cooling crystallisation of sulfamerzine (Liu *et al.*, 2013). Mechanistic insights into the early stages of crystallisation phenomena such as molecular cluster formation, crystal nucleation and growth were also obtained through analysis of the changes in resonant frequency and resistance. In that study, a quartz sensor with gold electrodes was used where gold also acted as the contact surface for crystallisation. By using sensors with glass or silica coating, the silanisation method used for template preparation in this study can be utilised for creating sensors with different surface chemistry that can double as the template surface for crystallisation. Apart from detecting nucleation event, difference in solute-template interactions and solute aggregation at template interfaces on templates with different surface chemistry could be monitored in real time. This could provide further information on the molecular mechanism of template-induced nucleation and the influence of template chemistry on prenucleation cluster development.

7.2.2. Scale up of template-induced crystallisation process

A primary limitation for practical application of the template-induced nucleation study undertaken in this thesis work is the small batch volume as well as the unstirred crystallisation conditions used. Scaling up the process for achieving polymorph selective crystallisation is a significant challenge. The template surface area per volume of the crystallising solution will become a major factor for achieving preferential nucleation. Development of alternative

particles that can act as template surfaces which could then be used as seeds during crystallisation can be a possible approach to overcome template surface area limitation. Large scale crystallisation will inherently involve stirring of the solution, an important factor that can influence nucleation of polymorphs (Liu *et al.*, 2014). Hence, prior to volumetric scale-up, influence of flow conditions on template induced nucleation will have to be studied. The efficiency of templates for obtaining preferential nucleation can be studied by creating TiPoD plots similar to those developed in this study, but with agitation rate or power per unit volume of solution considered as a design parameter.

Towards the scale up of a template-induced crystallisation process, it is important to develop benign and cost-effective techniques for large scale functionalisation of template surfaces. Techniques to develop stable surface coatings with various surface chemistries and their applicability in crystallisation systems would need to be studied. Also, development of patterned functionalised surfaces would enable application of template-induced nucleation approach for high-throughput polymorph screening.

7.2.3. Investigation of other model systems

Studying the influence of template chemistry on other model compounds is another important step required to establish the wider applicability of this approach. Nucleation of other model drug or excipient systems with different polymorphs needs to be studied with similar templates with different surface chemistries. A limitation of CBZ model system used in this study was the acicular morphology of form II crystals obtained in the study which constrained characterisation of surface properties of the individual facets of

crystal. Other model systems that exhibit polymorphism and which has well defined crystal morphology that aid surface characterisation could benefit developing experimental correlations between crystal and template surface properties.

7.3. Scope for application of template chemistry for nucleation control

With precise knowledge on the fundamental mechanism of template-induced nucleation, this approach can be used to control crystal nucleation in various technological applications. Some of the possible applications that could be foreseen with template-induced nucleation approach are highlighted here.

7.3.1. Polymorph screening

Polymorph screening is an essential step in crystallisation process development of any new drug molecule that needs to be formulated as a solid dosage form. At this stage, the operating and solution conditions influencing polymorphic crystallisation are screened by conducting hundreds of small-volume batch crystallisation experiments simultaneously (Cross *et al.*, 2002). High-throughput crystallisation experiments using well plate method is commonly used in polymorph screenings (Morissette *et al.*, 2004). The surface functionality of these well plates could be modified to induce heterogeneous nucleation under the influence of a wide range of properties such surface energy, polarity, hydrogen-donating or accepting functional groups. The small volume (typically <0.5 ml) of these wells make it ideal for template-induced nucleation due to the high surface area to volume ratio. Medium-throughput multi-batch crystallisers (such as Avantium Crystal16® or CrystalBreeder®

systems) commonly used for early stage crystallisation studies could also be modified to incorporate the templating effect on nucleation. Such crystallisers typically use glass vessels which can be silanised to produce the desired surface chemistry. As revealed through this study, surface interactions at the walls of the vessel could potentially nucleate either metastable or stable polymorphs. Furthermore, interactions with the template surface may stabilise metastable polymorphs, which otherwise could have been missed in the screening process due to fast solution-mediated polymorphic conversions.

7.3.2. Polymorphic purity

Nucleation of polymorphs under the influence of template surfaces could be utilised for either promoting or hindering the formation of specific polymorphs. The latter strategy is particularly helpful in avoiding unwanted nucleation during crystallisation which might affect product purity. Surface chemistry at interfaces in contact with the solution could be analysed and modified towards this goal. Molecular modelling could be used as a tool for predicting the effect of surface chemistry in promoting or inhibiting nucleation of specific polymorphs.

In small scale, template-induced nucleation could be achieved through immersing functionalised template surfaces in crystallising solution. However, with the development of new crystallisation reactor systems, the application of surface chemistry for polymorph control could take up new scenarios as discussed below.

7.3.2.1. Continuous crystallisation

Development of continuous crystallisation has received much attention recently. Many different configurations of continuous crystallisers have been

proposed for achieving consistent product quality in terms of crystal size distribution, polymorphism and yield (Zhang *et al.*, 2014). Two of the promising continuous crystalliser configurations are plug flow crystalliser and continuous oscillatory baffled crystalliser (Alvarez & Myerson, 2010; Zhao *et al.*, 2014). The walls of these crystallisers comprising of long tubes can act as templates that could trigger heterogeneous nucleation. Fouling or encrustation at the wall surface due to crystal growth has been reported as an obstacle in developing continuous flow crystallisation systems (Jiang *et al.*, 2014). Modelling approach used for template-induced nucleation could be used for screening suitable surface chemistry either for promoting nucleation of suitable polymorphs or for hindering nucleation. By functionalising the wall surfaces with suitable chemistry further control on crystallisation could be obtained in continuous crystallisers.

7.3.2.2. Producing nanocrystals

Formulation of drug crystals in the size range less than 100 nm is suggested to significantly improve the bioavailability of poorly water-soluble drugs (Elsayed *et al.*, 2014). With a significant proportion of the new drugs in pharmaceutical development pipeline possessing low aqueous solubility, methods for producing nanocrystal is becoming more and more significant (Keck & Müller, 2006). Several production routes such as precipitation, milling and high pressure homogenisation have been adopted by pharmaceutical industries for producing drug nanocrystals (Junghanns & Müller, 2008). Nonetheless, direct synthesis of nanoscale crystals through controlled crystallisation could overcome limitations of high energy input, multiple processing stages and low yield associated with top-down approaches

where the larger sized crystals are broken down to nano-scale particles (de Waard *et al.*, 2008). In thin-film crystallisation methods commonly used for producing inorganic nanocrystals, surface chemistry of the evaporating surface is known to play a significant role in controlling nucleation kinetics. On adapting this method for organic systems, knowledge developed through template-induced nucleation studies could be utilised for selective nucleation of nanocrystals polymorphs.

7.3.3. Seeding

Seeding is the most commonly used industrial practice to ensure polymorphic selectivity. The process involves addition of small seed crystals of the required polymorphic form into the crystallising solution to grow and/or nucleate the same crystal form. However, it is known that different processing routes used for generating seed crystals can produce crystals with different surface properties (Shah *et al.*, 2014). Milling of crystals could expose inner planes of crystals which are otherwise inaccessible and can modify the surface polarity of seed crystals (Ho *et al.*, 2012). In such cases, the effect of seed surface properties on polymorph control could be better understood by tracking the polymorphic domains via template-induced nucleation approach, i.e. by plotting TiPoD for various surface chemistries. Moreover, in cases where heterogeneous seeding is acceptable, template particles with different surface chemistries could be used to produce different polymorphs under identical crystallization conditions. For instance, crystal surfaces of excipient molecules such as mannitol could themselves act as heterogeneous seeds or could be functionalised to exhibit different surface chemistries. However, it is to be acknowledged that usage of heterogeneous seeds for pharmaceutical

crystallisation could be a major challenge due to regulatory issues. Nonetheless, heterogeneous seeding could be adopted in other industrial crystallisations such as agrochemical industry where the use of appropriate heterogeneous seeds would not be a serious roadblock for development and commercial approval.

7.4. Concluding remarks

Nucleation of CBZ crystal polymorphs was found to be influenced by the chemistry of the template surfaces used to induce heterogeneous nucleation. Template-induced polymorphic domain (TiPoD) plots capture the effect of surface chemistry, temperature and solution supersaturation on polymorph nucleation. TiPoD plots provide insight into the design considerations for utilising template-induced nucleation process. It could also lead to new interpretations and implications of the conventional phase diagrams used for crystallisation design purpose. The free energy calculations based on TiPoD plots and interaction energy calculations through molecular modelling underscores the propensity of different templates on selective polymorphic nucleation. Templates are found to be effective in different solvents though their impact is less in highly polar solvents.

Studying crystal nucleation through template-induced nucleation approach could provide valuable information on heterogeneous nucleation process and help control the process better. Advance techniques such as QCM could potentially provide real time information on template-solute interaction and track nucleation from early stages. Utilising other model systems for template-induced nucleation will enable to create a wider acceptance and understanding of the process. Furthermore, development of new template

surfaces with different surface properties could enhance the efficiency of polymorph screening and crystallisation. With more and more rigorous and elaborate polymorph screening methods being developed following McCrone's (1965) opinion that "the number of forms known for a given compound is proportional to the time and money spend in research on that compound", template surfaces could provide a valuable handle in future screening methods. However, understanding template–solute interactions during template-induced nucleation could also complement computational tools that predict polymorphism, to provide suitable template substrates that result in the nucleation of predicted crystal forms. Moreover, effect of surface properties of seeds or other particulates on crystallisation could also be better comprehended with the help of template-induced nucleation approach. Further work on template-induced nucleation can also aid in developing modelling tools that can incorporate the effect of surface properties on crystallisation process.

The different chemistries of surfaces that come in contact with the crystallisation solution is often overlooked in general crystallisation process. The results in this study show that the surface chemistry of the crystallisation vessel, agitator or probes could potentially alter the nucleation behaviour of the solute. The effect of surfaces on nucleation would become more relevant when the surface area to volume ratio is high. This consideration could be potentially utilised in developing novel designs for continuous crystallisation process. High-throughput devices for polymorph screening and new crystallisation techniques for generating nano-crystals are also probable to

exhibit high surface area volume ratio where template effect would be important.

References

Aitipamula, S., & Nangia, A. (2012). Polymorphism: Fundamentals and Applications *Supramolecular Chemistry*: John Wiley & Sons, Ltd.

Aizenberg, J., Black, A. J., & Whitesides, G. M. (1999). Oriented Growth of Calcite Controlled by Self-Assembled Monolayers of Functionalized Alkanethiols Supported on Gold and Silver. *Journal of the American Chemical Society, 121*(18), 4500-4509.

Allesø, M., van den Berg, F., Cornett, C., Jørgensen, F. S., Halling-Sørensen, B., de Diego, H. L., . . . Rantanen, J. (2008). Solvent diversity in polymorph screening. *Journal of Pharmaceutical Sciences, 97*(6), 2145-2159.

Alvarez, A. J., & Myerson, A. S. (2010). Continuous Plug Flow Crystallization of Pharmaceutical Compounds. *Crystal Growth & Design, 10*(5), 2219-2228.

Alvarez, A. J., Singh, A., & Myerson, A. S. (2009). Polymorph Screening: Comparing a Semi-Automated Approach with a High Throughput Method. *Crystal Growth & Design, 9*(9), 4181-4188.

Arlin, J. B., Price, L. S., Price, S. L., & Florence, A. J. (2011). A strategy for producing predicted polymorphs: catemeric carbamazepine form V. *Chem Commun (Camb), 47*(25), 7074-7076.

Arwin, H. (2000). Ellipsometry on thin organic layers of biological interest: characterization and applications. *Thin Solid Films, 377–378*(0), 48-56.

Babu, N. J., Cherukuvada, S., Thakuria, R., & Nangia, A. (2010). Conformational and Synthon Polymorphism in Furosemide (Lasix). *Crystal Growth & Design, 10*(4), 1979-1989.

Babu, N. J., & Nangia, A. (2007). High *Z'* polymorphs have shorter C-HO interactions and O-HO hydrogen bonds. *CrystEngComm, 9*(11), 980-983.

Bernardes, C. E. S., Lopes, M. L. S. M., Ascenso, J. R., & da Piedade, M. E. M. (2014). From Molecules to Crystals: The Solvent Plays an Active Role Throughout the Nucleation Pathway of Molecular Organic Crystals. *Crystal Growth & Design, 14*(11), 5436-5441.

Bernstein, J. (2007). *Polymorphism in Molecular Crystals*. Oxford: Oxford University Press.

Bernstein, J., Davey, R. J., & Henck, J.-O. (1999). Concomitant Polymorphs. *Angewandte Chemie International Edition, 38*, 3440-3461.

Bruckenstein, S., & Shay, M. (1985). Experimental aspects of use of the quartz crystal microbalance in solution. *Electrochimica Acta, 30*(10), 1295-1300.

Bučar, D.-K., Day, G. M., Halasz, I., Zhang, G. G. Z., Sander, J. R. G., Reid, D. G., . . . Jones, W. (2013). The curious case of (caffeine)·(benzoic acid): how heteronuclear seeding allowed the formation of an elusive cocrystal. *Chemical Science, 4*(12), 4417.

Burger, A., & Ramberger, R. (1979a). On the polymorphism of pharmaceuticals and other molecular crystals. I. *Microchimica Acta, 72*(3-4), 259-271.

Burger, A., & Ramberger, R. (1979b). On the polymorphism of pharmaceuticals and other molecular crystals. II. *Microchimica Acta, 72*(3-4), 273-316.

Byrn, S., Pfeiffer, R., Ganey, M., Hoiberg, C., & Poochikian, G. (1995). Pharmaceutical Solids: A Strategic Approach to Regulatory Considerations. *Pharmaceutical Research, 12*(7), 945-954.

Campbell, J. M., Meldrum, F. C., & Christenson, H. K. (2013). Characterization of Preferred Crystal Nucleation Sites on Mica Surfaces. *Crystal Growth & Design, 13*(5), 1915-1925.

Capacci-Daniel, C., Gaskell, K. J., & Swift, J. A. (2010). Nucleation and Growth of Metastable Polymorphs on Siloxane Monolayer Templates. *Crystal Growth & Design, 10*(2), 952-962.

Capes, J. S., & Cameron, R. E. (2007). Contact line crystallisation to obtain metastable polymorphs. *Crystal Growth & Design, 7*(1), 108-112.

Cardew, P. T., & Davey, R. J. (1982). *Kinetic factors in the appearance and transformation of metastable phases.* Paper presented at the Tailoring of Crystal growth: Control of purity, form and size distribution, Institute of Chemical Engineers (North-Western Branch).

Caridi, A., Kulkarni, S. A., Di Profio, G., Curcio, E., & ter Horst, J. H. (2014). Template-Induced Nucleation of Isonicotinamide Polymorphs. *Crystal Growth & Design, 14*(3), 1135-1141.

Chadwick, K., Chen, J., Myerson, A. S., & Trout, B. L. (2012). Toward the Rational Design of Crystalline Surfaces for Heteroepitaxy: Role of Molecular Functionality. *Crystal Growth & Design, 12*(3), 1159-1166.

Chaudhuri, K. R. (2008). Crystallisation within transdermal rotigotine patch: is there cause for concern? *Expert Opinion on Drug Delivery*, *5*(11), 1169-1171.

Chen, J., Sarma, B., Evans, J. M. B., & Myerson, A. S. (2011). Pharmaceutical Crystallization. *Crystal Growth & Design, 11*(4), 887-895.

Chen, S., Guzei, I. A., & Yu, L. (2005a). New Polymorphs of ROY and New Record for Coexisting Polymorphs of Solved Structures. *Journal of the American Chemical Society*, *127*(27), 9881-9885.

Chen, S., Xi, H., & Yu, L. (2005b). Cross-Nucleation between ROY Polymorphs. *Journal of the American Chemical Society, 127*(49), 17439-17444.

Cimarosti, Z., Castagnoli, C., Rossetti, M., Scarati, M., Day, C., Johnson, B., & Westerduin, P. (2010). Development of Drug Substances as Mixture of Polymorphs: Studies to Control Form 3 in Casopitant Mesylate. *Organic Process Research & Development, 14*(6), 1337-1346.

Cote, A., Zhou, G., & Stanik, M. (2009). A Novel Crystallization Methodology To Ensure Isolation of the Most Stable Crystal Form. *Organic Process Research & Development, 13*(6), 1276-1283.

Cras, J. J., Rowe-Taitt, C. A., Nivens, D. A., & Ligler, F. S. (1999). Comparison of chemical cleaning methods of glass in preparation for silanization. *Biosensors and Bioelectronics, 14*(8–9), 683-688.

Cross, W. I., Blagden, N., Davey, R. J., Pritchard, R. G., Neumann, M. A., Roberts, R. J., & Rowe, R. C. (2002). A Whole Output Strategy for Polymorph Screening: Combining Crystal Structure Prediction, Graph Set Analysis, and Targeted Crystallization Experiments in the Case of Diflunisal. *Crystal Growth & Design, 3*(2), 151-158.

Cruz Cabeza, A. J., Day, G. M., Motherwell, W. D. S., & Jones, W. (2006). Amide Pyramidalization in Carbamazepine: A Flexibility Problem in Crystal Structure Prediction? *Crystal Growth & Design, 6*(8), 1858-1866.

Curcio, E., López-Mejías, V., Di Profio, G., Fontananova, E., Drioli, E., Trout, B. L., & Myerson, A. S. (2014). Regulating Nucleation Kinetics through Molecular Interactions at the Polymer–Solute Interface. *Crystal Growth & Design, 14*(2), 678-686.

Dabros, M., & Thalladi, V. R. (2007). Effect of alkyl chain parity on the face-selective crystal growth of a drug polymorph. *Chemical Communications*(24), 2476-2478.

Datta, S., & Grant, D. J. W. (2005). Effect of supersaturation on the crystallization of phenylbutazone polymorphs. *Crystal Research and Technology, 40*(3), 233-242.

Davey, R. J. (2003). Pizzas, polymorphs and pills. *Chemical Communications*(13), 1463-1467.

Davey, R. J., Allen, K., Blagden, N., Cross, W. I., Lieberman, H. F., Quayle, M. J., . . . Tiddy, G. J. T. (2002). Crystal engineering - nucleation, the key step. *CrystEngComm, 4*(47), 257.

Davey, R. J., Blagden, N., Righini, S., Alison, H., Quayle, M. J., & Fuller, S. (2001). Crystal polymorphism as a probe for molecular self-assembly during nucleation from solutions: The case of 2,6-Dihydroxybenzoic acid. *Crystal Growth & Design, 1*(1), 59-65.

Davey, R. J., Schroeder, S. L., & ter Horst, J. H. (2013). Nucleation of organic crystals - A molecular perspective. *Angew Chem Int Ed Engl, 52*(8), 2166-2179.

De Villiers, M. M., van der Watt, J. G., & Lötter, A. P. (1992). Kinetic study of the solid-state photolytic degradation of two polymorphic forms of furosemide. *International Journal of Pharmaceutics, 88*(1–3), 275-283.

de Waard, H., Hinrichs, W. L. J., & Frijlink, H. W. (2008). A novel bottom–up process to produce drug nanocrystals: Controlled crystallization during freeze-drying. *Journal of Controlled Release, 128*(2), 179-183.

Della Volpe, C., Maniglio, D., Brugnara, M., Siboni, S., & Morra, M. (2004). The solid surface free energy calculation. I. In defense of the multicomponent approach. *J Colloid Interface Sci, 271*(2), 434-453.

Desiraju, G. R. (1995). Supramolecular Synthons in Crystal Engineering—A New Organic Synthesis. *Angewandte Chemie International Edition in English, 34*(21), 2311-2327.

Di Profio, G., Fontananova, E., Curcio, E., & Drioli, E. (2012). From Tailored Supports to Controlled Nucleation: Exploring Material Chemistry, Surface Nanostructure, and Wetting Regime Effects in Heterogeneous Nucleation of Organic Molecules. *Crystal Growth & Design, 12*(7), 3749-3757.

Diao, Y., Helgeson, M. E., Myerson, A. S., Hatton, T. A., Doyle, P. S., & Trout, B. L. (2011a). Controlled Nucleation from Solution Using Polymer Microgels. *Journal of the American Chemical Society, 133*(11), 3756-3759.

Diao, Y., Helgeson, M. E., Siam, Z. A., Doyle, P. S., Myerson, A. S., Hatton, T. A., & Trout, B. L. (2011b). Nucleation under Soft Confinement: Role of Polymer–Solute Interactions. *Crystal Growth & Design, 12*(1), 508-517.

Diao, Y., Myerson, A. S., Hatton, T. A., & Trout, B. L. (2011c). Surface Design for Controlled Crystallization: The Role of Surface Chemistry and Nanoscale Pores in Heterogeneous Nucleation. *Langmuir, 27*(9), 5324-5334.

Dixon, M. C. (2008). Quartz Crystal Microbalance with Dissipation Monitoring: Enabling Real-Time Characterization of Biological Materials and Their Interactions. *Journal of Biomolecular Techniques : JBT, 19*(3), 151-158.

Docherty, R., Clydesdale, G., Roberts, K. J., & Bennema, P. (1991). Application of Bravais-Friedel-Donnay-Harker, attachment energy and Ising models to predicting and understanding the morphology of molecular crystals. *Journal of Physics D: Applied Physics, 24*(2), 89.

Dressler, D. H., & Mastai, Y. (2007). Controlling Polymorphism by Crystallization on Self-Assembled Multilayers. *Crystal Growth & Design, 7*(5), 847-850.

Du, W., Yin, Q., Gong, J., Bao, Y., Zhang, X., Sun, X., . . . Hao, H. (2014). Effects of Solvent on Polymorph Formation and Nucleation of Prasugrel Hydrochloride. *Crystal Growth & Design, 14*(9), 4519-4525.

Ectors, P., Duchstein, P., & Zahn, D. (2014). Nucleation Mechanisms of a Polymorphic Molecular Crystal: Solvent-Dependent Structural Evolution of Benzamide Aggregates. *Crystal Growth & Design, 14*(6), 2972-2976.

Edwards, A. D., Shekunov, B. Y., Forbes, R. T., Grossmann, J. G., & York, P. (2001). Time-resolved X-ray scattering using synchrotron radiation applied to the study of a polymorphic transition in carbamazepine. *Journal of Pharmaceutical Sciences, 90*(8), 1106-1114.

Elsayed, I., Abdelbary, A. A., & Elshafeey, A. H. (2014). Nanosizing of a poorly soluble drug: technique optimization, factorial analysis, and pharmacokinetic study in healthy human volunteers *International Journal of Nanomedicine, 9*(1), 2943-2953.

Erdemir, D., Lee, A. Y., & Myerson, A. S. (2009). Nucleation of Crystals from Solution: Classical and Two-Step Models. *Accounts of Chemical Research, 42*(5), 621-629.

Fernandes, P., Shankland, K., Florence, A. J., Shankland, N., & Johnston, A. (2007). Solving molecular crystal structures from X-ray powder diffraction data: The challenges posed by γ-carbamazepine and chlorothiazide N,N,-dimethylformamide (1/2) solvate. *Journal of Pharmaceutical Sciences, 96*(5), 1192-1202.

Ferraria, A. M., Lopes da Silva, J. D., & Botelho do Rego, A. M. (2003). XPS studies of directly fluorinated HDPE: problems and solutions. *Polymer, 44*(23), 7241-7249.

Filobelo, L. F., Galkin, O., & Vekilov, P. G. (2005). Spinodal for the solution-to-crystal phase transformation. *The Journal of Chemical Physics, 123*(1), 014904.

Fisher, C. J. (1948). The Fracture of Liquids. *Journal of Applied Physics, 19*, 1062-1067.

Florence, A. J., Johnston, A., Price, S. L., Nowell, H., Kennedy, A. R., & Shankland, N. (2006). An automated parallel crystallisation search for

predicted crystal structures and packing motifs of carbamazepine. *Journal of Pharmaceutical Sciences, 95*(9), 1918-1930.

Fowkes, F. M. (1962). Determination of Interfacial Tensions, Contact Angles, and Dispersion Forces in Surfaces by Assuming Additivity of Intermolecular Interactions in Surfaces. *The Journal of Physical Chemistry, 66*(2), 382-382.

Freeman, C. L., Harding, J. H., & Duffy, D. M. (2008). Simulations of Calcite Crystallization on Self-Assembled Monolayers. *Langmuir, 24*(17), 9607-9615.

Gavezzotti, A. (2005). Quantitative Ranking of Crystal Packing Modes by Systematic Calculations on Potential Energies and Vibrational Amplitudes of Molecular Dimers. *Journal of Chemical Theory and Computation, 1*(5), 834-840.

Gavezzotti, A. (2007). *Molecular Aggregation: Structural analysis and molecular simulation of crystals and liquids*: Oxford University Press.

Gebauer, D., & Cölfen, H. (2011). Prenucleation clusters and non-classical nucleation. *Nano Today, 6*(6), 564-584.

Gelbrich, T., Hughes, D. S., Hursthouse, M. B., & Threlfall, T. L. (2008). Packing similarity in polymorphs of sulfathiazole. *CrystEngComm, 10*(10), 1328-1334.

Grant, D. J. W. (1999). Theory and origin of polymorphism. In H. G. Brittain (Ed.), *Polymorphism in pharmaceutical solids* (2 ed.): CRC Press.

Graubner, G., Rengarajan, G. T., Anders, N., Sonnenberger, N., Enke, D., Beiner, M., & Steinhart, M. (2013). Morphology of Porous Hosts Directs Preferred Polymorph Formation and Influences Kinetics of Solid/Solid Transitions of Confined Pharmaceuticals. *Crystal Growth & Design, 14*(1), 78-86.

Gregory, E. A. (1995). Physical and Mechanical Property Characterization of Powders *Physical Characterization of Pharmaceutical Solids* (pp. 281-319): CRC Press.

Grzesiak, A. L., Lang, M., Kim, K., & Matzger, A. J. (2003). Comparison of the four anhydrous polymorphs of carbamazepine and the crystal

structure of form I. *Journal of Pharmaceutical Sciences, 92*(11), 2260-2271.

Gu, C.-H., Li, H., Gandhi, R. B., & Raghavan, K. (2004). Grouping solvents by statistical analysis of solvent property parameters: implication to polymorph screening. *International Journal of Pharmaceutics, 283*(1–2), 117-125.

Gu, C.-H., Young, V., & Grant, D. J. W. (2001). Polymorph screening: Influence of solvents on the rate of solvent-mediated polymorphic transformation. *Journal of Pharmaceutical Sciences, 90*(11), 1878-1890.

Ha, J.-M., Wolf, J. H., Hillmyer, M. A., & Ward, M. D. (2004). Polymorph Selectivity under Nanoscopic Confinement. *Journal of the American Chemical Society, 126*(11), 3382-3383.

Haisa, M., Kashino, S., & Maeda, H. (1974). The orthorhombic form of p-hydroxyacetanilide. *Acta Crystallographica Section B, 30*(10), 2510-2512.

Haleblian, J., & McCrone, W. (1969). Pharmaceutical applications of polymorphism. *Journal of Pharmaceutical Sciences, 58*(8), 911-929.

Halliwell, C. M., & Cass, A. E. G. (2001). A Factorial Analysis of Silanization Conditions for the Immobilization of Oligonucleotides on Glass Surfaces. *Analytical Chemistry, 73*(11), 2476-2483.

Hamad, S., Moon, C., Catlow, C. R. A., Hulme, A. T., & Price, S. L. (2006). Kinetic Insights into the Role of the Solvent in the Polymorphism of 5-Fluorouracil from Molecular Dynamics Simulations. *The Journal of Physical Chemistry B, 110*(7), 3323-3329.

Hammond, R. B., Pencheva, K., & Roberts, K. J. (2007). Molecular Modeling of Crystal−Crystal Interactions between the α- and β-Polymorphic Forms of l-Glutamic Acid Using Grid-Based Methods. *Crystal Growth & Design, 7*(5), 875-884.

Harding, J. H., Freeman, C. L., & Duffy, D. M. (2014). Oriented crystal growth on organic monolayers. *CrystEngComm, 16*(8), 1430-1438.

Harris, R. K., Ghi, P. Y., Puschmann, H., Apperley, D. C., Griesser, U. J., Hammond, R. B., . . . Pickard, C. J. (2005). Structural Studies of the Polymorphs of Carbamazepine, Its Dihydrate, and Two Solvates. *Organic Process Research & Development, 9*(6), 902-910.

Hartman, P., & Bennema, P. (1980). The attachment energy as a habit controlling factor: I. Theoretical considerations. *Journal of Crystal Growth, 49*(1), 145-156.

Heng, J. Y. Y. (2005). *Anisotropic surface properties of crystalline pharmaceutical solids.* (Doctor of Philosophy), University of London, London.

Hillier, A., & Ward, M. (1996). Epitaxial interactions between molecular overlayers and ordered substrates. *Physical Review B, 54*(19), 14037-14051.

Himes, V. L., Mighell, A. D., & De Camp, W. H. (1981). Structure of carbamazepine: 5H-dibenz[b,f]azepine-5-carboxamide. *Acta Crystallographica Section B, 37*(12), 2242-2245.

Hiremath, R., Basile, J. A., Varney, S. W., & Swift, J. A. (2005). Controlling molecular crystal polymorphism with self-assembled monolayer templates. *Journal of the American Chemical Society, 127*(51), 18321-18327.

Hiremath, R., Varney, S. W., & Swift, J. A. (2004). Oriented Crystal Growth of 4-Iodo-4'-nitrobiphenyl on Polar Self-Assembled Monolayer Templates: A Case for "Chemical Epitaxy". *Chemistry of Materials, 16*(24), 4948-4954.

Ho, R., Naderi, M., Heng, J. Y., Williams, D., Thielmann, F., Bouza, P., . . . Burnett, D. (2012). Effect of Milling on Particle Shape and Surface Energy Heterogeneity of Needle-Shaped Crystals. *Pharmaceutical Research, 29*(10), 2806-2816.

Ho, R., Wilson, D. A., & Heng, J. Y. Y. (2009). Crystal Habits and the Variation in Surface Energy Heterogeneity. *Crystal Growth & Design, 9*(11), 4907-4911.

Hulme, A. T., Johnston, A., Florence, A. J., Fernandes, P., Shankland, K., Bedford, C. T., . . . Price, S. L. (2007). Search for a Predicted Hydrogen Bonding Motif − A Multidisciplinary Investigation into the

Polymorphism of 3-Azabicyclo[3.3.1]nonane-2,4-dione. *Journal of the American Chemical Society*, *129*(12), 3649-3657.

Hunter, C. A., McCabe, J. F., & Spitaleri, A. (2012). Solvent effects of the structures of prenucleation aggregates of carbamazepine. *CrystEngComm, 14*(21), 7115.

Igarashi, K., Azuma, M., Kato, J., & Ooshima, H. (1999). The initial stage of crystallization of lysozyme: a differential scanning calorimetric (DSC) study. *Journal of Crystal Growth*, *204*(1–2), 191-200.

Jiang, M., Zhu, Z., Jimenez, E., Papageorgiou, C. D., Waetzig, J., Hardy, A., . . . Braatz, R. D. (2014). Continuous-Flow Tubular Crystallization in Slugs Spontaneously Induced by Hydrodynamics. *Crystal Growth & Design*, *14*(2), 851-860.

Jiang, S., & ter Horst, J. H. (2010). Crystal Nucleation Rates from Probability Distributions of Induction Times. *Crystal Growth & Design, 11*(1), 256-261.

Junghanns, J.-U. A. H., & Müller, R. H. (2008). Nanocrystal technology, drug delivery and clinical applications. *International Journal of Nanomedicine, 3*(3), 295-310.

Karami, S., Li, Y., Hughes, D. S., Hursthouse, M. B., Russell, A. E., Threlfall, T. L., . . . Roberts, R. (2006). Further errors in polymorph identification: furosemide and finasteride. *Acta Crystallographica Section B, 62*(4), 689-691.

Keck, C. M., & Müller, R. H. (2006). Drug nanocrystals of poorly soluble drugs produced by high pressure homogenisation. *European Journal of Pharmaceutics and Biopharmaceutics, 62*(1), 3-16.

Keiji Kanazawa, K., & Gordon Ii, J. G. (1985). The oscillation frequency of a quartz resonator in contact with liquid. *Analytica Chimica Acta, 175*(0), 99-105.

Khoshkhoo, S., & Anwar, J. (1993). Crystallization of polymorphs: the effect of solvent. *Journal of Physics D: Applied Physics*, *26*(8B), B90.

Kitamura, M. (2004). Controlling Factors and Mechanism of Polymorphic Crystallization. *Crystal Growth & Design, 4*(6), 1153-1159.

Kogan, A., Popov, I., Uvarov, V., Cohen, S., Aserin, A., & Garti, N. (2007). Crystallization of Carbamazepine Pseudopolymorphs from Nonionic Microemulsions. *Langmuir, 24*(3), 722-733.

Konkel, J. T., & Myerson, A. S. (2011). Empirical Molecular Modeling of Suspension Stabilization with Polysorbate 80 *Industrial Applications of Molecular Simulations* (pp. 195-202): CRC Press.

Kuhs, M., Zeglinski, J., & Rasmuson, Å. C. (2014). Influence of History of Solution in Crystal Nucleation of Fenoxycarb: Kinetics and Mechanisms. *Crystal Growth & Design, 14*(3), 905-915.

Kulkarni, S. A., Weber, C. C., Myerson, A. S., & ter Horst, J. H. (2014). Self-association during heterogeneous nucleation onto well-defined templates. *Langmuir, 30*(41), 12368-12375.

Kwokal, A., & Roberts, K. J. (2014). Direction of the polymorphic form of entacapone using an electrochemical tuneable surface template. *CrystEngComm, 16*(17), 3487-3493.

Landau, E. M., Levanon, M., Leiserowitz, L., Lahav, M., & Sagiv, J. (1985). Transfer of structural information from Langmuir monolayers to three-dimensional growing crystals. *Nature, 318*(6044), 353-356.

Lang, M., Kampf, J. W., & Matzger, A. J. (2002). Form IV of carbamazepine. *Journal of Pharmaceutical Sciences, 91*(4), 1186-1190.

Lang, M. D., Grzesiak, A. L., & Matzger, A. J. (2002). The use of polymer heteronuclei for crystalline polymorph selection. *Journal of the American Chemical Society, 124*(50), 14834-14835.

Lee, A. Y., Erdemir, D., & Myerson, A. S. (2011). Crystal Polymorphism in Chemical Process Development. *Annual Review of Chemical and Biomolecular Engineering, 2*(1), 259-280.

Lee, A. Y., Lee, I. S., Dette, S. S., Boerner, J., & Myerson, A. S. (2005). Crystallization on Confined Engineered Surfaces: A Method to Control Crystal Size and Generate Different Polymorphs. *Journal of the American Chemical Society, 127*(43), 14982-14983.

Lee, A. Y., Lee, I. S., & Myerson, A. S. (2006). Factors Affecting the Polymorphic Outcome of Glycine Crystals Constrained on Patterned Substrates. *Chemical Engineering & Technology, 29*(2), 281-285.

Lee, A. Y., Ulman, A., & Myerson, A. S. (2002). Crystallization of amino acids on self-assembled monolayers of rigid thiols on gold. *Langmuir, 18*(15), 5886-5898.

Lee, D., Monin, G., Duong, N. T., Lopez, I. Z., Bardet, M., Mareau, V., . . . De Paepe, G. (2014). Untangling the condensation network of organosiloxanes on nanoparticles using 2D (29)Si-(29)Si solid-state NMR enhanced by dynamic nuclear polarization. *J Am Chem Soc, 136*(39), 13781-13788.

Lefebvre, C., Guyot-Hermann, A. M., Draguet-Brughmans, M., Bouché, R., & Guyot, J. C. (1986). Polymorphic Transitions of Carbamazepine During Grinding and Compression. *Drug Development and Industrial Pharmacy, 12*(11-13), 1913-1927.

Leiserowitz, L. (1976). Molecular packing modes. Carboxylic acids. *Acta Crystallographica Section B, 32*(3), 775-802.

Liu, J., Svärd, M., & Rasmuson, Å. C. (2014). Influence of Agitation and Fluid Shear on Nucleation ofm-Hydroxybenzoic Acid Polymorphs. *Crystal Growth & Design, 14*(11), 5521-5531.

Liu, L.-S., Kim, J., Chang, S.-M., Choi, G. J., & Kim, W.-S. (2013). Quartz Crystal Microbalance Technique for Analysis of Cooling Crystallization. *Analytical Chemistry, 85*(9), 4790-4796.

Liu, W., Dang, L., Black, S., & Wei, H. (2008). Solubility of Carbamazepine (Form III) in Different Solvents from (275 to 343) K. *Journal of Chemical & Engineering Data, 53*(9), 2204-2206.

Lopez-Mejias, V., Kampf, J. W., & Matzger, A. J. (2009). Polymer-Induced Heteronucleation of Tolfenamic Acid: Structural Investigation of a Pentamorph. *Journal of the American Chemical Society, 131*(13), 4554-4555.

López-Mejías, V., Myerson, A. S., & Trout, B. L. (2013). Geometric Design of Heterogeneous Nucleation Sites on Biocompatible Surfaces. *Crystal Growth & Design, 13*(8), 3835-3841.

Louhi-Kultanen, M., Karjalainen, M., Rantanen, J., Huhtanen, M., & Kallas, J. (2006). Crystallization of glycine with ultrasound. *Int J Pharm, 320*(1-2), 23-29.

Lovette, M. A., & Doherty, M. F. (2013). Needle-Shaped Crystals: Causality and Solvent Selection Guidance Based on Periodic Bond Chains. *Crystal Growth & Design, 13*(8), 3341-3352.

Lowes, M. M. J., Caira, M. R., Lotter, A. P., & Van Watt, J. G. D. (1987). Physicochemical properties and x-ray structural studies of the trigonal polymorph of carbamazepine. *Journal of Pharmaceutical Sciences, 76*(9), 744-752.

Lucklum, R., & Hauptmann, P. (2000). The quartz crystal microbalance: mass sensitivity, viscoelasticity and acoustic amplification. *Sensors and Actuators B: Chemical, 70*(1–3), 30-36.

Maeda, T., Takenaka, H., Yamahira, Y., & Noguchi, T. (1980). Use of Rabbits for Absorption Studies on Polymorphs of Chloramphenicol Palmitate. *Chemical & pharmaceutical bulletin, 28*(2), 431-436.

Marciniak, B. (2002). Density and ultrasonic velocity of undersaturated and supersaturated solutions of fluoranthene in trichloroethylene, and study of their metastable zone width. *Journal of Crystal Growth, 236*(1–3), 347-356.

Mattei, A., & Li, T. (2011). Polymorph Formation and Nucleation Mechanism of Tolfenamic Acid in Solution: An Investigation of Pre-nucleation Solute Association. *Pharmaceutical Research, 29*(2), 460-470.

McCrone, W. C. (1965). Polymorphism. In D. Fox, M. M. Labes & A. Weissberger (Eds.), *Physics and Chemistry of the Organic Solid State* (Vol. 2, pp. 725-767). New York: Wiley Interscience.

Meenan, P. A., Anderson, S. R., & Klug, D. L. (2002). The influence of impurities and solvents on crystallization. In A. S. Myerson (Ed.), *Handbook of Industrial Crystallization (Second Edition)* (pp. 67-100). Woburn: Butterworth-Heinemann.

Mitchell, C. A., Yu, L., & Ward, M. D. (2001). Selective Nucleation and Discovery of Organic Polymorphs through Epitaxy with Single Crystal Substrates. *Journal of the American Chemical Society, 123*(44), 10830-10839.

Modi, S. R., Dantuluri, A. K. R., Perumalla, S. R., Sun, C. C., & Bansal, A. K. (2014). Effect of Crystal Habit on Intrinsic Dissolution Behavior of Celecoxib Due to Differential Wettability. *Crystal Growth & Design, 14*(10), 5283-5292.

Morissette, S. L., Almarsson, Ö., Peterson, M. L., Remenar, J. F., Read, M. J., Lemmo, A. V., . . . Gardner, C. R. (2004). High-throughput crystallization: polymorphs, salts, co-crystals and solvates of pharmaceutical solids. *Advanced Drug Delivery Reviews, 56*(3), 275-300.

Muller, F. L., Fielding, M., & Black, S. (2009). A Practical Approach for Using Solubility to Design Cooling Crystallisations. *Organic Process Research & Development, 13*(6), 1315-1321.

Munroe, A., Croker, D., Hodnett, B. K., & Seaton, C. C. (2011). Epitaxial growth of polymorphic systems: The case of sulfathiazole. *CrystEngComm, 13*(19), 5903-5907.

Muramatsu, H., Tamiya, E., & Karube, I. (1988). Computation of equivalent circuit parameters of quartz crystals in contact with liquids and study of liquid properties. *Analytical Chemistry, 60*(19), 2142-2146.

Myrdal, P. B., & Jozwiakowski, M. J. (2008). Alteration of the solid state of the drug substances: Polymorphs, solvates and amorphous forms. In R. Liu (Ed.), *Water-insoluble Drug Formulation* (2 ed., pp. 531-566): CRC Press.

Nordström, F. L., Svärd, M., Malmberg, B., & Rasmuson, Å. C. (2012). Influence of Solution Thermal and Structural History on the Nucleation of m-Hydroxybenzoic Acid Polymorphs. *Crystal Growth & Design, 12*(9), 4340-4348.

O'Mahony, M., Seaton, C. C., Croker, D. M., Veesler, S., Rasmuson, A. C., & Hodnett, B. K. (2014). Investigating the dissolution of the metastable triclinic polymorph of carbamazepine using in situ microscopy. *CrystEngComm, 16*(20), 4133-4141.

O'Mahony, M. A., Croker, D. M., Rasmuson, Å. C., Veesler, S., & Hodnett, B. K. (2013). Measuring the Solubility of a Quickly Transforming Metastable Polymorph of Carbamazepine. *Organic Process Research & Development, 17*(3), 512-518.

O'Sullivan, C. K., & Guilbault, G. G. (1999). Commercial quartz crystal microbalances – theory and applications. *Biosensors and Bioelectronics, 14*(8–9), 663-670.

Ostwald, W. (1897). Studies on the formation and transformation of solid bodies. *Zeitschrift fur physikalische Chemie, 22*, 289-330.

Otsuka, M., Hasegawa, H., & Matsuda, Y. (1999). *Effect of polymorphic forms of bulk powders on pharmaceutical properties of carbamazepine granules* (Vol. 47). Tokyo, JAPON: JAACC.

Owen, M. J., & Williams, D. E. (1991). Surface modification by fluoroalkyl-functional silanes. *Journal of Adhesion Science and Technology, 5*(4), 307-320.

Owens, D. K., & Wendt, R. C. (1969). Estimation of the surface free energy of polymers. *Journal of Applied Polymer Science, 13*(8), 1741-1747.

Parks, G. S., Snyder, L. J., & Cattoir, F. R. (1934). Studies on Glass. XI. Some Thermodynamic Relations of Glassy and Alpha-Crystalline Glucose. *The Journal of Chemical Physics, 2*(9), 595.

Parsons, A. R., Black, S. N., & Colling, R. (2003). Automated Measurement of Metastable Zones for Pharmaceutical Compounds. *Chemical Engineering Research and Design, 81*(6), 700-704.

Payne, R. S., Roberts, R. J., Rowe, R. C., & Docherty, R. (1999). Examples of successful crystal structure prediction: polymorphs of primidone and progesterone. *International Journal of Pharmaceutics, 177*(2), 231-245.

Peterson, M. L., McIlroy, D., Shaw, P., Mustonen, J. P., Oliveira, M., & Almarsson, Ö. (2003). Crystallization and Transformation of Acetaminophen Trihydrate. *Crystal Growth & Design, 3*(5), 761-765.

Pohlmann, H., Gulde, C., Jahn, R., & Pfeifer, S. (1975). Polymorphism, particle-size and blood level values of Carbamazepine. *Pharmazie, 30*(11), 709-711.

Pokroy, B., Chernow, V. F., & Aizenberg, J. (2009). Crystallization of malonic and succinic acids on SAMs: toward the general mechanism

of oriented nucleation on organic monolayers. *Langmuir, 25*(24), 14002-14006.

Poornachary, S. K., Chow, P. S., & Tan, R. B. H. (2007). Influence of Solution Speciation of Impurities on Polymorphic Nucleation in Glycine. *Crystal Growth & Design, 8*(1), 179-185.

Poornachary, S. K., Chow, P. S., & Tan, R. B. H. (2012). Application of Molecular Modeling in Pharmaceutical Crystallization and Formulation *Molecular Modeling for the Design of Novel Performance Chemicals and Materials* (pp. 157-185): CRC Press.

Poornachary, S. K., Parambil, J. V., Chow, P. S., Tan, R. B. H., & Heng, J. Y. Y. (2013). Nucleation of Elusive Crystal Polymorphs at the Solution–Substrate Contact Line. *Crystal Growth & Design, 13*(3), 1180-1186.

Price, C. P., Grzesiak, A. L., & Matzger, A. J. (2005). Crystalline Polymorph Selection and Discovery with Polymer Heteronuclei. *Journal of the American Chemical Society, 127*(15), 5512-5517.

Price, S. L. (2008). From crystal structure prediction to polymorph prediction: interpreting the crystal energy landscape. *Physical Chemistry Chemical Physics, 10*(15), 1996-2009.

Prohens, R., Font-Bardia, M., & Barbas, R. (2013). Water wires in the nanoporous form II of carbamazepine: a single-crystal X-ray diffraction analysis. *CrystEngComm, 15*(5), 845-847.

Quigley, D., Rodger, P. M., Freeman, C. L., Harding, J. H., & Duffy, D. M. (2009). Metadynamics simulations of calcite crystallization on self-assembled monolayers. *The Journal of Chemical Physics, 131*(9), -.

Rabesiaka, M., Porte, C., Bonnin-Paris, J., & Havet, J.-L. (2011). An automatic method for the determination of saturation curve and metastable zone width of lysine monohydrochloride. *Journal of Crystal Growth, 332*(1), 75-80.

Reboul, J. P., Cristau, B., Soyfer, J. C., & Astier, J. P. (1981). 5H-Dibenz[b,f]azepinecarboxamide-5 (carbamazepine). *Acta Crystallographica Section B, 37*(10), 1844-1848.

Robertson, J. M., & Ubbelohde, A. R. (1938). A New Form of Resorcinol. II. Thermodynamic Properties in Relation to Structure. *Proceedings of the Royal Society of London. Series A, Mathematical and Physical Sciences, 167*(928), 136-147.

Rodahl, M., Höök, F., Krozer, A., Brzezinski, P., & Kasemo, B. (1995). Quartz crystal microbalance setup for frequency and Q-factor measurements in gaseous and liquid environments. *Review of Scientific Instruments, 66*(7), 3924-3930.

Roy, S., & Matzger, A. J. (2009). Unmasking a Third Polymorph of a Benchmark Crystal-Structure-Prediction Compound(). *Angewandte Chemie (International ed. in English), 48*(45), 8505-8508.

Rustichelli, C., Gamberini, G., Ferioli, V., Gamberini, M. C., Ficarra, R., & Tommasini, S. (2000). Solid-state study of polymorphic drugs: carbamazepine. *Journal of Pharmaceutical and Biomedical Analysis, 23*(1), 41-54.

Sauerbrey, G. (1959). Verwendung von Schwingquarzen zur Wägung dünner Schichten und zur Mikrowägung. *Zeitschrift für Physik, 155*(2), 206-222.

Savage, J. R., & Dinsmore, A. D. (2009). Experimental Evidence for Two-Step Nucleation in Colloidal Crystallization. *Physical Review Letters, 102*(19), 198302.

Schakenraad, J. M., Busscher, H. J., Wildevuur, C. R. H., & Arends, J. (1986). The influence of substratum surface free energy on growth and spreading of human fibroblasts in the presence and absence of serum proteins. *Journal of Biomedical Materials Research, 20*(6), 773-784.

Schreiber, F. (2000). Structure and growth of self-assembling monolayers. *Progress in Surface Science, 65*(5–8), 151-257.

Shah, U. V., Amberg, C., Diao, Y., Yang, Z., & Heng, J. Y. Y. (2015). Heterogeneous nucleants for crystallogenesis and bioseparation. *Current Opinion in Chemical Engineering, 8*, 69-75.

Shah, U. V., Olusanmi, D., Narang, A. S., Hussain, M. A., Gamble, J. F., Tobyn, M. J., & Heng, J. Y. Y. (2014). Effect of crystal habits on the surface energy and cohesion of crystalline powders. *International Journal of Pharmaceutics, 472*(1-2), 140-147.

Shekunov, B. Y., & York, P. (2000). Crystallization processes in pharmaceutical technology and drug delivery design. *Journal of Crystal Growth, 211*(1-4), 122-136.

Singh, A., Lee, I. S., Kim, K., & Myerson, A. S. (2011). Crystal growth on self-assembled monolayers. *CrystEngComm, 13*(1), 24.

Singh, A., & Myerson, A. S. (2010). Chiral self assembled monolayers as resolving auxiliaries in the crystallization of valine. *Journal of Pharmaceutical Sciences, 99*(9), 3931-3940.

Singhal, D., & Curatolo, W. (2004). Drug polymorphism and dosage form design: a practical perspective. *Advanced Drug Delivery Reviews, 56*(3), 335-347.

Snyder, L. R. (1974). Classification of the solvent properties of common liquids. *Journal of Chromatography A, 92*(2), 223-230.

Stahly, G. P. (2007). Diversity in Single- and Multiple-Component Crystals. The Search for and Prevalence of Polymorphs and Cocrystals. *Crystal Growth & Design, 7*(6), 1007-1026.

Streets, A. M., & Quake, S. R. (2010). Ostwald Ripening of Clusters during Protein Crystallization. *Physical Review Letters, 104*(17), 178102.

Sudha, C., Nandhini, R., & Srinivasan, K. (2014). Polymer-Induced Selective Nucleation of Mono or Ortho Polymorphs of Paracetamol through Swift Cooling of Boiled Aqueous Solution. *Crystal Growth & Design, 14*(2), 705-715.

Sullivan, R. A., Davey, R. J., Sadiq, G., Dent, G., Back, K. R., ter Horst, J. H., . . . Hammond, R. B. (2014). Revealing the Roles of Desolvation and Molecular Self-Assembly in Crystal Nucleation from Solution: Benzoic and p-Aminobenzoic Acids. *Crystal Growth & Design, 14*(5), 2689-2696.

Sun, C., & Grant, D. W. (2001). Influence of Crystal Structure on the Tableting Properties of Sulfamerazine Polymorphs. *Pharmaceutical Research, 18*(3), 274-280.

Sun, H. (1998). COMPASS: An ab Initio Force-Field Optimized for Condensed-Phase Applications Overview with Details on Alkane and

Benzene Compounds. *The Journal of Physical Chemistry B, 102*(38), 7338-7364.

Sun, X., Garetz, B. A., & Myerson, A. S. (2006). Supersaturation and Polarization Dependence of Polymorph Control in the Nonphotochemical Laser-Induced Nucleation (NPLIN) of Aqueous Glycine Solutions. *Crystal Growth & Design, 6*(3), 684-689.

Sypek, K., Burns, I. S., Florence, A. J., & Sefcik, J. (2012). In Situ Monitoring of Stirring Effects on Polymorphic Transformations during Cooling Crystallization of Carbamazepine. *Crystal Growth & Design, 12*(10), 4821-4828.

Teychené, S., & Biscans, B. (2008). Nucleation Kinetics of Polymorphs: Induction Period and Interfacial Energy Measurements. *Crystal Growth & Design, 8*(4), 1133-1139.

Thallapally, P. K., Jetti, R. K. R., Katz, A. K., Carrell, H. L., Singh, K., Lahiri, K., . . . Desiraju, G. R. (2004). Polymorphism of 1,3,5-Trinitrobenzene Induced by a Trisindane Additive. *Angewandte Chemie International Edition, 43*(9), 1149-1155.

Thomason, J. L. (2009). The Role of Polarity in the Structure of Silanes Employed in Surface Modification *Silanes and Other Coupling Agents, Volume 5* (pp. 51-64): CRC Press.

Tian, F., Zeitler, J. A., Strachan, C. J., Saville, D. J., Gordon, K. C., & Rades, T. (2006). Characterizing the conversion kinetics of carbamazepine polymorphs to the dihydrate in aqueous suspension using Raman spectroscopy. *Journal of Pharmaceutical and Biomedical Analysis, 40*(2), 271-280.

Tokumitsu, S., Liebich, A., Herrwerth, S., Eck, W., Himmelhaus, M., & Grunze, M. (2002). Grafting of Alkanethiol-Terminated Poly(ethylene glycol) on Gold. *Langmuir, 18*(23), 8862-8870.

Towler, C. S., Davey, R. J., Lancaster, R. W., & Price, C. J. (2004). Impact of Molecular Speciation on Crystal Nucleation in Polymorphic Systems: The Conundrum of γ Glycine and Molecular 'Self Poisoning'. *Journal of the American Chemical Society, 126*(41), 13347-13353.

Trabattoni, S., Moret, M., Campione, M., Raimondo, L., & Sassella, A. (2013). Epitaxial Growth of Organic Semiconductor Polymorphs on

Natural Amino Acid Single Crystals. *Crystal Growth & Design, 13*(10), 4268-4278.

Ueno, S., Hamada, Y., & Sato, K. (2003). Controlling Polymorphic Crystallization of n-Alkane Crystals in Emulsion Droplets through Interfacial Heterogeneous Nucleation. *Crystal Growth & Design, 3*(6), 935-939.

Upadhyay, P., Dantuluri, A. K., Kumar, L., & Bansal, A. K. (2012). Estimating relative stability of polymorphs by generation of configurational free energy phase diagram. *Journal of Pharmaceutical Sciences, 101*(5), 1843-1851.

Urbelis, J. H., & Swift, J. A. (2014). Phase-Selective Crystallization of Perylene on Monolayer Templates. *Crystal Growth & Design, 14*(10), 5244-5251.

Van Oss, C. J., Chaudhury, M. K., & Good, R. J. (1988). Interfacial Lifshitz-van der Waals and polar interactions in macroscopic systems. *Chemical Reviews, 88*(6), 927-941.

Van Oss, C. J., Good, R. J., & Chaudhury, M. K. (1986). The role of van der Waals forces and hydrogen bonds in "hydrophobic interactions" between biopolymers and low energy surfaces. *Journal of Colloid and Interface Science, 111*(2), 378-390.

Van Oss, C. J., Good, R. J., & Chaudhury, M. K. (1988). Additive and nonadditive surface tension components and the interpretation of contact angles. *Langmuir, 4*(4), 884-891.

Vekilov, P. G. (2004). Dense Liquid Precursor for the Nucleation of Ordered Solid Phases from Solution. *Crystal Growth & Design, 4*(4), 671-685.

Vekilov, P. G. (2010). Nucleation. *Crystal Growth & Design, 10*(12), 5007-5019.

Vericat, C., Vela, M. E., Benitez, G., Carro, P., & Salvarezza, R. C. (2010). Self-assembled monolayers of thiols and dithiols on gold: new challenges for a well-known system. *Chemical Society Reviews, 39*(5), 1805-1834.

Volpe, C. D., & Siboni, S. (1997). Some Reflections on Acid–Base Solid Surface Free Energy Theories. *Journal of Colloid and Interface Science, 195*(1), 121-136.

Wan, C.-Q., Li, A.-M., Al-Thabaiti, S. A., El-Mosslamy, E.-S. H., & Mak, T. C. W. (2014). Efficient solvent-controlled crystallization of pure polymorphs of 1-nitro-4-(4-nitrophenylmethylthio)benzene. *CrystEngComm, 16*(38), 8960-8968.

Ward, M. D. (2001). Bulk Crystals to Surfaces: Combining X-ray Diffraction and Atomic Force Microscopy to Probe the Structure and Formation of Crystal Interfaces. *Chemical Reviews, 101*(6), 1697-1725.

Yamano, M. (2011). Development of new drug and crystal polymorphs. In T. Shioiri, K. Izawa & T. Konoike (Eds.), *Pharmaceutical Process Chemistry* (pp. 401-419). Weinheim: Wiley-VCH Verlag GmbH & Co. KGaA.

Yang, H., Svärd, M., Zeglinski, J., & Rasmuson, Å. C. (2014). Influence of Solvent and Solid-State Structure on Nucleation of Parabens. *Crystal Growth & Design, 14*(8), 3890-3902.

Yongan Peter, G. (2007). Glass Surfaces: Electrokinetic and Wetting Properties *Encyclopedia of Surface and Colloid Science, Second Edition* (Vol. 4, pp. 2711-2723): Taylor & Francis.

Yoshihashi, Y., Yonemochi, E., & Terada, K. (2002). Estimation of Initial Dissolution Rate of Drug Substance by Thermal Analysis: Application for Carbamazepine Hydrate. *Pharmaceutical Development and Technology, 7*(1), 89-95.

Young, T. (1805). An Essay on the Cohesion of Fluids. *Philosophical Transactions of the Royal Society of London, 95*, 65-87.

Yu, L. (2003). Nucleation of one polymorph by another. *Journal of American Chemical Society, 125*(21), 6380-6381.

Zenkiewicz, M. (2007). Methods for the calculation of surface free energy of solids. *Journal of Achievements in Materials and Manufacturing Engineering, 24*(1), 137-145.

Zhang, H., Lakerveld, R., Heider, P. L., Tao, M., Su, M., Testa, C. J., . . . Evans, J. M. B. (2014). Application of Continuous Crystallization in an Integrated Continuous Pharmaceutical Pilot Plant. *Crystal Growth & Design, 14*(5), 2148-2157.

Zhang, J., Liu, A., Han, Y., Ren, Y., Gong, J., Li, W., & Wang, J. (2011). Effects of Self-Assembled Monolayers on Selective Crystallization of Tolbutamide. *Crystal Growth & Design, 11*(12), 5498-5506.

Zhao, L., Raval, V., Briggs, N. E. B., Bhardwaj, R. M., McGlone, T., Oswald, I. D. H., & Florence, A. J. (2014). From discovery to scale-up: α-lipoic acid : nicotinamide co-crystals in a continuous oscillatory baffled crystalliser. *CrystEngComm, 16*(26), 5769-5780.

Zisman, W. A. (1964). Relation of the Equilibrium Contact Angle to Liquid and Solid Constitution. *43*, 1-51.

Publications

This thesis resulted in the following journal articles and conference presentations.

Journal articles

Parambil, J. V., Poornachary, S. K., Tan, R. B. H., & Heng, J. Y. Y. (2014). Template-induced polymorphic selectivity: the effects of surface chemistry and solute concentration on carbamazepine crystallisation. *CrystEngComm, 16*, 4927-4930.

Parambil, J. V., Poornachary, S. K., Hinder, S. J., Tan, R. B. H., & Heng, J. Y. Y. (2015) Establishing template-induced polymorphic domains for API crystallisation: The case of carbamazepine. *CrystEngComm.* 17, 6384-6392.

Parambil, J. V., Poornachary, S. K., Tan, R. B. H., & Heng, J. Y. Y. Influence of solvents on template-induced polymorphic domains. *Journal of Crystal Growth*. In preparation

Conference presentations

Parambil, J. V., Poornachary, S. K., Tan, R. B. H., & Heng, J. Y. Y. "Influencing polymorph crystallisation through template-mediated nucleation." Oral presentation at 45th Annual British Association for Crystal Growth (BACG) conference, 2014, Leeds, United Kingdom.

Parambil, J. V., Poornachary, S. K., Tan, R. B. H., & Heng, J. Y. Y. "Template-mediated nucleation for controlling crystal polymorphism." Oral presentation at International Conference in Advances in Chemical Engineering (ICACE), 2014, Kollam, India.

Parambil, J. V., Poornachary, S. K., Tan, R. B. H., & Heng, J. Y. Y. "Effects of surface chemistry on polymorph selective nucleation of carbamazepine." Poster presentation at Annual meeting of International Fine Particle Research Institute, 2014, Edinburgh, United Kingdom.

Parambil, J. V., Poornachary, S. K., Tan, R. B. H., & Heng, J. Y. Y. "Polymorph selective crystallisation of carbamazepine on silanised glass templates." Poster presentation at 44th Annual British Association for Crystal Growth (BACG) conference, 2013, Manchester, United Kingdom.

Parambil, J. V., Poornachary, S. K., Tan, R. B. H., & Heng, J. Y. Y. "Selective polymorphic crystallisation on modified glass templates." Poster presentation at Continuous Manufacturing and Crystallisation (CMAC) Annual meeting, 2013, Glassgow, United Kingdom.

Parambil, J. V., Poornachary, S. K., Tan, R. B. H., & Heng, J. Y. Y. "Templates for nucleation control." Poster presentation at CrystallisAbility workshop organised by EPSRC Directed Assembly Grand Challenge Network, 2013, Berkshire, United Kingdom.

Appendix – A

Theory of Quartz Crystal Microbalance (QCM)

QCM is basically a very sensitive mass balance which utilises the piezoelectric properties of a quartz crystal. It consists of a quartz crystal disc with electrodes on either side. When an oscillating potential is applied across the electrodes, the quartz crystal oscillates laterally due to its piezoelectric properties and an acoustic wave propagates perpendicular to the crystal surface. The frequency of this oscillation depends on the fundamental resonant frequency of the crystal which is determined by the mass and thickness of the crystal. When additional mass is attached to the oscillating crystal, the frequency of oscillation decreases as expressed below:

$$\Delta f = -\frac{f}{t_q \rho_q}\Delta m = -n\frac{2f_0^2}{v_q \rho_q}\Delta m = -n\frac{1}{C}\Delta m \qquad (7.1)$$

where, Δm and Δf represents the change in mass and frequency shift respectively; t_q, ρ_q, v_q, f_0, n and C stands for thickness and density of the quartz crystal, velocity of sound through quartz, fundamental frequency of the crystal, overtone number and mass sensitivity (a constant) of the crystal. This linear relationship between frequency shift and mass shift is referred to as the Sauerbrey equation in honour of Gunter Sauerbury who put forward the equation (1959). With a frequency resolution of 0.1 Hz in liquid, a QCM is capable of detecting mass changes which are just a few nanograms per cm^2. However, this relationship is applicable only under certain ideal conditions. It assumes that there is a no slip condition between the crystal and adsorbed material and that the adsorbed material is a rigid solid mass. Although these could be applicable for vacuum deposition of metals on a quartz surface, these

assumptions are not completely applicable for a quartz crystal in liquid or when the adsorbed material exhibits viscoelastic properties (Bruckenstein & Shay, 1985). The shift in the resonant frequency of the sensor when in contact with a Newtonian liquid is given by the relationship,

$$\Delta f = f_0^{3/2} \sqrt{\frac{\rho_L \eta_L}{\pi \rho_q \mu_q}} \qquad (7.2)$$

where, ρ_L, η_L and μ_q represents liquid density, dynamic viscosity of liquid and shear modulus of the crystal (Keiji Kanazawa & Gordon Ii, 1985). When a solid mass adsorbs on to the crystal surface in liquid medium, frequency shifts caused by increased mass is additive to the contribution from liquid. Thus both mass of the adsorbed solid and viscosity of the liquid will cause shift in resonant frequency in a liquid phase QCM measurement (Lucklum & Hauptmann, 2000).

It is shown that by creating electrical circuit analogue for the oscillating quartz crystal in QCM, more information on the viscoelastic properties of the adsorbed layer can be obtained (Muramatsu *et al.*, 1988). An equivalent circuit for quartz crystal as proposed by Muramastu *et al*. is shown in Figure A1. Based on the equivalent circuit, the resonant frequency of the crystal can be expressed as,

$$f_0 = 1/\left(2\pi \sqrt{C_1 L_1}\right) \qquad (7.3)$$

where, C_1 and L_1 represents the capacitance and inductance of the crystal, which in turn reflects the elasticity and mass of the quartz crystal. The resonant resistance (R_1) in the circuit reflects the degree of mechanical vibration energy loss due to damping in a viscous liquid (Liu *et al.*, 2013) and can be expressed as,

$$R_1 = A\sqrt{2\pi f_0 \rho_L \eta_L}/\mathrm{K}^2 \qquad (7.4)$$

where K is the electromagnetic coupling factor of the quartz resonator. Similarly, the dissipation factor (*D*) can be expressed by the equation,

$$D = R_1/(\omega L_1) \qquad (7.5),$$

where ω is the angular frequency at resonance (Rodahl *et al.*, 1995). The dissipation factor can provide valuable information on the molecular structure of the liquid or solid interacting with the resonator and the surface-liquid coupling at interface (Dixon, 2008). Using the above relationships, the mass, thickness, viscosity and elasticity of the liquid and solid phases surrounding the quartz crystal can be estimated.

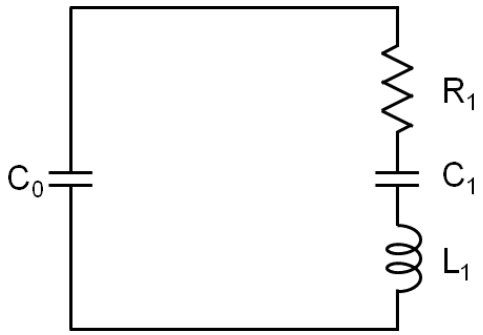

Figure A1. Electrical equivalent circuit of quartz crystal.